Cosmological surveys

Lecture 2

Will Percival

ICG Portsmouth
University of Portsmouth

Science & Technology Facilities Council
erc

Cosmology from surveys

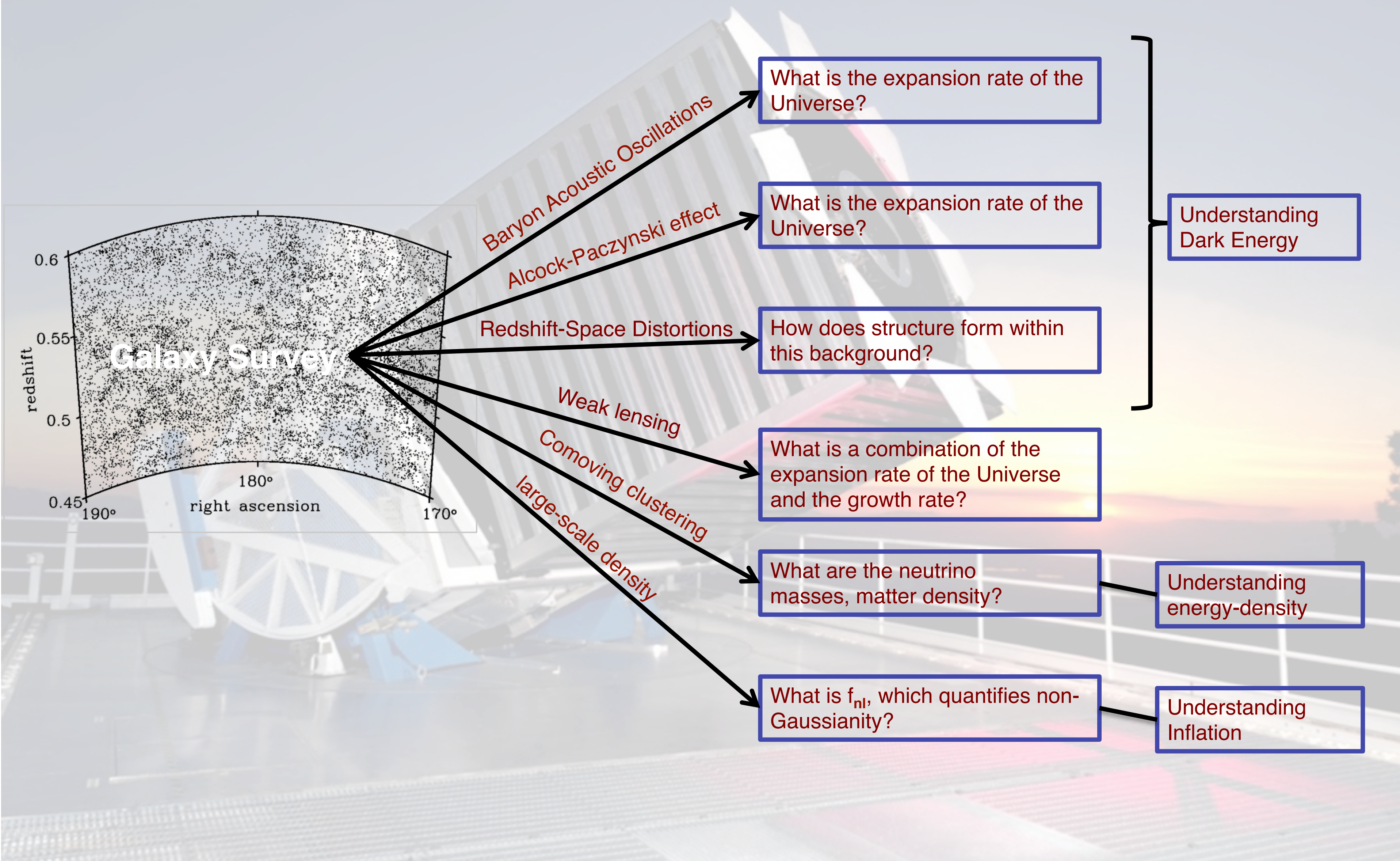

Weak lensing

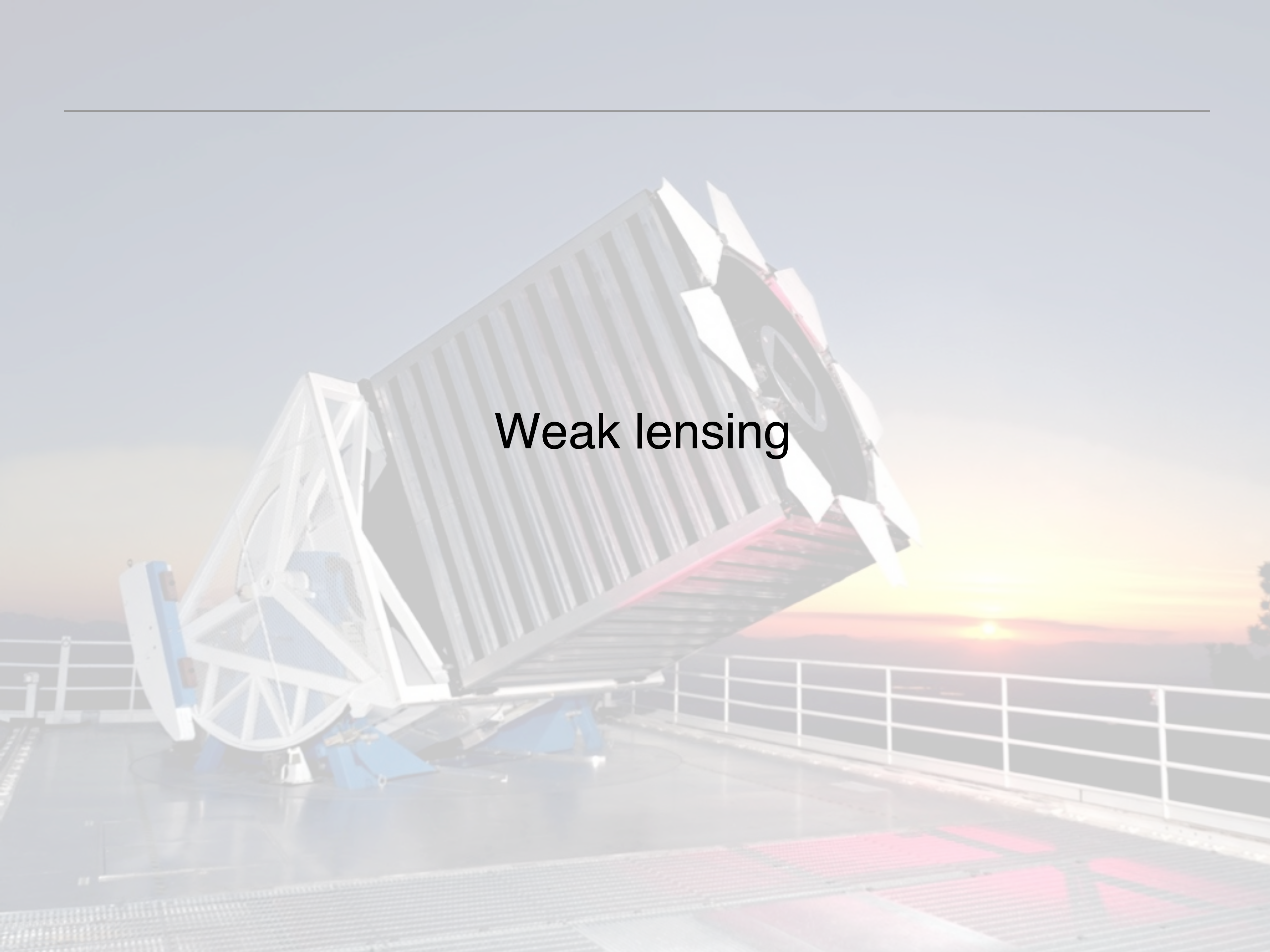

Gravitational lensing

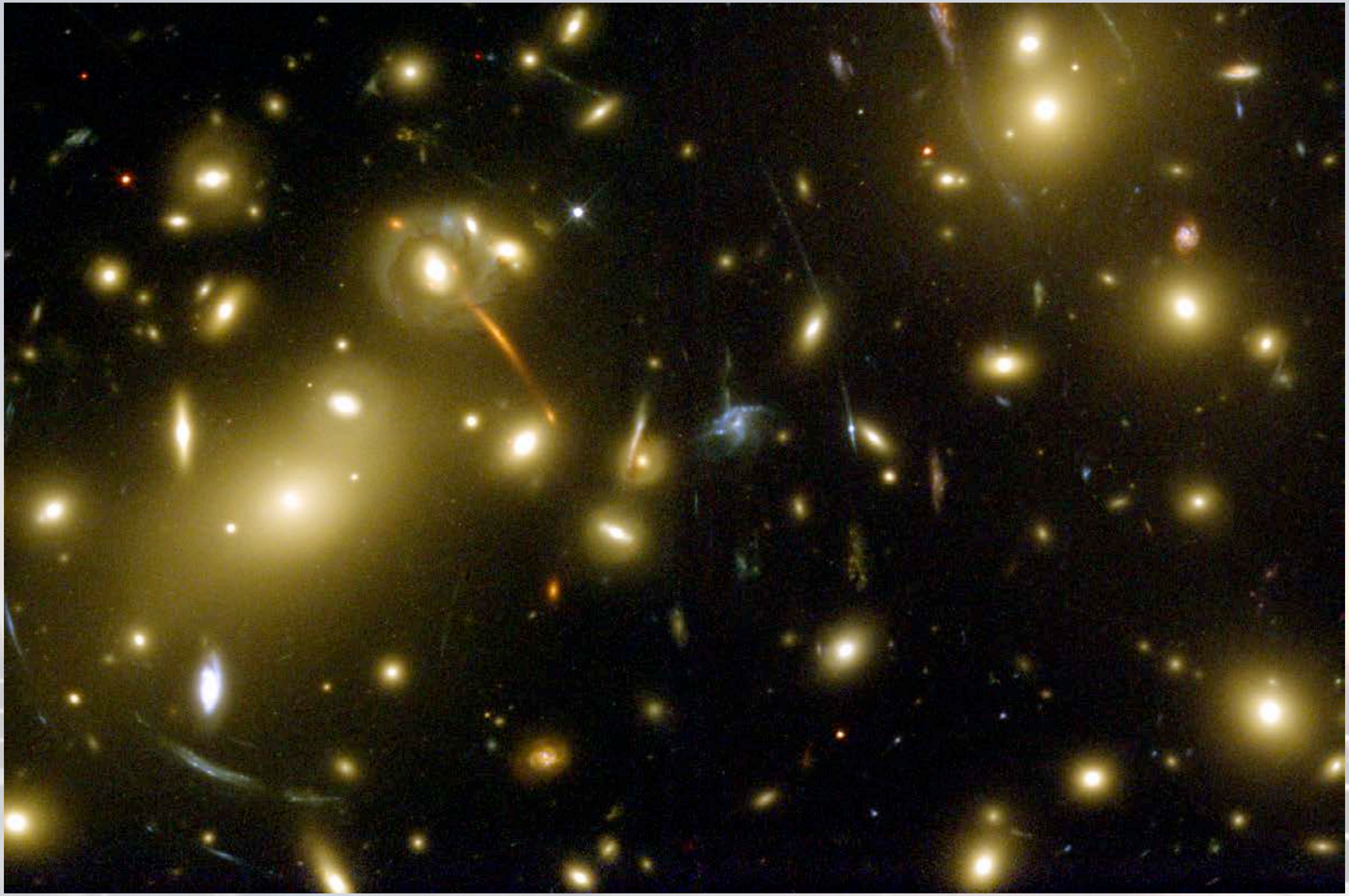

Abell 2218
Cluster of galaxies 2 billion light years away,
Background galaxies 6 billion light years away

So what's happening?

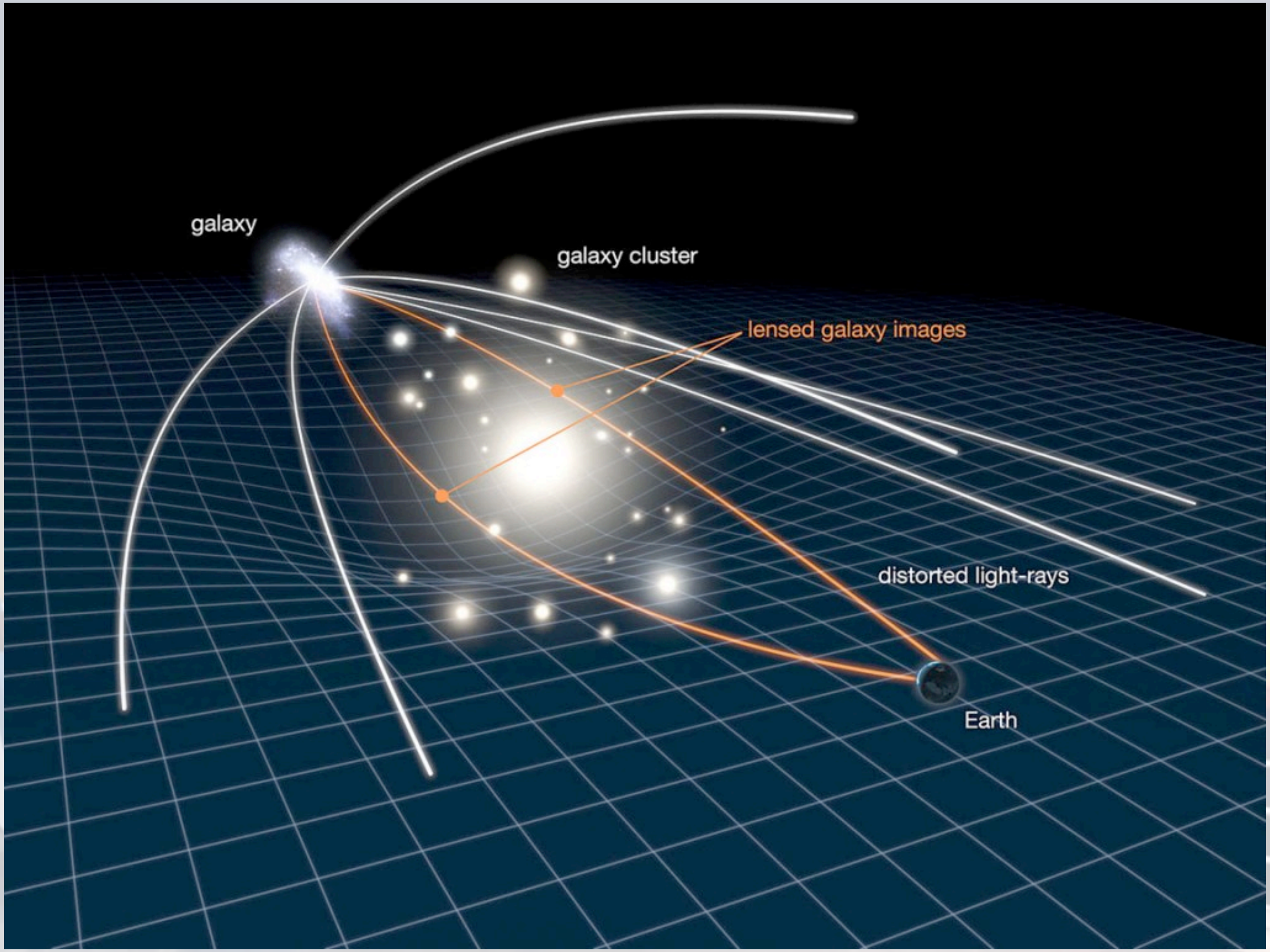

Weak-lensing

Assumptions:

- weak field limit $v^2/c^2 \ll 1$
- stationary field $t_{dyn}/t_{cross} \ll 1$
- thin lens approximation $L_{lens}/L_{bench} \ll 1$
- transparent lens
- small deflection angle

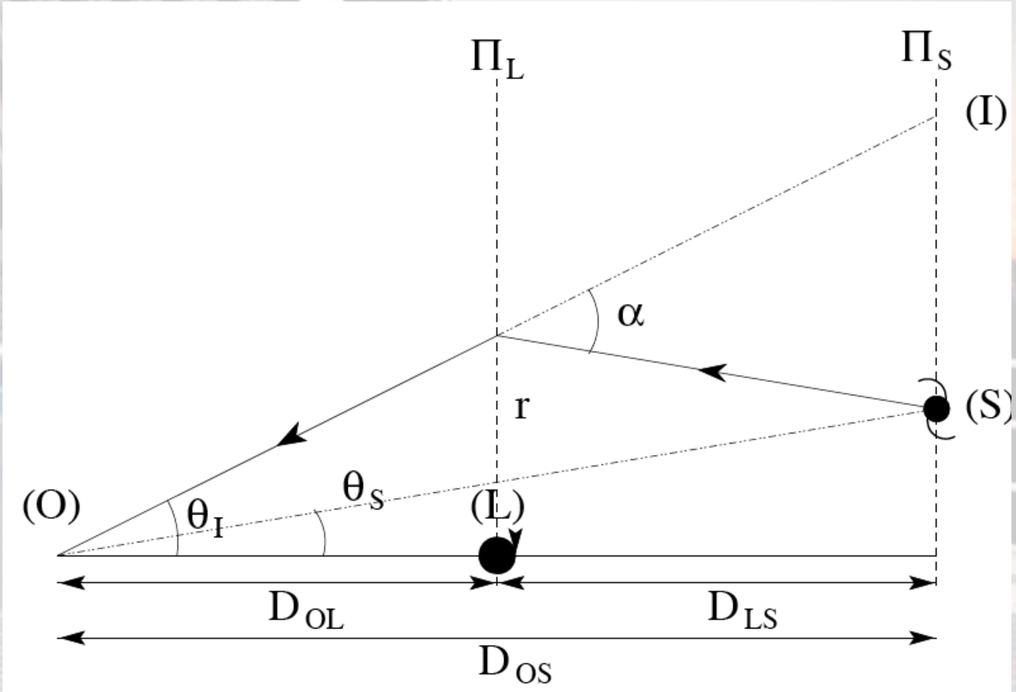

Weak-lensing

Photons travel along null geodesics

Solve for photon path by extremizing the Lagrangian for force-free motion

$$L = \frac{1}{2} g_{\mu\nu} \dot{x}^\mu \dot{x}^\nu$$

This leads to the following Euler-Lagrange equations

$$\frac{dp_\mu}{d\lambda} = \frac{\partial L}{\partial x^\mu}; \;\; p_\mu = \frac{\partial L}{\partial \dot{x}^\mu}$$

For the weak-field metric

$$ds^2 = -(1 + 2\Phi)dt^2 + (1 - 2\Phi)d\mathbf{x}^2$$

We obtain to first order in ϕ

$$p_\parallel^{-1} \frac{dp_\perp}{d\lambda} = -2\nabla_\perp \Phi \dot{x}_\parallel$$

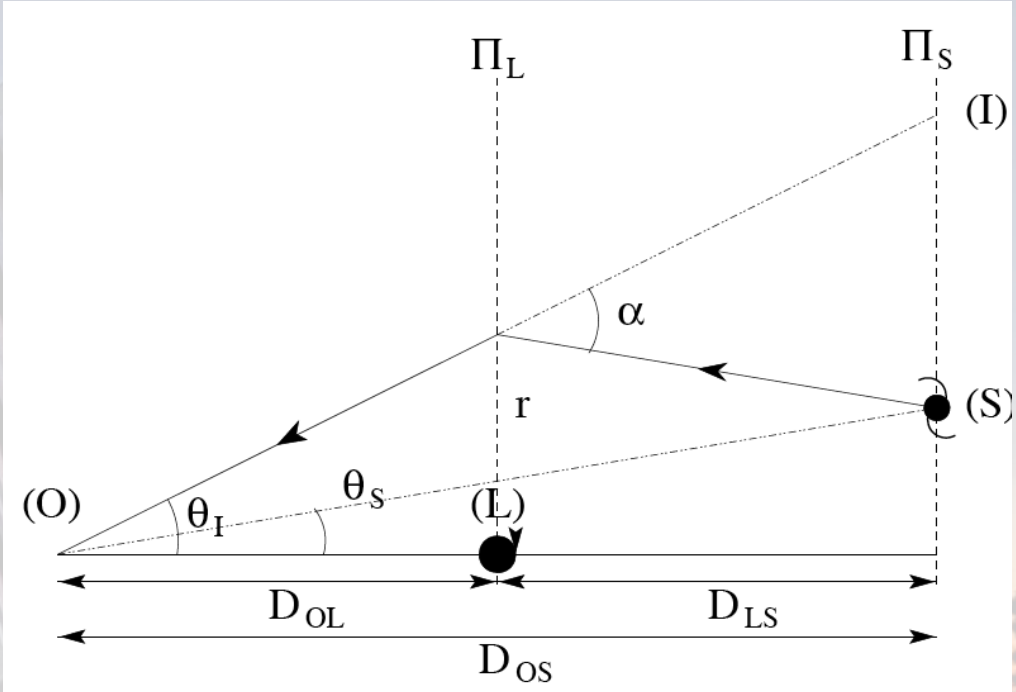

Weak-lensing

The bend angle depends on the gravitational potential through

$$\alpha = \frac{2}{c}\int \nabla_{\perp}\Phi d\ell$$

So the lens equation can be written in terms of a lensing potential

$$\theta_I - \theta_S = \frac{D_{LS}}{D_{OS}}\alpha \equiv \nabla_\theta \psi(\theta_I)$$

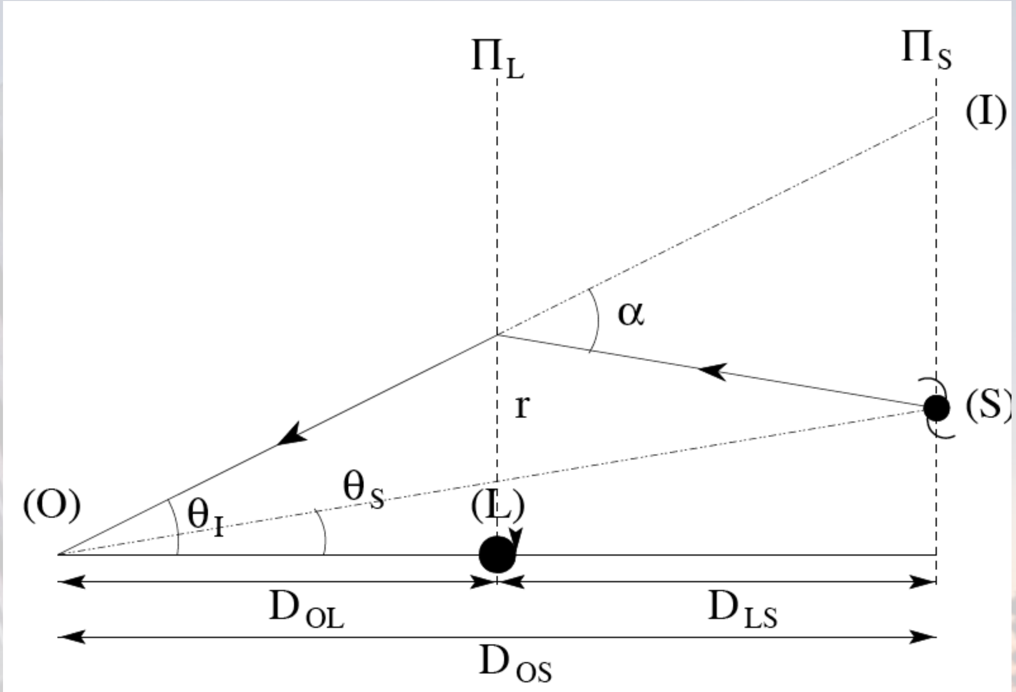

The lensing will produce a first order mapping distortion (Jacobian of the lens mapping)

$$\frac{d\theta_S}{d\theta_I} = A = \begin{pmatrix} 1 - \partial_{xx}\psi & -\partial_{xy}\psi \\ -\partial_{xy}\psi & 1 - \partial_{yy}\psi \end{pmatrix}$$

Weak-lensing

We can write the Jacobian of the lens mapping as

$$A = \begin{pmatrix} 1-\kappa-\gamma_1 & -\gamma_2 \\ -\gamma_2 & 1-\kappa+\gamma_1 \end{pmatrix} = (1-\kappa)\begin{pmatrix} 1 & 0 \\ 0 & 1 \end{pmatrix} + \begin{pmatrix} -\gamma_1 & -\gamma_2 \\ -\gamma_2 & +\gamma_1 \end{pmatrix}$$

In terms of the convergence

$$\kappa = \frac{1}{2}[\partial_{xx}\psi + \partial_{yy}\psi]$$

And shear

$$\gamma = (\gamma_1, \gamma_2) = [(\partial_{yy}\psi - \partial_{xx}\psi)/2, \partial_{xy}\psi]$$

κ represents an isotropic magnification. It transforms a circle into a larger / smaller circle

γ Represents an anisotropic magnification. It transforms a circle into an ellipse with axes

$$b = (1-\kappa+\gamma)^{-1}, \quad a = (1-\kappa-\gamma)^{-1}$$

Weak-lensing

Galaxy ellipticities provide a direct measurement of the shear field (in the weak lensing limit)

Need an expression relating the lensing field to the matter field, which will be an integral over galaxy distances χ

$$P_\kappa(\ell) = \frac{9\pi}{4\ell}\Omega_m^2 H_0^4 \int_0^{\chi_\infty} d\chi \frac{g^2(\chi)}{\chi^2 a^2(\chi)} P_m(\ell/\chi)$$

The weight function, which depends on the galaxy distribution is

$$g(\chi) \equiv 2\chi \int_\chi^{\chi_\infty} d\chi' \left(1 - \frac{\chi}{\chi'}\right) W(\chi')$$

The shear power spectra are related to the convergence power spectrum by

$$P_{\gamma_1}(\ell, \phi_\ell) = \cos^2(2\phi_\ell) P_\kappa(\ell)$$
$$P_{\gamma_2}(\ell, \phi_\ell) = \sin^2(2\phi_\ell) P_\kappa(\ell)$$

As expected, from a measurement of the convergence power spectrum we can constrain the matter power spectrum (mainly amplitude) and geometry

Weak-lensing

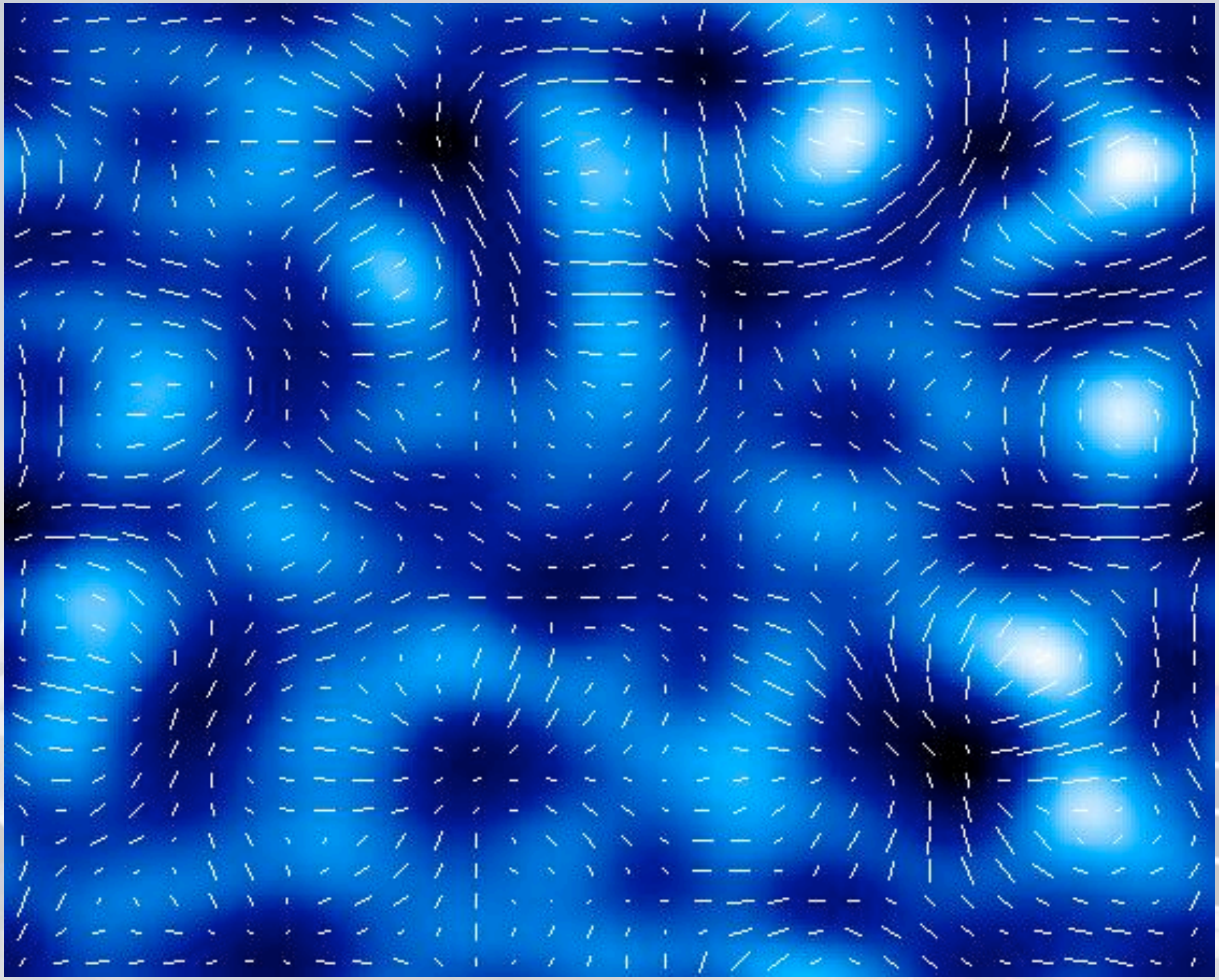

Comparison of convergence and shear fields

In practice

- Convergence field can be measured by cross-correlating foreground galaxies with background galaxies
  - expect galaxies to be brighter behind mass concentrations
- Shear field can be measured from galaxy ellipticities
  - percent level effect
  - requires accurate knowledge of PSF

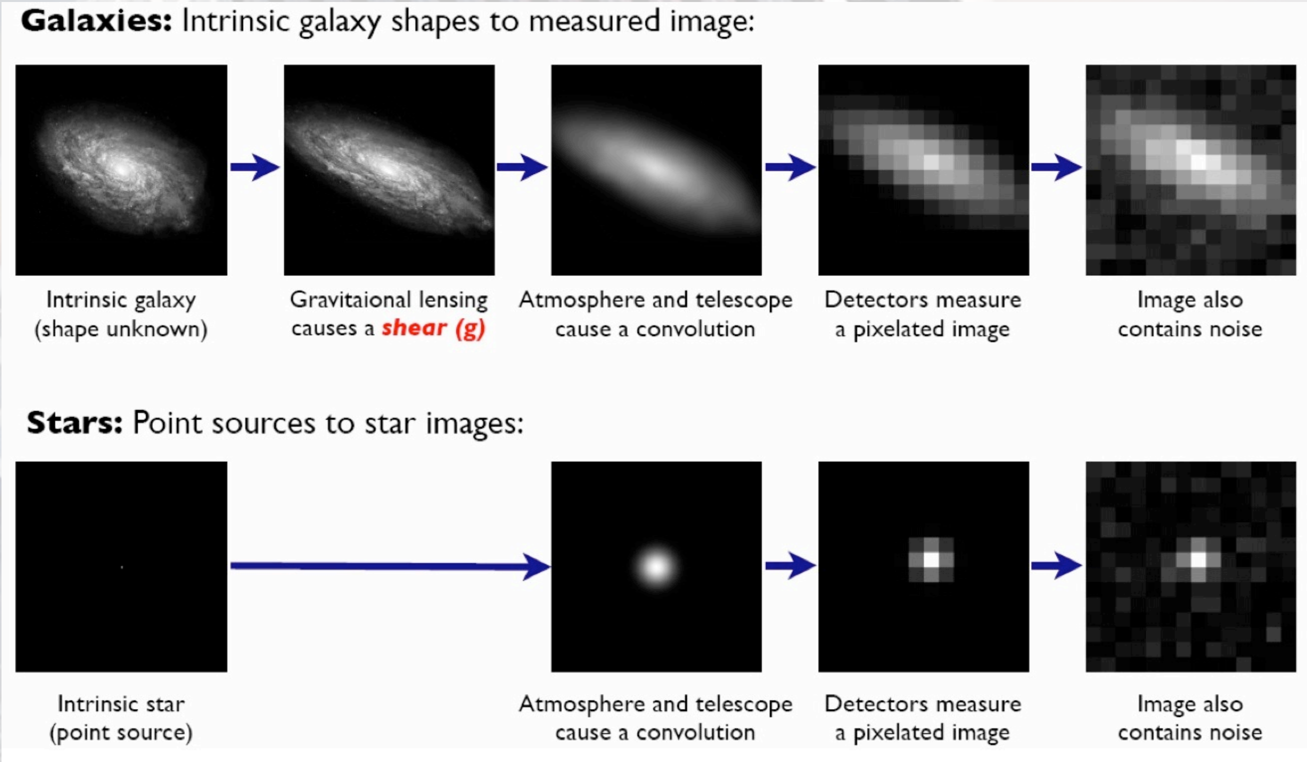

Intrinsic alignments

- Galaxy formation processes can align galaxies, giving a false shear signal
  - correlations can be galaxy-galaxy
  - correlations can be galaxy-shear

- In general, these have a different dependence with redshift compared with the weak lensing signal itself

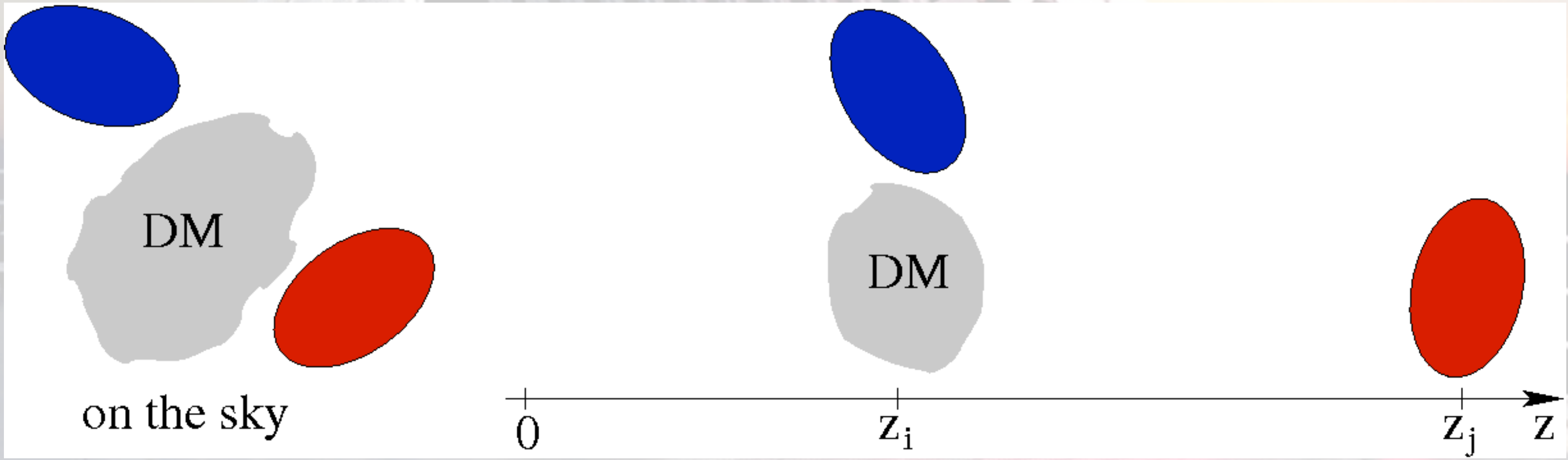

Directly depends on the mass distribution

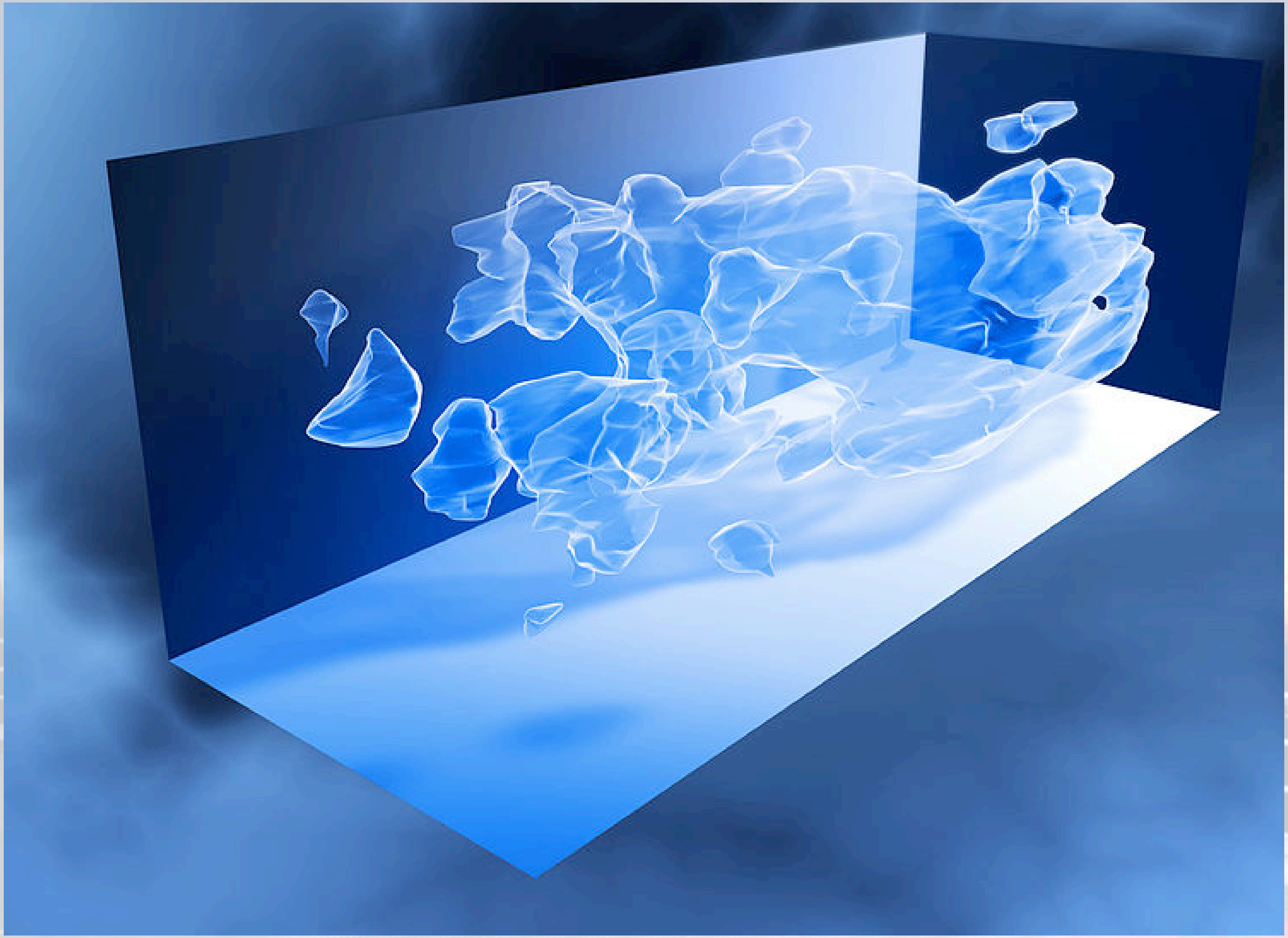

Massey et al. 2008; HST COSMOS analysis; 2 deg^2

CFHTLenS

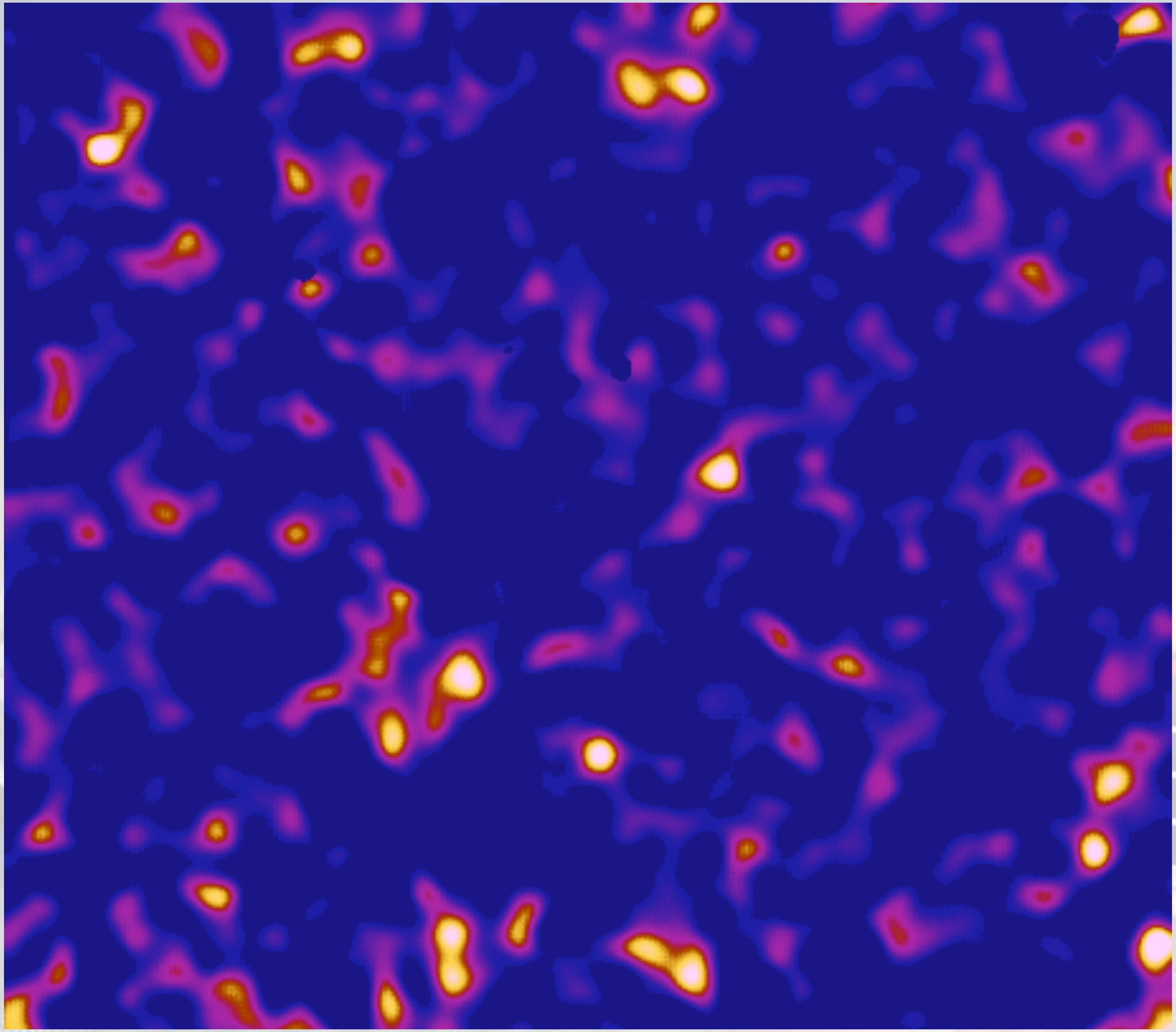

CFHT Lensing Survey: 154deg^2 of deep multi-colour imaging

CFHTLenS

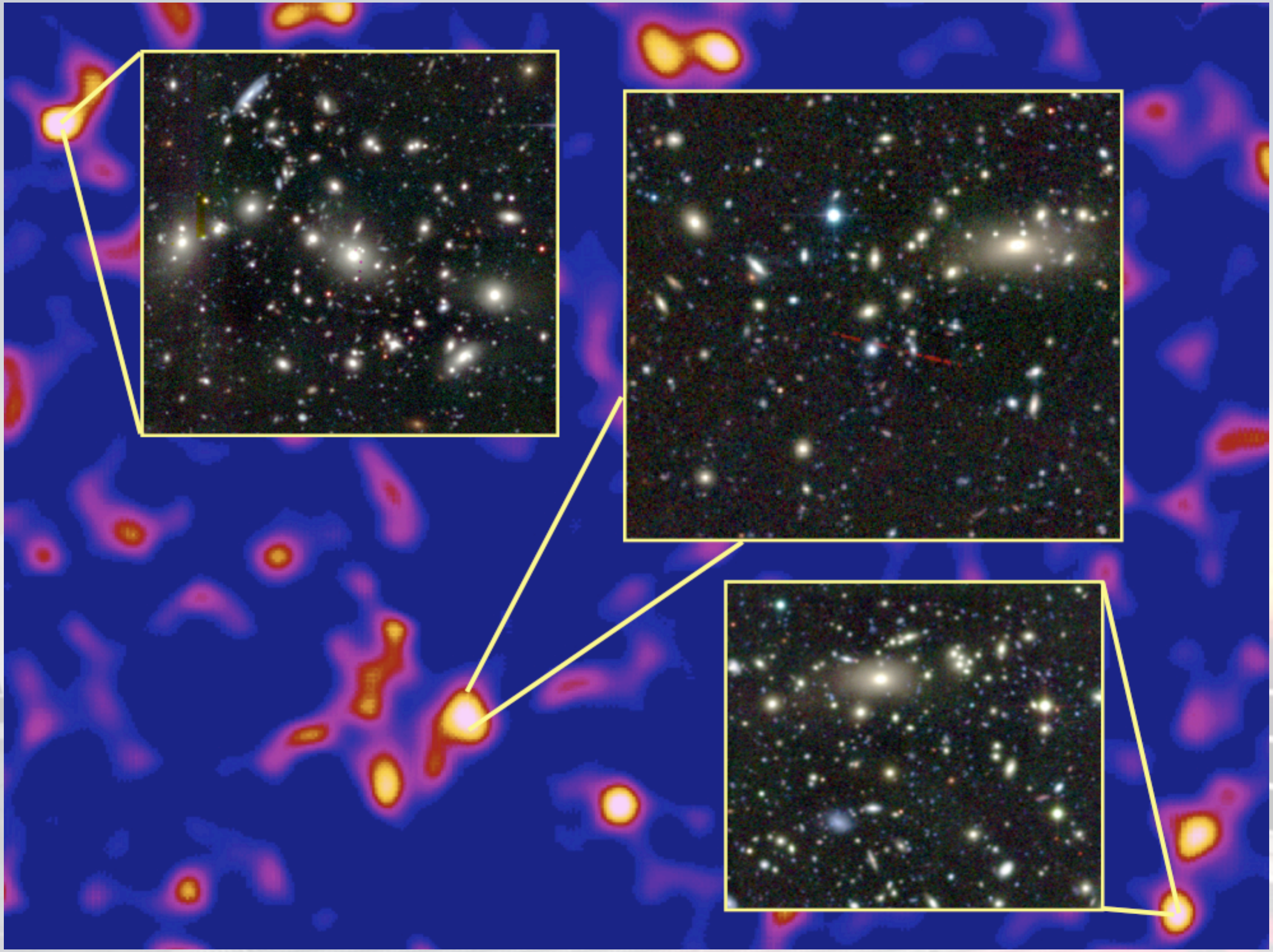

CFHT Lensing Survey: 154deg^2 of deep multi-colour imaging

Recent CFHTLenS results

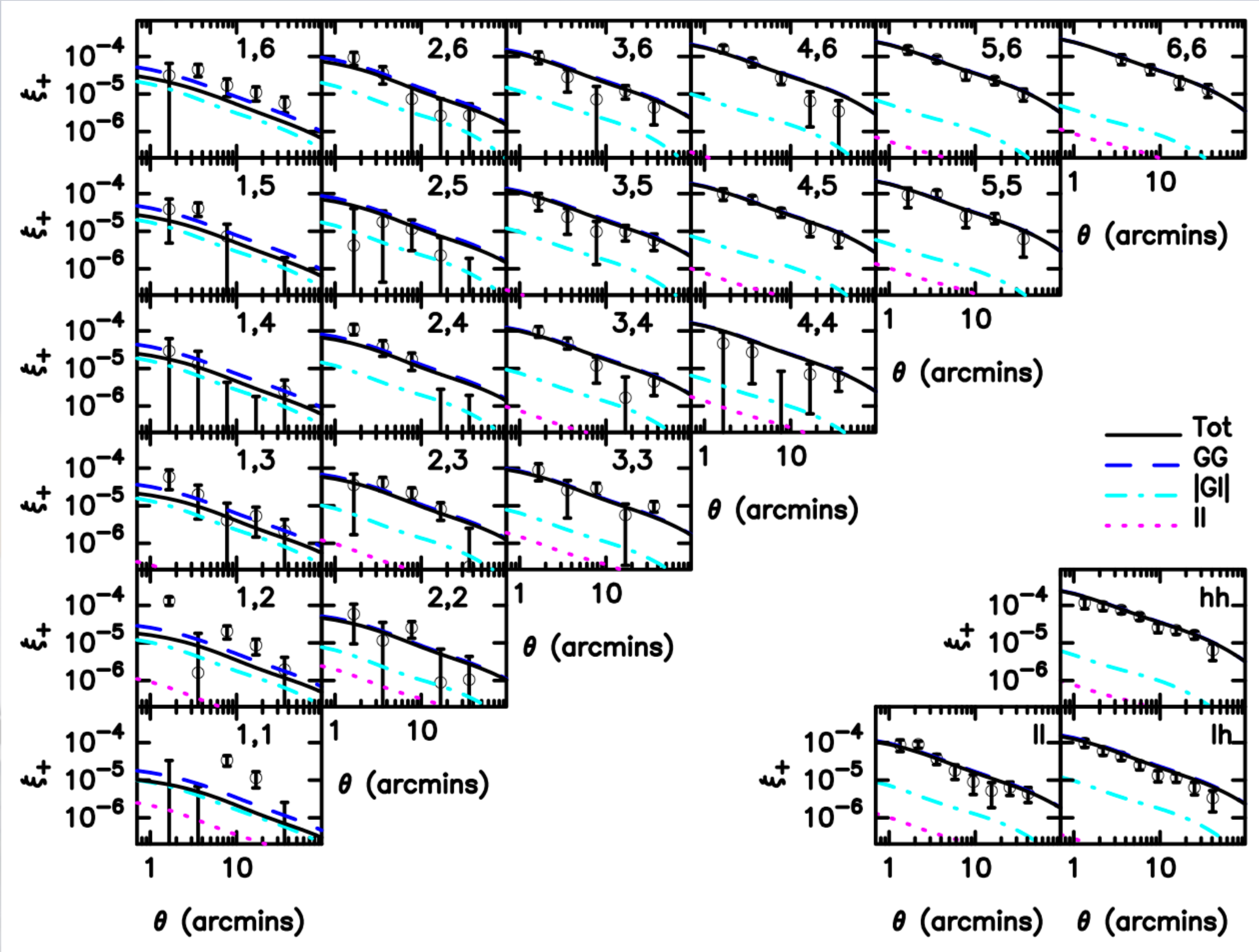

Heymans et al. 2013; arXiv:1303.1808

Recent CFHTLenS results

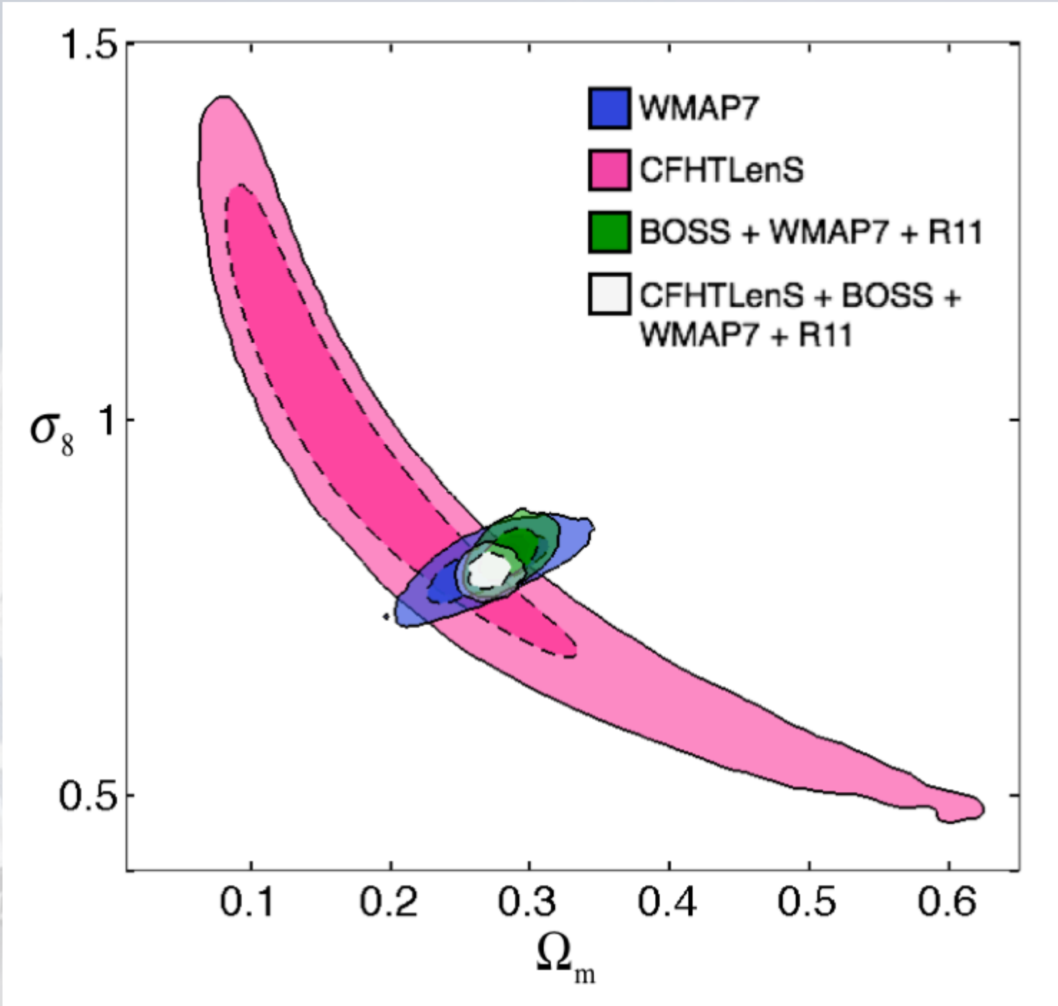

Heymans et al. 2013; arXiv:1303.1808

Redshift-space distortions

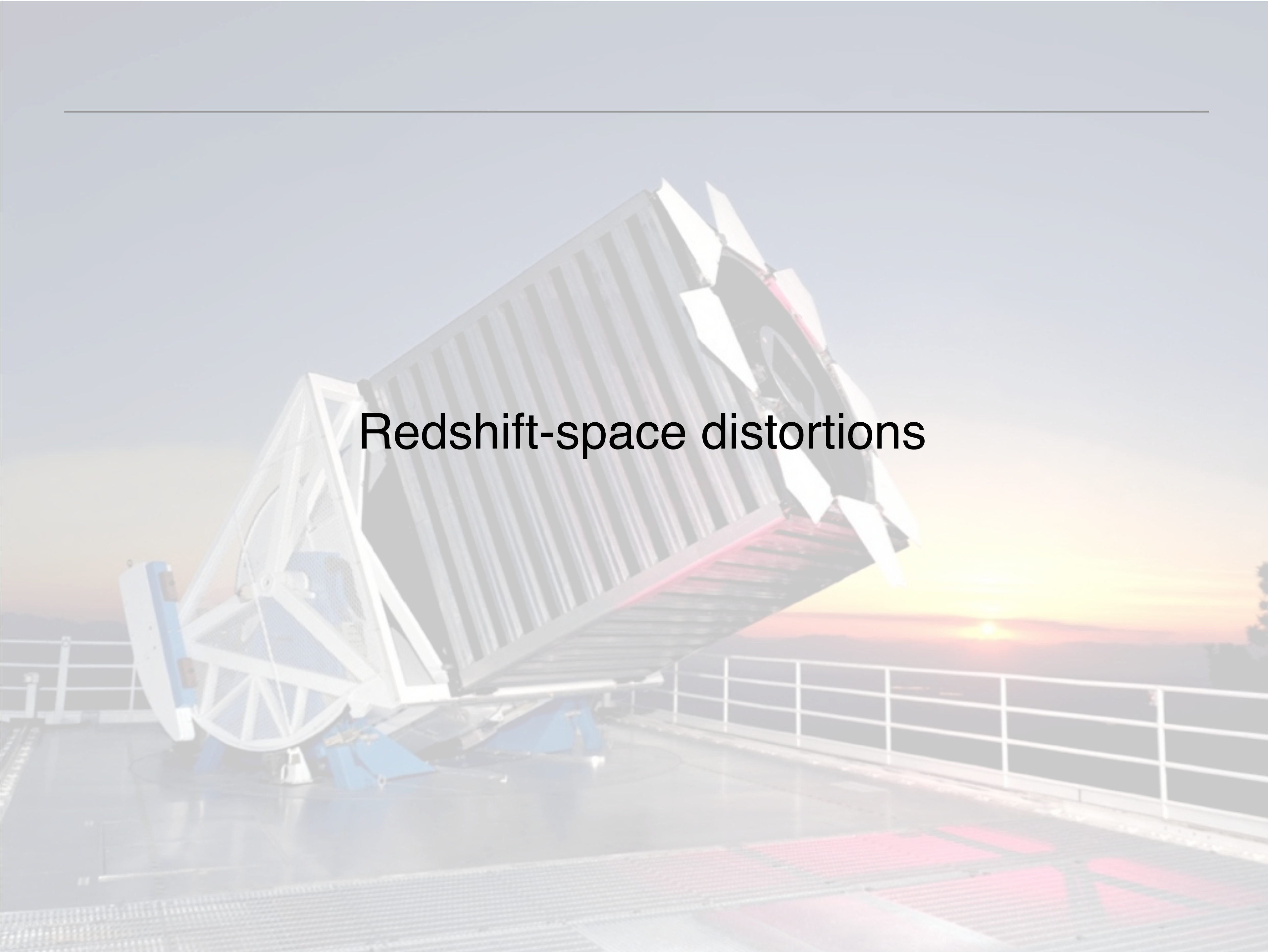

Comoving velocities

Locally, galaxies act as test particles in the flow of matter

On large-scales, the distribution of galaxy velocities is unbiased if galaxies fully sample the velocity field

expect a small peak velocity-bias due to motion of peaks in Gaussian random fields differing from that of the mass

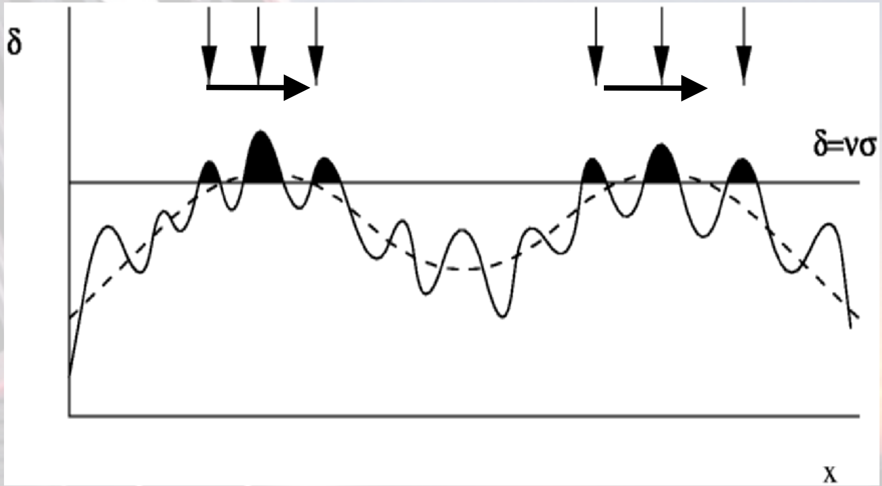

Redshift-Space Distortions

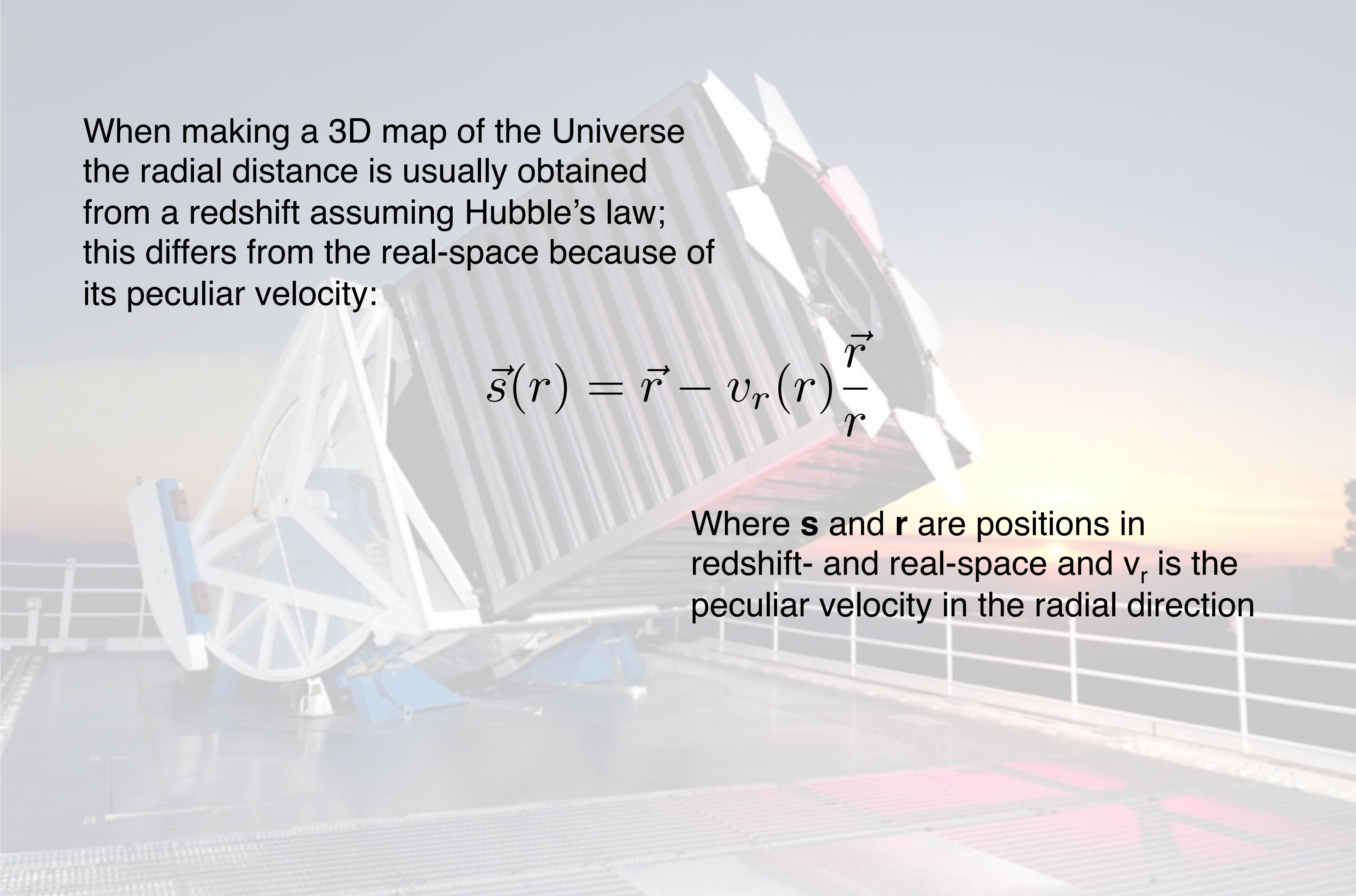

When making a 3D map of the Universe the radial distance is usually obtained from a redshift assuming Hubble's law; this differs from the real-space because of its peculiar velocity:

$$\vec{s}(r) = \vec{r} - v_r(r)\frac{\vec{r}}{r}$$

Where **s** and **r** are positions in redshift- and real-space and v_r is the peculiar velocity in the radial direction

Two key regimes of interest

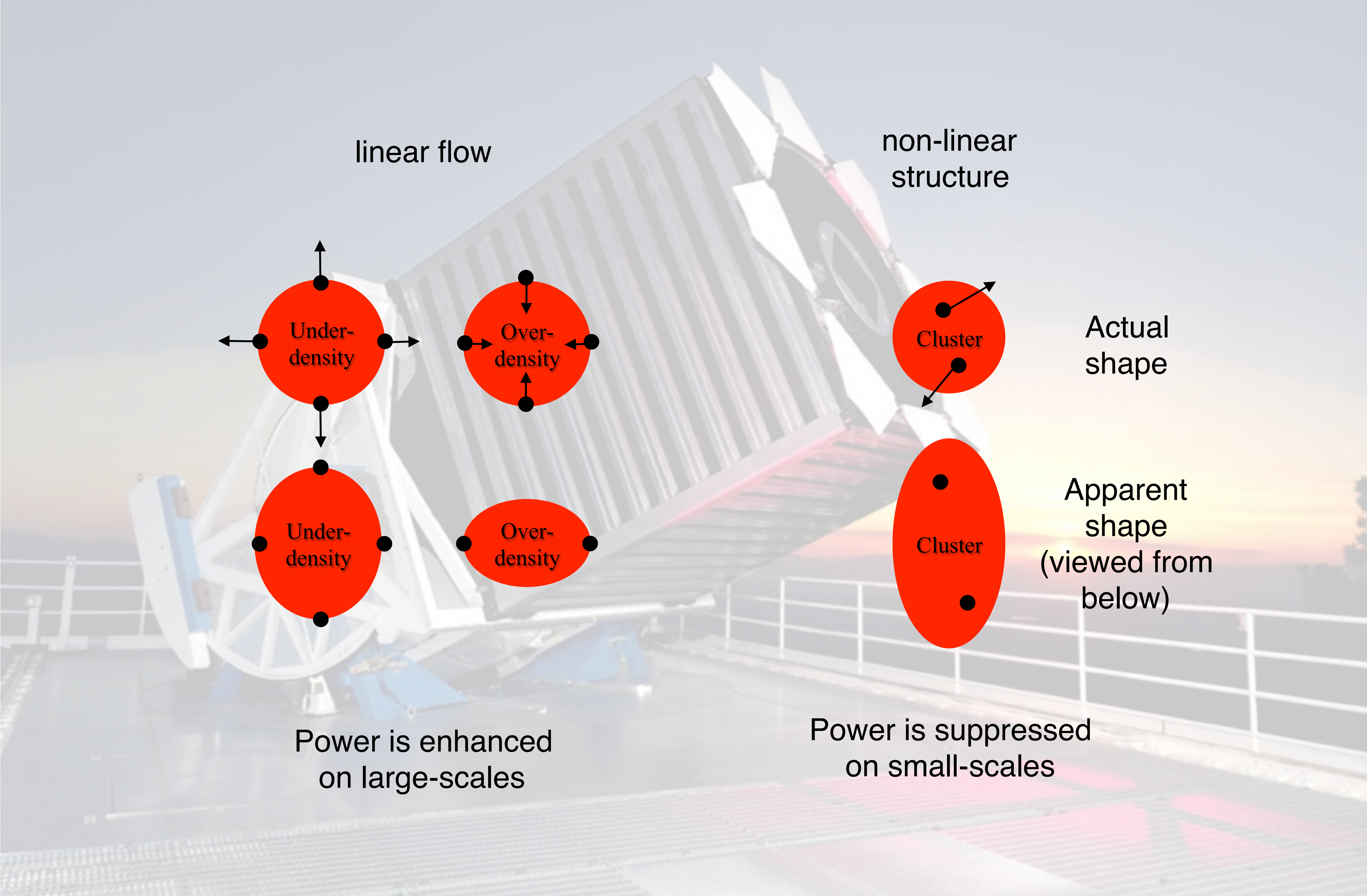

Fingers-of-God clearly visible in maps

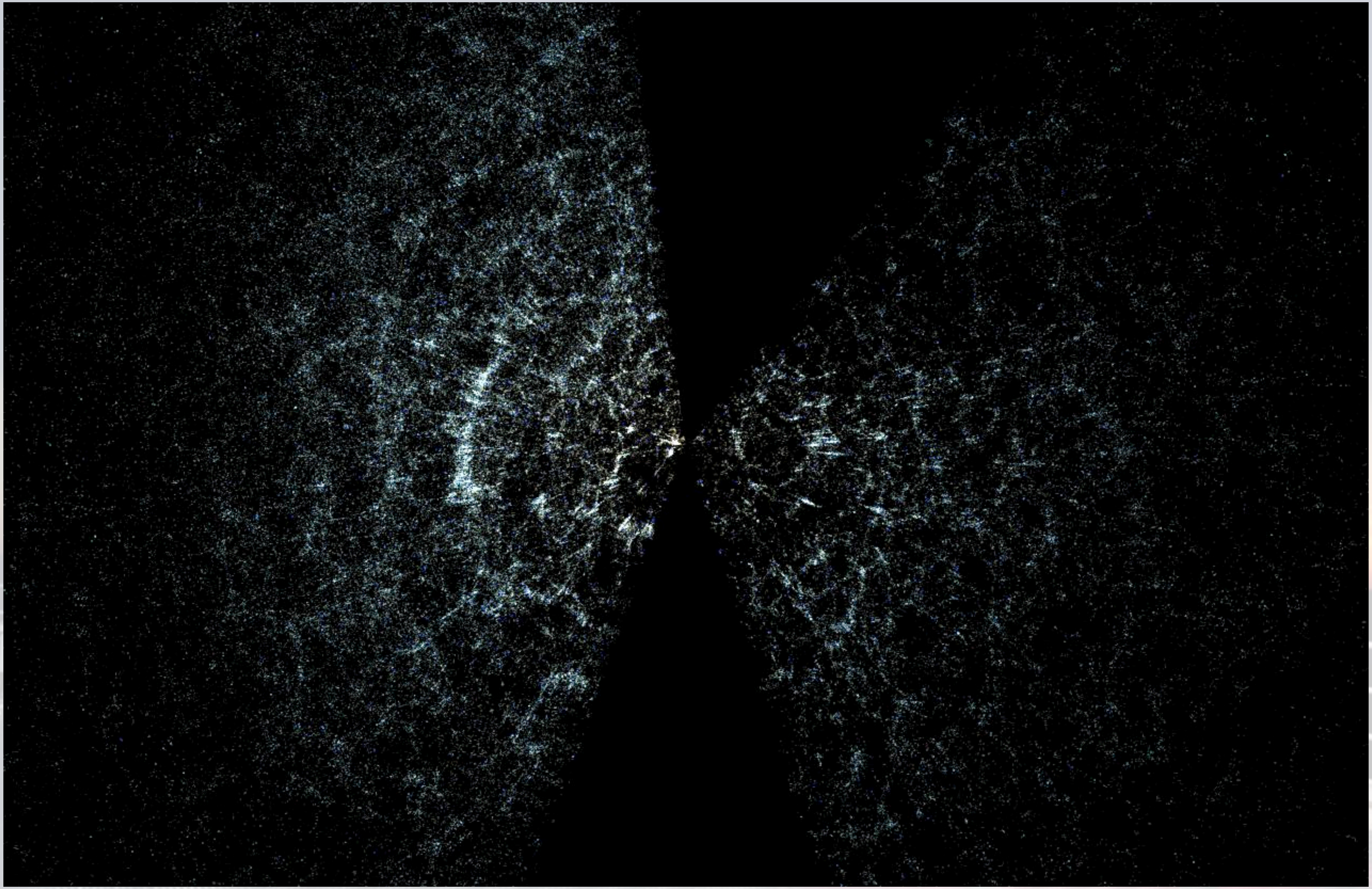

Image of SDSS, from U. Chicago

Linear plane-parallel redshift-space

Transition from real to redshift space, with peculiar velocity v **in units of the Hubble flow**

$$\mathbf{s} = \mathbf{r} + v_{\rm los}\hat{\mathbf{r}}_{\rm los}$$

$$\begin{aligned}\mu &= cos(\alpha)\\ \theta &= \nabla \cdot \mathbf{u}\end{aligned}$$

Jacobian for transformation

$$\frac{d^3s}{d^3r} = \left(1 + \frac{v_{\rm los}}{r_{\rm los}}\right)^2 \left(1 + \frac{dv_{\rm los}}{dr_{\rm los}}\right)$$

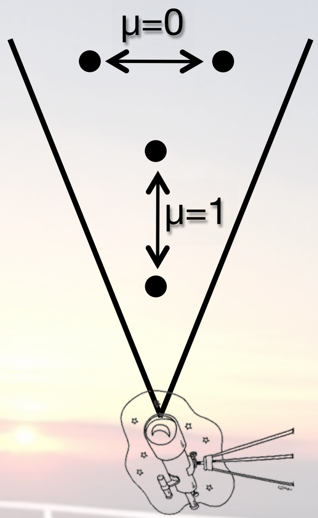

Conservation of galaxy number

$$n^r(\mathbf{r})d^3r = n^s(\mathbf{s})d^3s \qquad 1 + \delta_g^s = (1 + \delta_g^r)\frac{d^3r}{d^3s}\frac{\bar{n}^r(\mathbf{r})}{\bar{n}^s(\mathbf{s})}$$

Trick to understand velocity field derivative

$$\frac{\partial v_{\rm los}}{\partial r_{\rm los}} = \left(\frac{\partial}{\partial r_{\rm los}}\right)^2 \nabla^{-2}\theta = \left(\frac{k_{\rm los}}{k}\right)^2 \theta = \mu^2\theta, \;\; \theta = \nabla \cdot \mathbf{v}$$

Gives to first order

$$\delta_g^s = \delta_g^r - \mu^2\theta$$

Kaiser 1987, MNRAS, 227, 1

what do linear z-space distortions measure?

linear scales,

$$\begin{aligned} \delta_g^s(\mu) &= \delta_g + \mu^2\theta \\ P_g^s(\mu) &= \langle|\delta_g + \mu^2\theta|^2\rangle \\ &= P_{gg} + 2\mu^2 P_{g\theta} + \mu^4 P_{\theta\theta} \end{aligned}$$

$$\begin{aligned} \mu &= cos(\alpha) \\ \theta &= \nabla\cdot\mathbf{u} \end{aligned}$$

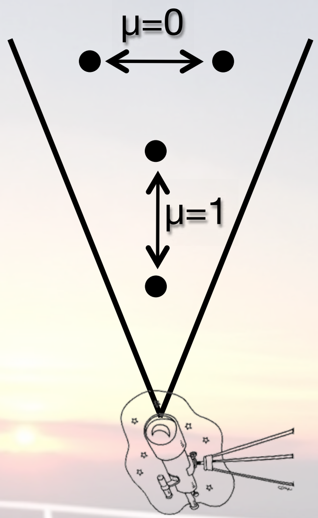

Galaxy-galaxy power

Velocity-velocity power

Galaxy-velocity divergence cross power

In linear regime

$$\delta_g = b\delta(\text{mass}),\ \ \theta = -f\delta(\text{mass}),\ \ f \equiv \frac{d\ln G}{d\ln a}$$

Linear growth rate

So, the simplest model for the power spectrum is

$$P_g^s(k,\mu) = \left[b + \mu^2 f\right]^2 P_{\text{mass}}(k)$$

Kaiser 1987, MNRAS, 227, 1

Modeling redshift space distortions

Include model for both “regimes”

$$P_g^s(k,\mu) = \left[P_{gg}(k) + 2\mu^2 P_{g\theta}(k) + \mu^4 P_{\theta\theta}(k)\right] F(k,\mu^2)$$

Note that non-linear model is not necessarily more accurate then the linear one. If we assume linear bias

$$P_g^s(k,\mu) = P_m^r(k)\left[b^2 + 2\mu^2 f b + \mu^4 f^2\right] F(k,\mu^2)$$

On small scales, galaxies lose all knowledge of initial position. If pairwise velocity dispersion has an exponential distribution (superposition of Gaussians), then we get this damping term for the power spectrum.

$$F(k,\mu^2) = (1 + k^2\mu^2\sigma_p^2/2)^{-1}$$

Modeling redshift space distortions

Alternative for the data is to try to “correct” the data by “collapsing the clusters”

- Velocity dispersion of the Luminous Red Galaxies (LRGs) shifts them along the line of sight by ~ 9 h^{-1}Mpc, and the distribution of intrahalo velocities has long tails.

- Use an asymmetric “friends-of-friends” (FOF) finder to match galaxies in the same clusters, and collapse to spherical profile

- Parameters of FOF calculated by matching simulations

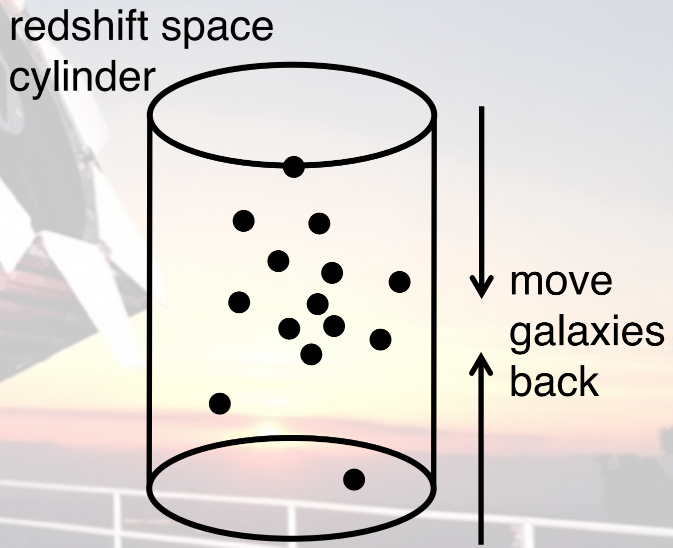

Reid et al. 2008, arXiv:0811.1025; Reid et al. 2009, arXiv:0907.1659

Cosmology improved with RSD

- Anisotropic clustering allows huge improvement on w!
- w = -0.95 ± 0.25 (WMAP + $D_V(0.57)/r_s$)
- w = -0.88 ± 0.055 (WMAP + anisotropic)
- Provided a number of GR tests

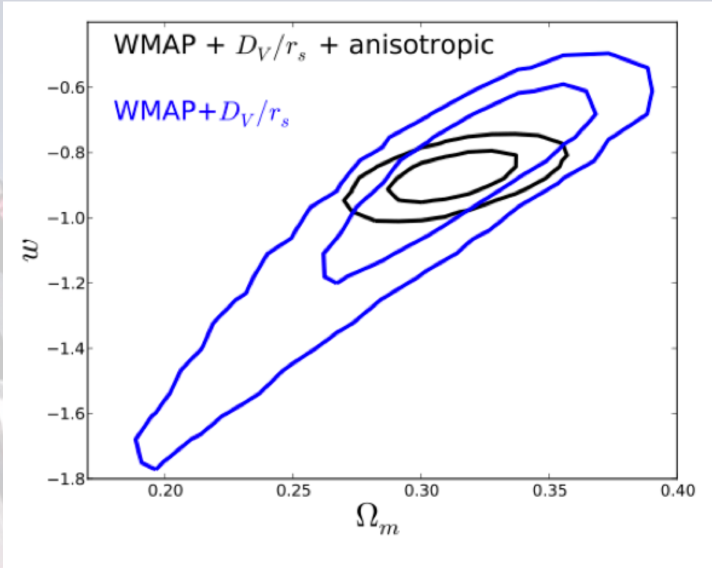

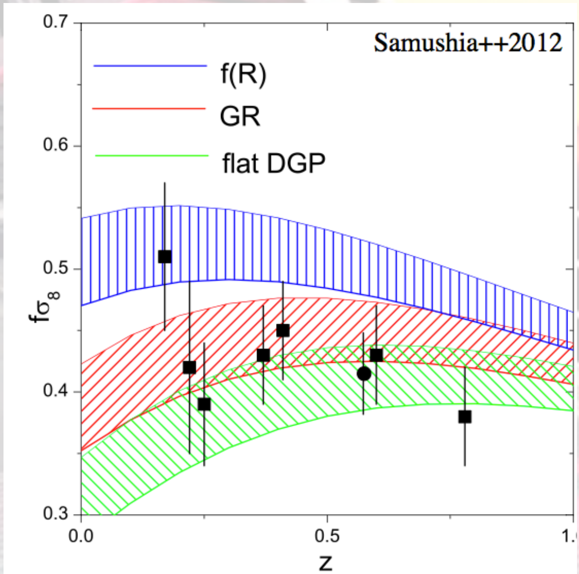

Samushia et al. 2012; arXiv:1206.5309

The Alcock-Paczynski Effect

The Alcock-Paczynski Effect

- If the Universe is isotropic, clustering is same radial & tangential
- Stretching at a single redshift slice (for galaxies expanding with Universe) depends on

  $H^{-1}(z)$ (radial)

  $D_A(z)$ (angular)

- Analyze with wrong model -> see anisotropy
- AP effect measures $D_A(z)H(z)$
- RSD limits test to scales where can be modeled

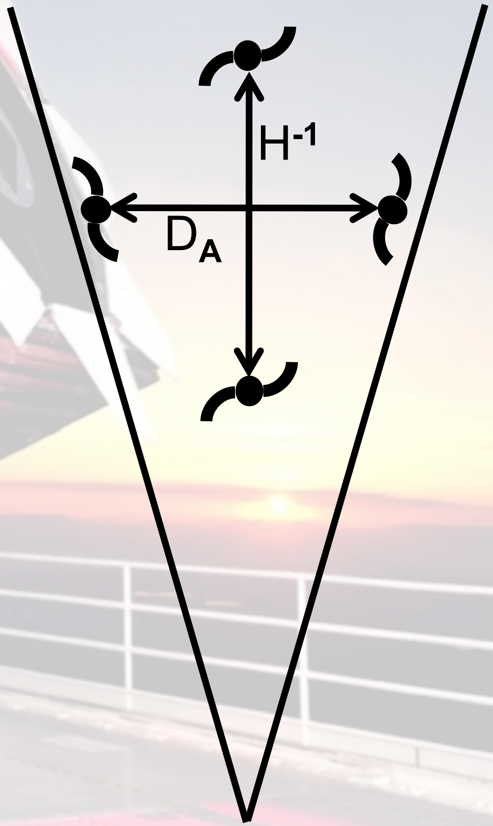

Anisotropic BAO fits …

monopole

$$\xi_2^s(r) = \frac{3}{2}\int_{-1}^{+1} d\mu\ \xi^s(r,\mu)$$

quadrupole

$$\xi_2^s(r) = \frac{5}{2}\int_{-1}^{+1} d\mu\ \xi^s(r,\mu)\frac{3\mu^2-1}{2}$$

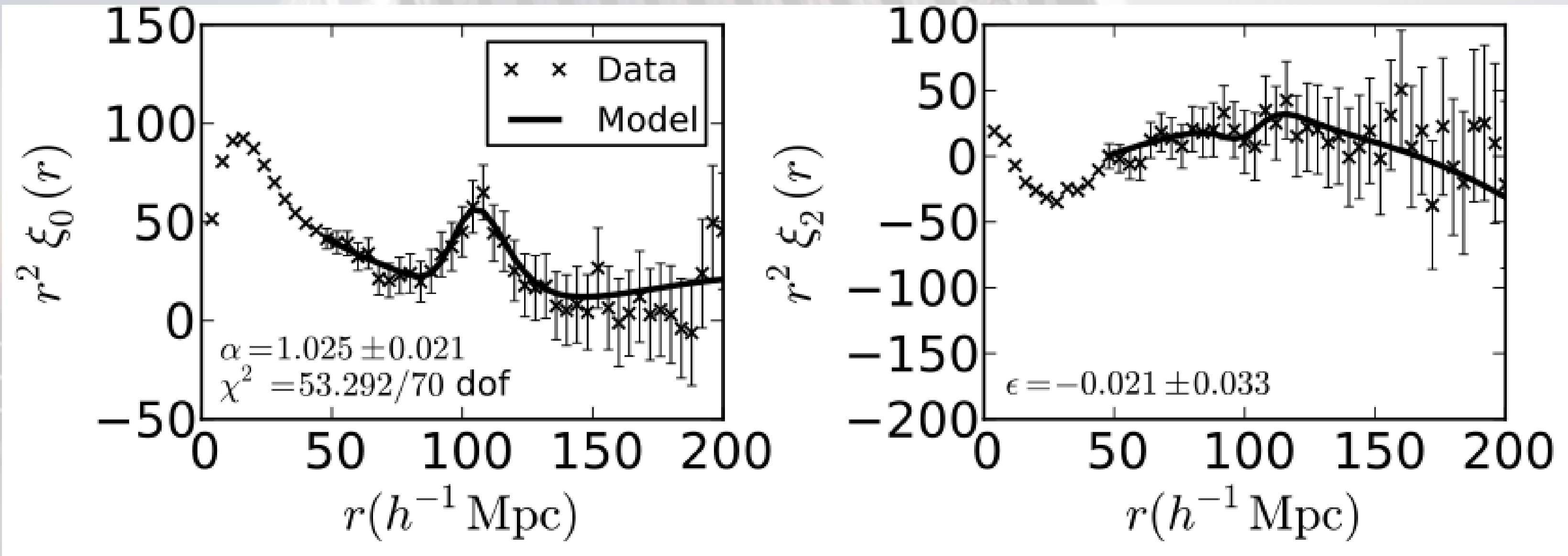

Anderson et al. 2013; arXiv:1303.4666

Anisotropic BAO fits …

	$D_A(z)(r_s^{\rm fid}/r_s)$	$H(z)(r_s/r_s^{\rm fid})$	$\rho_{D_A H}$
	Before Reconstruction		
$(\xi_0(s), \xi_2(s))$	1367 ± 44	86.6 ± 6.2	0.65
$(\xi_\perp(s), \xi_\parallel(s))$	1379 ± 42	88.3 ± 5.1	0.52
	After Reconstruction		
$(\xi_0(s), \xi_2(s))$	1424 ± 43	95.4 ± 7.5	0.63
$(\xi_\perp(s), \xi_\parallel(s))$	1386 ± 36	90.6 ± 6.7	0.50
Consensus	1408 ± 45	92.9 ± 7.8	0.55

- correlation function is easier to split into line-of-sight and transverse directions
- can decompose into multipoles or other bases (e.g. wedges – see Kazin et al. 2013)
- Results are consistent and a concordance value is given

Anderson et al. 2013; arXiv:1303.4666

Anisotropic BAO measurements vs CMB

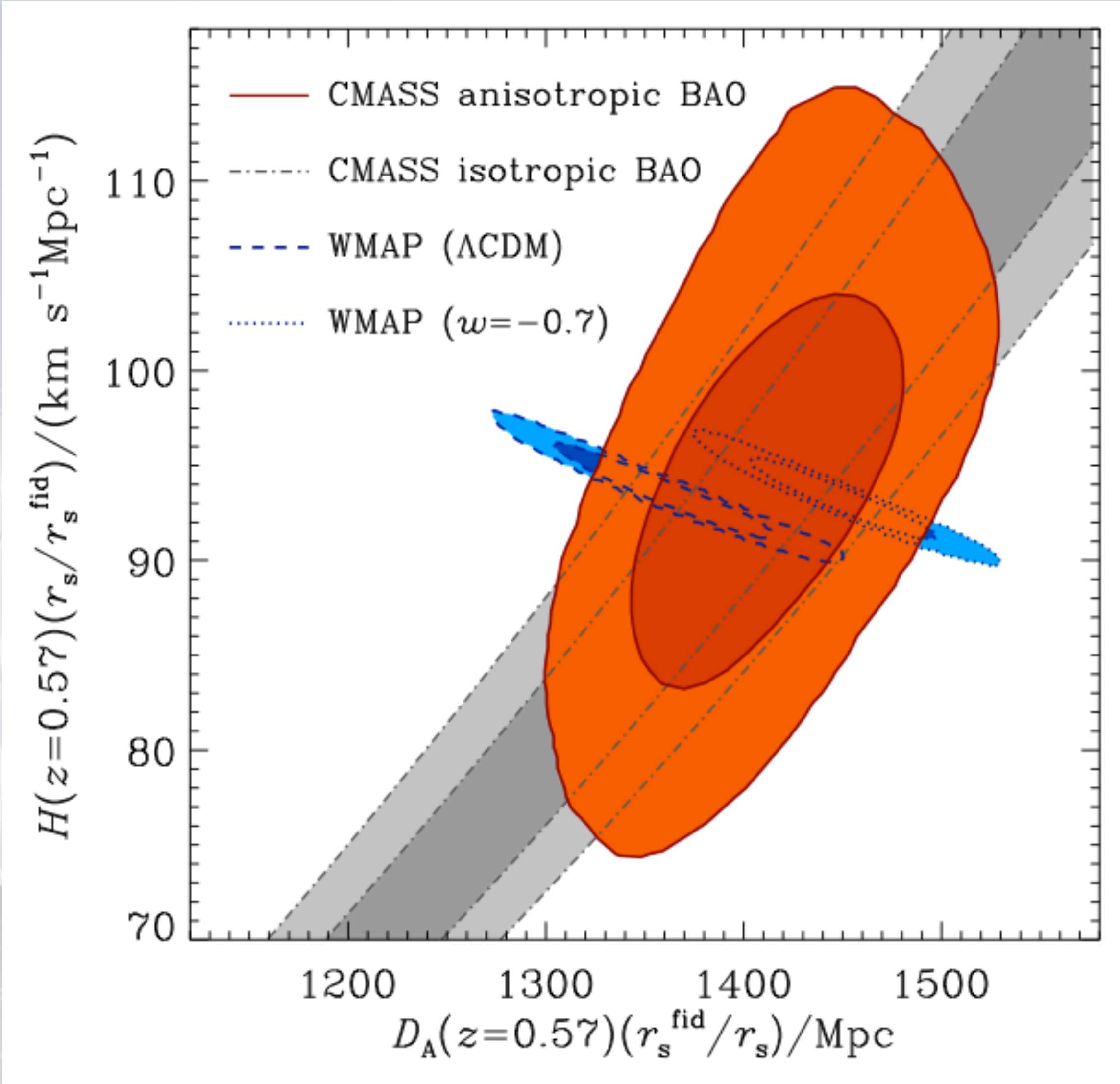

Anderson et al. 2013; arXiv:1303.4666

Can we use the AP effect on small scales?

use isolated galaxy pairs

Marinoni & Buzzi 2011

Nature 468, 539

Jennings et al. 2012

MNRAS 420, 1079

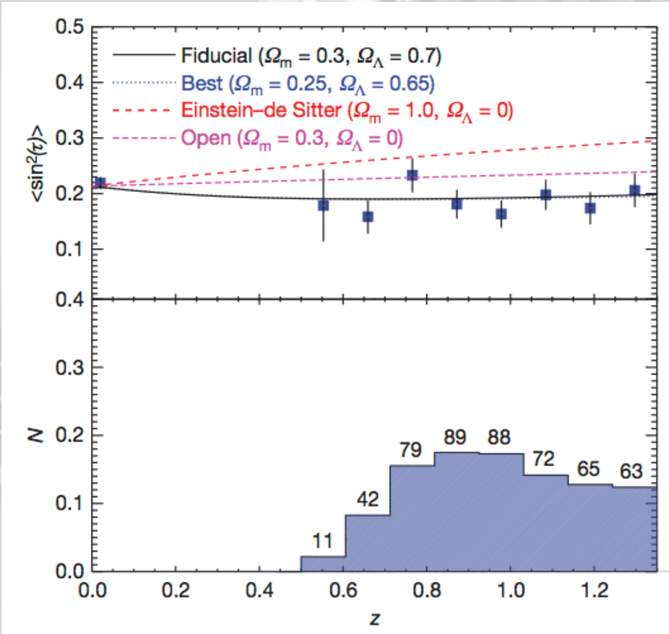

use voids

Lavaux & Wandelt 2011

arXiv:1110.0345

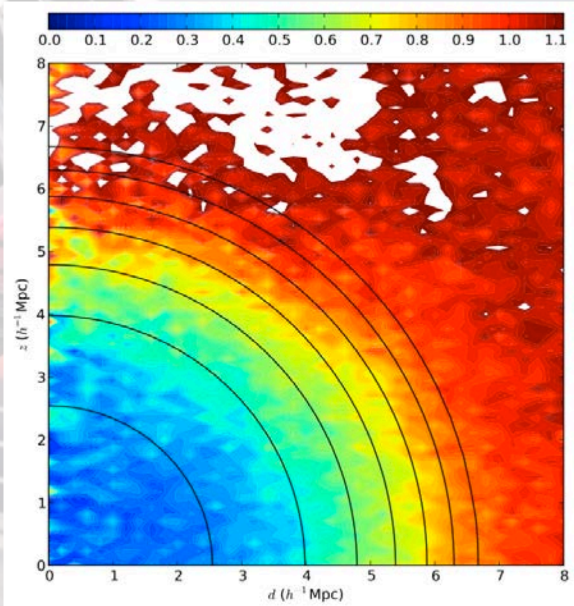

Both try to isolate objects where the RSD signal is known or weak

Collapsed structures

Live in static region of space-time

Velocity from growth exactly cancels Hubble expansion

Two static galaxies in same structure have same observed redshift irrespective of distance from us

Redshift difference only tells us properties of system

Two collapsed similar regions observed in different background cosmologies give same Δz

No cosmological information from Δz

Cannot be used for AP tests

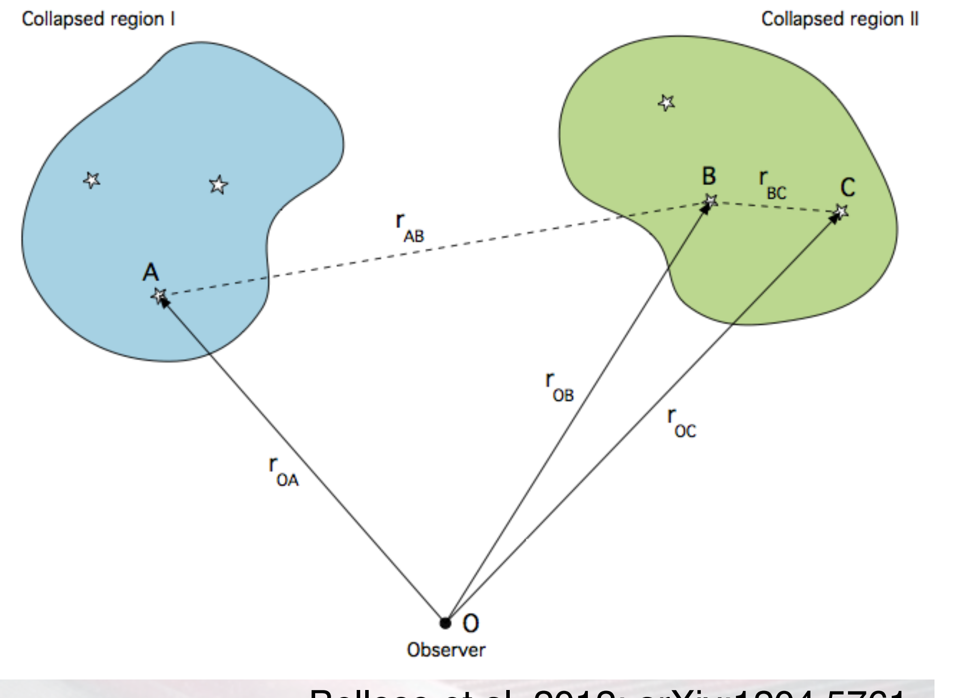

Belloso et al. 2012: arXiv:1204.5761

Large-scale RSD & AP measurements

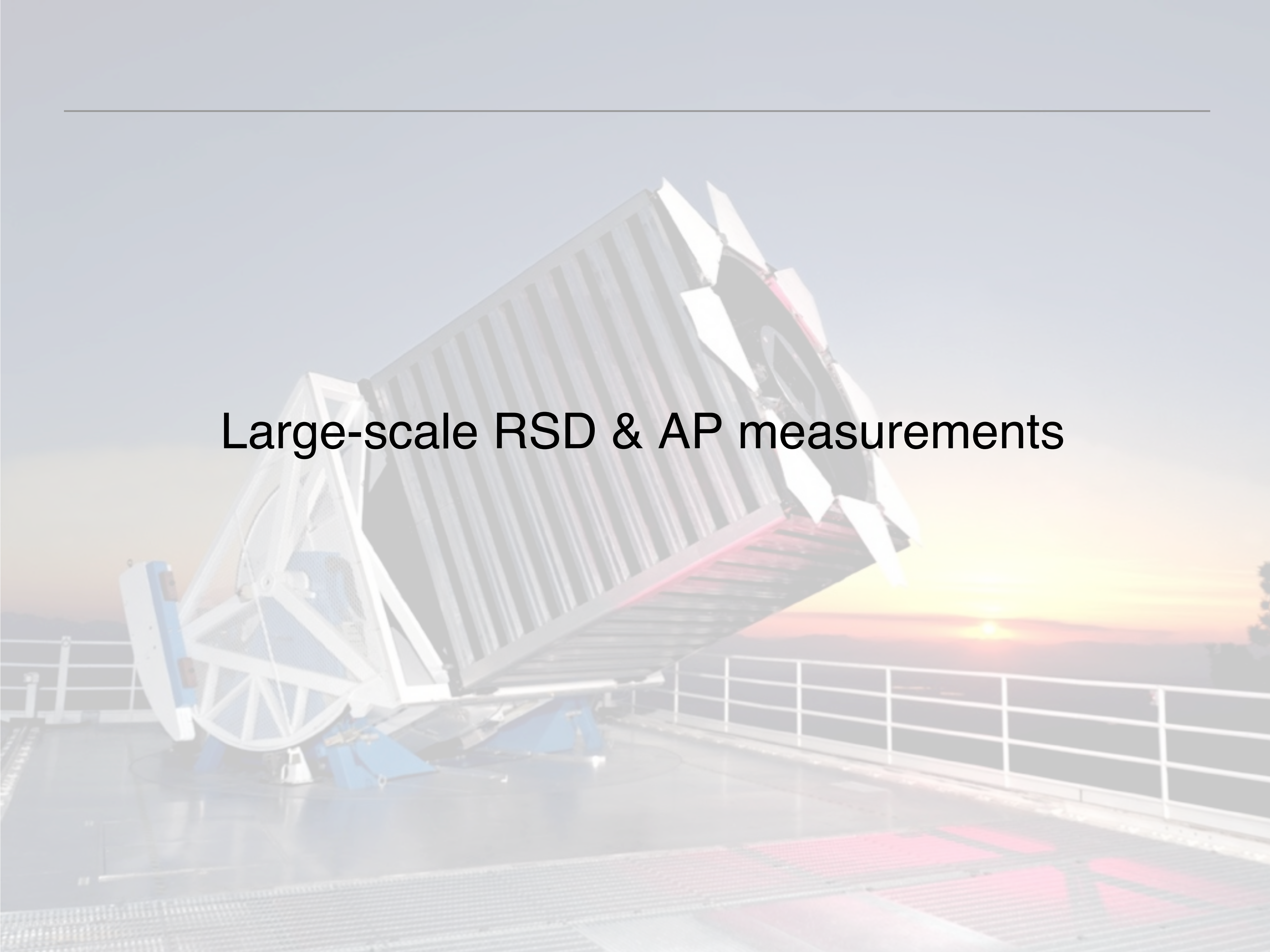

Linking z-space distortions and BAO

We should allow for the coupling between the redshift-space distortions and the geometrical squashing caused by getting the geometry wrong. Effects are not perfectly degenerate

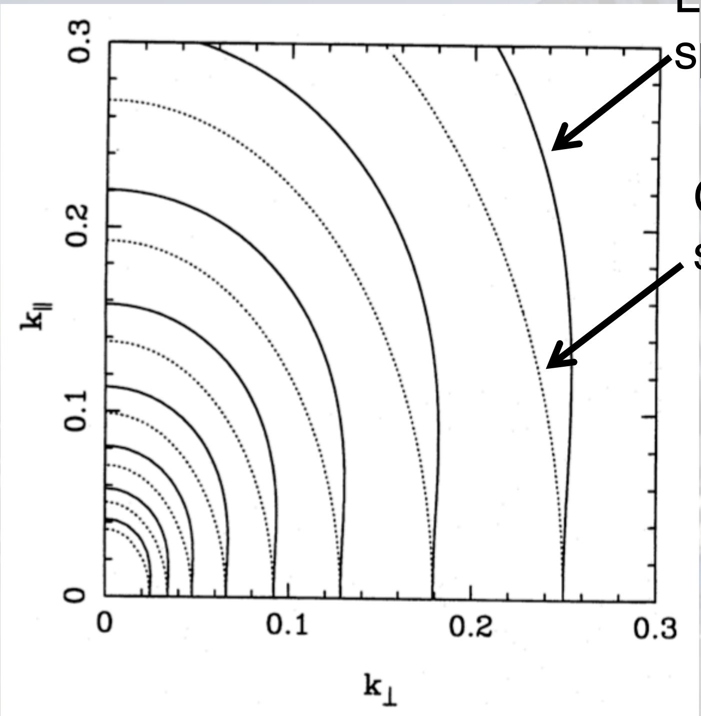

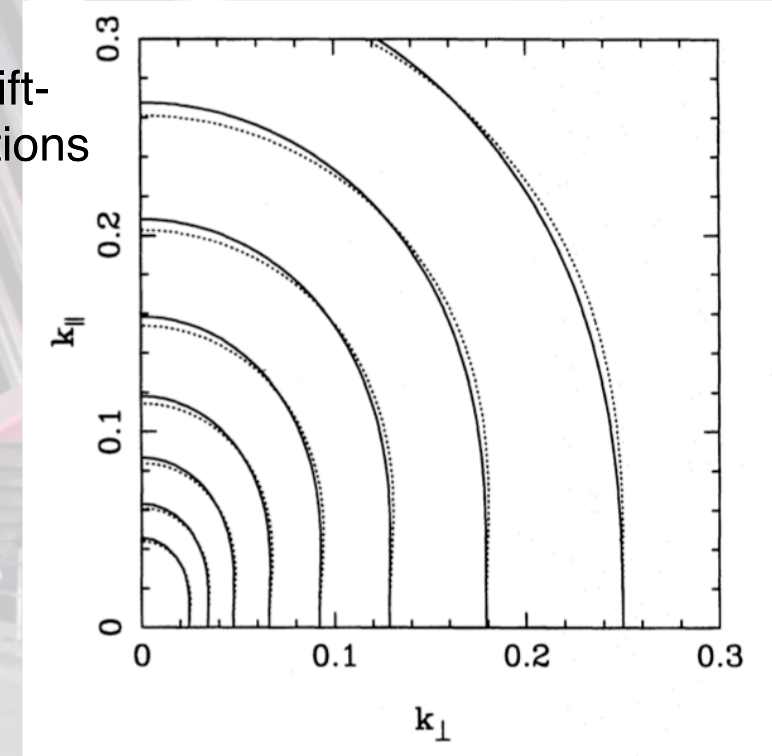

Fit to redshift-space distortions cannot mimic geometric squashing

Ballinger, Peacock & Heavens 1999, MNRAS, 282, 877

Measuring F & fσ_8

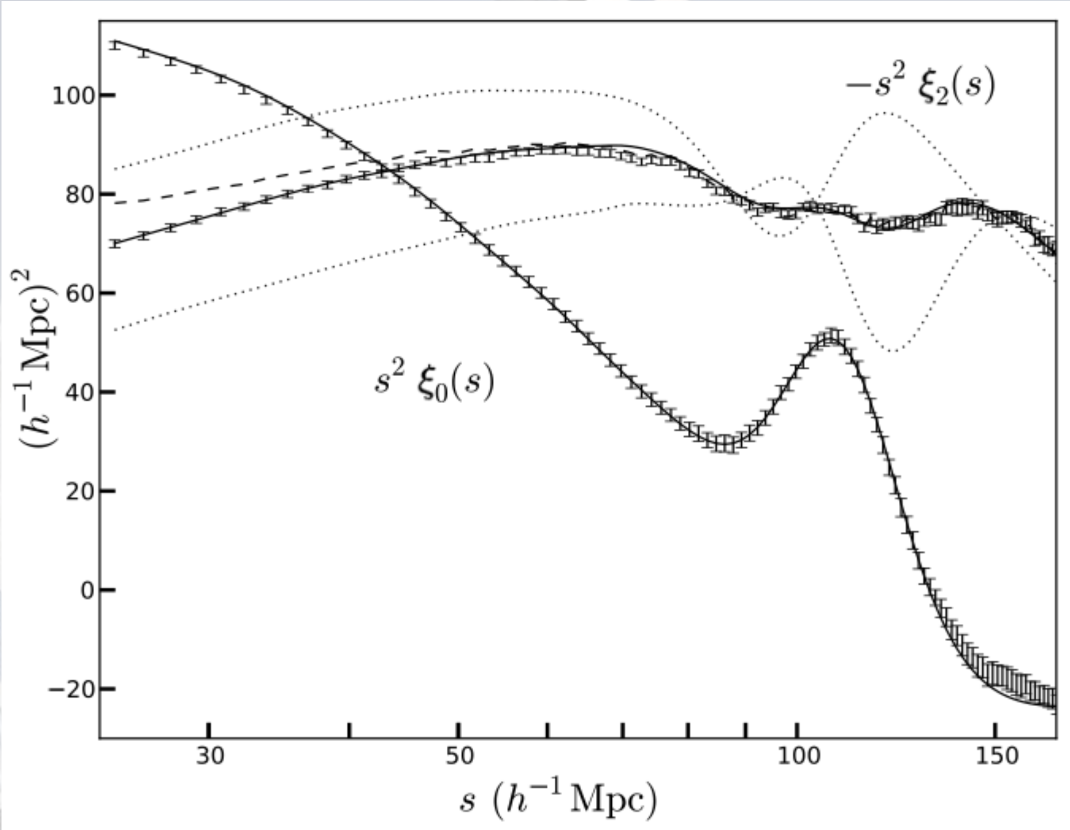

Varying F by 10%, while keeping D_V fixed

Scale-dependence of F variations allows measurements of F & fσ_8 to be separated

Reid et al. 2012; arXiv:1203.6641

Degradation of RSD measurements by AP effect

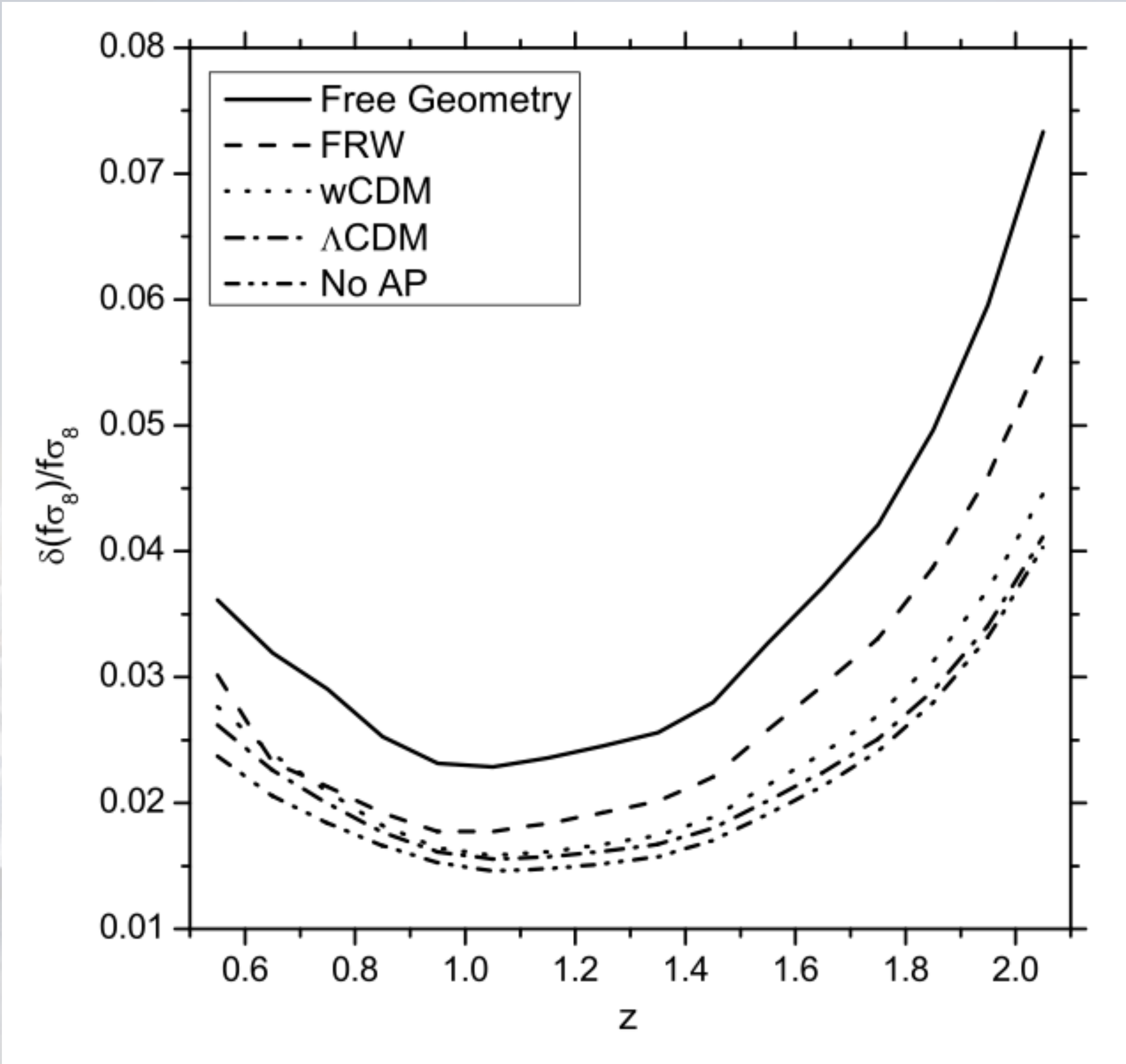

Samushia et al 2011, 410, 1993

BOSS AP & RSD measurement degeneracy

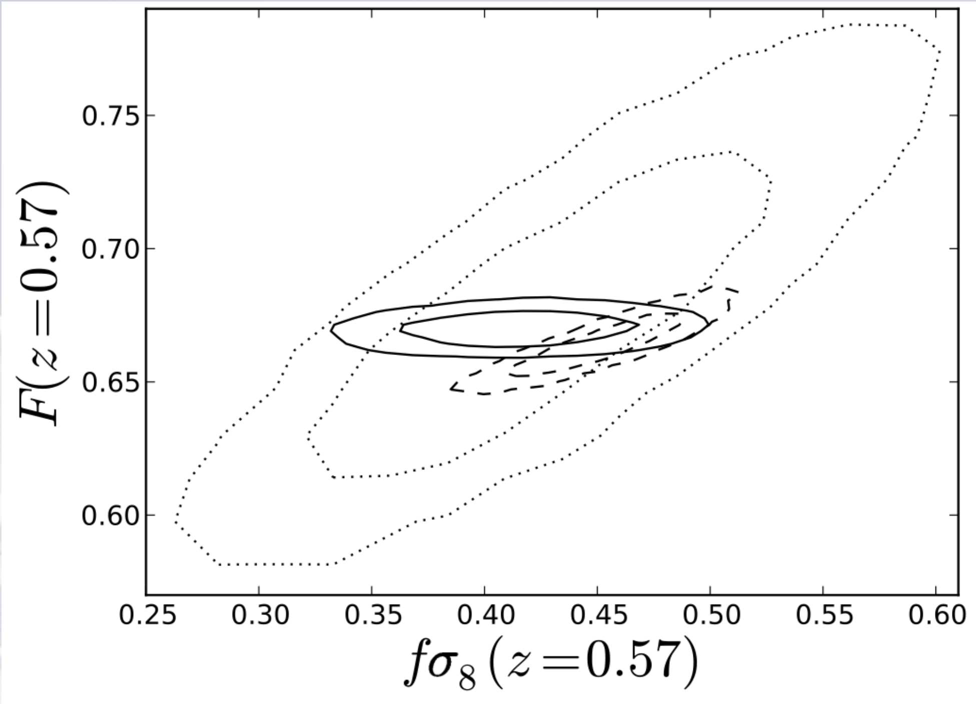

Dotted: free growth, geometry, ΛCDM prior on large-scale linear P(k) shape at z=0.57

Solid: F forced to match ΛCDM model

Dashed: WMAP ΛCDM+GR prediction

Reid et al. 2012; arXiv:1203.6641

BOSS F measurements in context

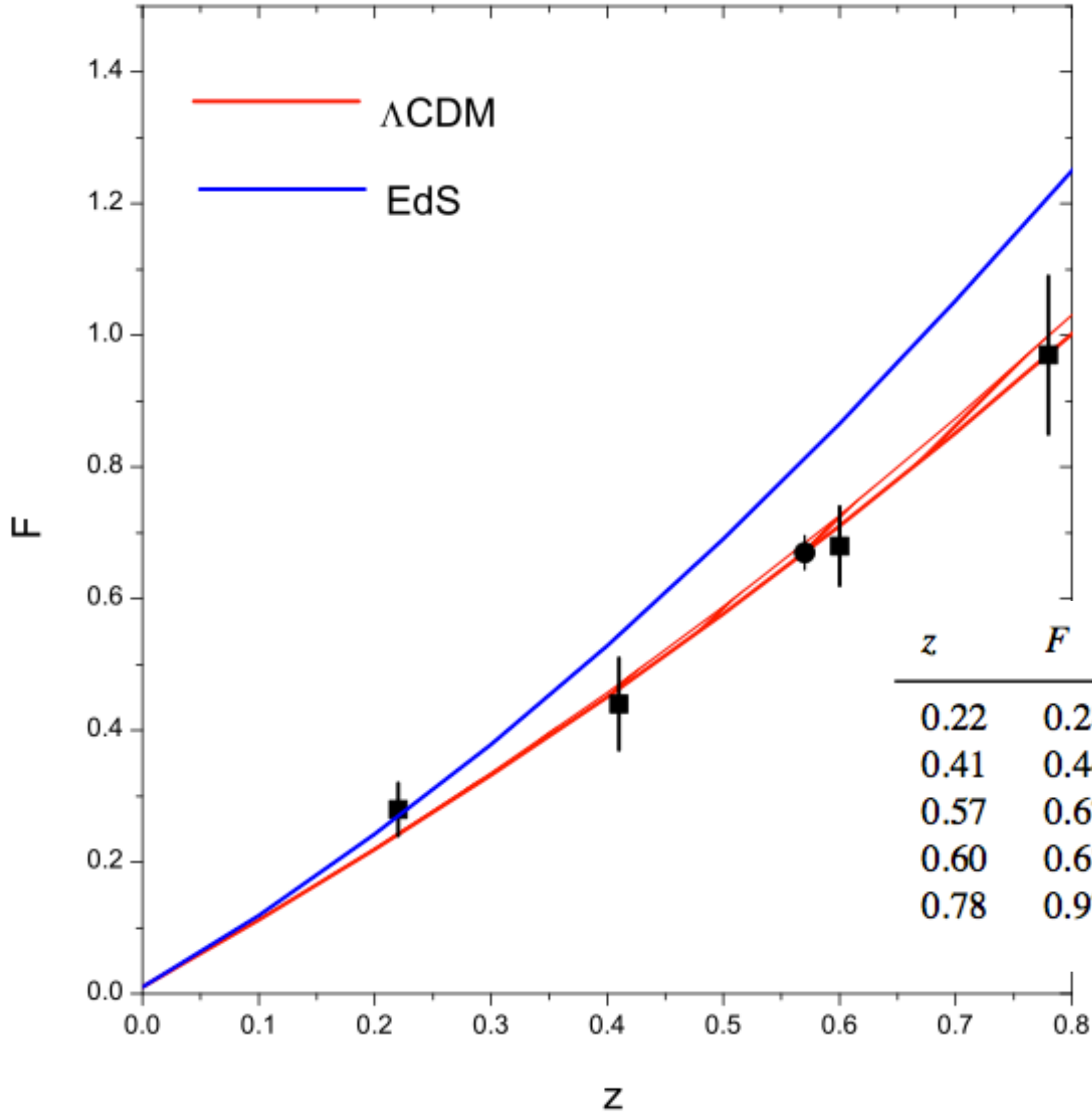

z	F	survey	reference
0.22	0.28 ± 0.04	WiggleZ	Blake, et al. (2011c)
0.41	0.44 ± 0.07	WiggleZ	Blake, et al. (2011c)
0.57	0.67 ± 0.026	BOSS	Reid et al. (2012)
0.60	0.68 ± 0.06	WiggleZ	Blake, et al. (2011c)
0.78	0.97 ± 0.12	WiggleZ	Blake, et al. (2011c)

Samushia et al. 2012; arXiv:1206.5309

BOSS RSD measurements in context

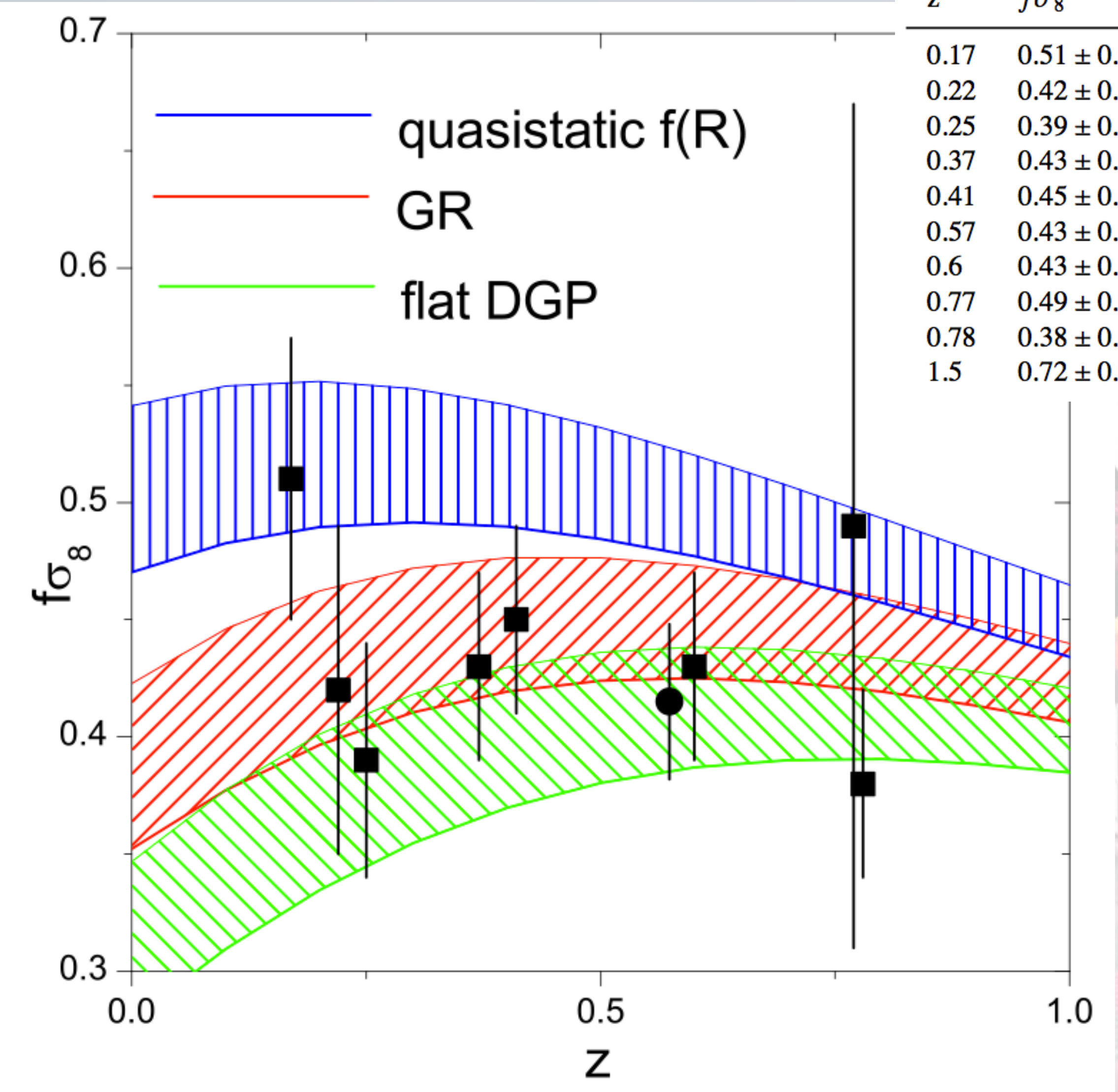

z	$f\sigma_8$	survey	reference
0.17	0.51 ± 0.06	2dFGRS	Percival et al. (2004)
0.22	0.42 ± 0.07	WiggleZ	Blake, et al. (2011b)
0.25	0.39 ± 0.05	SDSS	Samushia, Percival, & Raccanelli (2011)
0.37	0.43 ± 0.04	SDSS	Samushia, Percival, & Raccanelli (2011)
0.41	0.45 ± 0.04	WiggleZ	Blake, et al. (2011b)
0.57	0.43 ± 0.03	BOSS	Reid et al. (2012)
0.6	0.43 ± 0.04	WiggleZ	Blake, et al. (2011b)
0.77	0.49 ± 0.18	VVDS	Guzzo et al. (2007)
0.78	0.38 ± 0.04	WiggleZ	Blake, et al. (2011b)
1.5	0.72 ± 0.15	2SLAQ	da Angela et al. (2008)

Samushia et al. 2012; arXiv:1206.5309

Primordial non-Gaussianity

Measuring primordial non-Gaussianity: f_{NL} g_{NL}

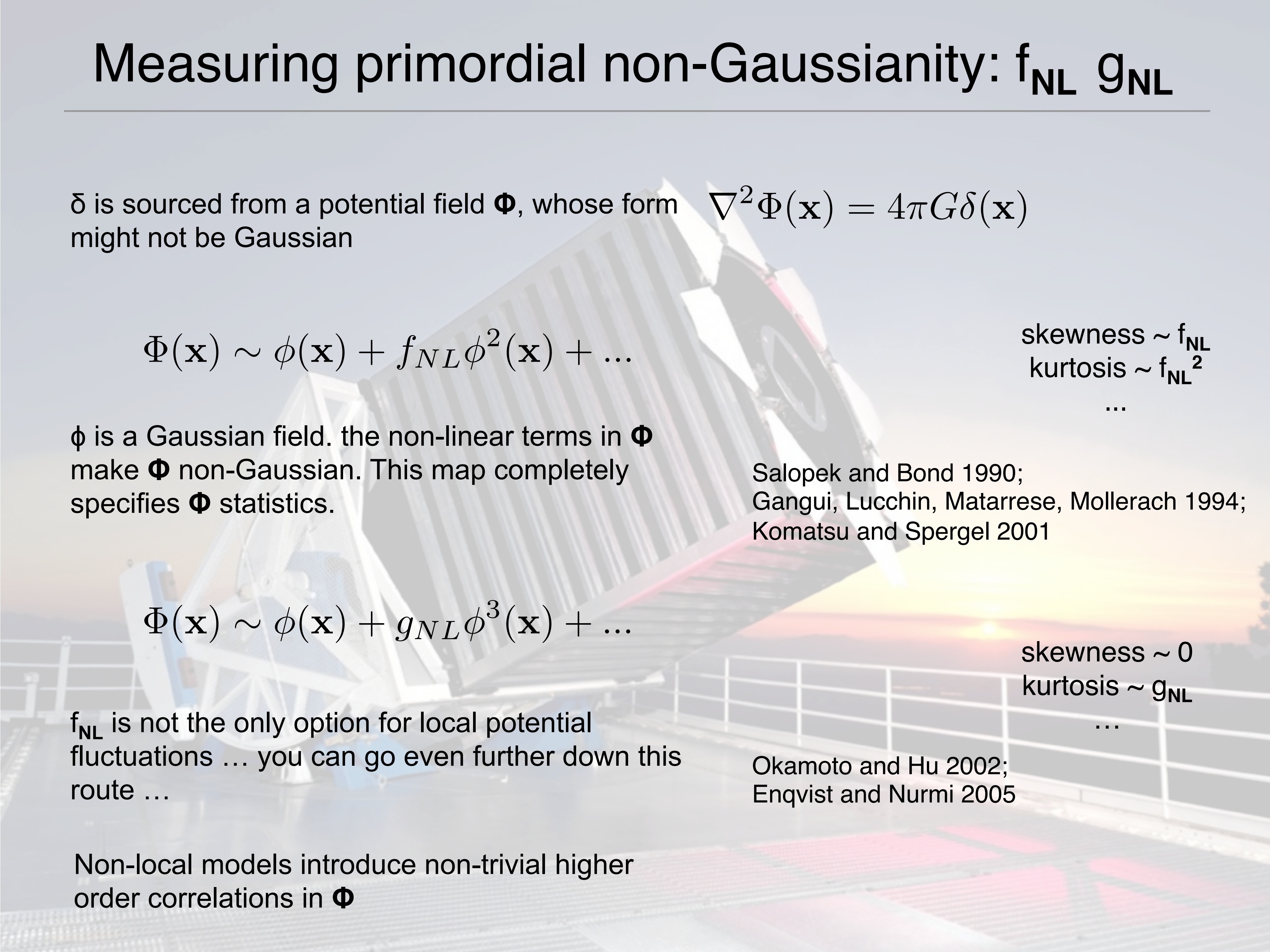

δ is sourced from a potential field **Φ**, whose form might not be Gaussian

$$\nabla^2 \Phi(\mathbf{x}) = 4\pi G \delta(\mathbf{x})$$

$$\Phi(\mathbf{x}) \sim \phi(\mathbf{x}) + f_{NL}\phi^2(\mathbf{x}) + ...$$

skewness ~ f_{NL}
kurtosis ~ f_{NL}^2
...

ϕ is a Gaussian field. the non-linear terms in **Φ** make **Φ** non-Gaussian. This map completely specifies **Φ** statistics.

Salopek and Bond 1990;
Gangui, Lucchin, Matarrese, Mollerach 1994;
Komatsu and Spergel 2001

$$\Phi(\mathbf{x}) \sim \phi(\mathbf{x}) + g_{NL}\phi^3(\mathbf{x}) + ...$$

skewness ~ 0
kurtosis ~ g_{NL}
…

f_{NL} is not the only option for local potential fluctuations … you can go even further down this route …

Okamoto and Hu 2002;
Enqvist and Nurmi 2005

Non-local models introduce non-trivial higher order correlations in **Φ**

Measuring non-Gaussianity: halo abundance

Dark matter halos form in the peaks of the density field

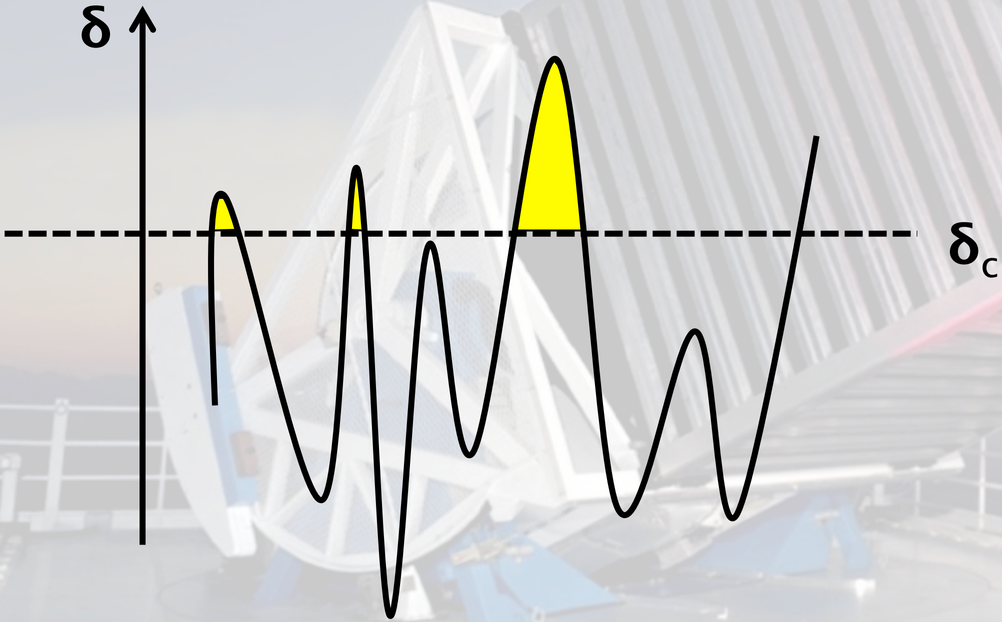

Non-Gaussianity changes the number density of the peaks

This in turn affects the halo mass function

Measuring non-Gaussianity: halo abundance

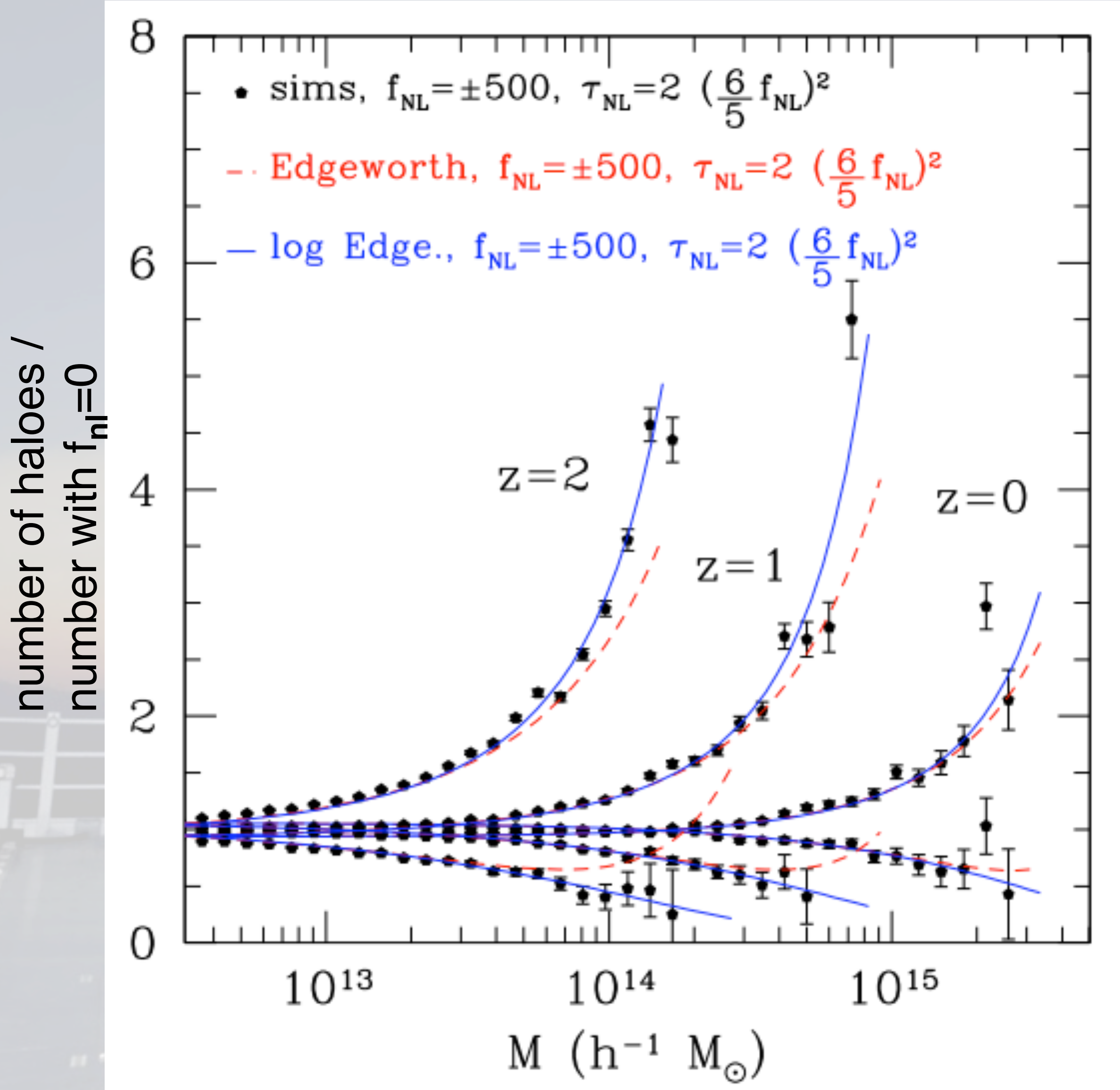

Largest effect is seen at highest masses

Insensitive to shape of bispectrum

But difficult to observe – relies on cluster masses being precisely known

LoVerde & Smith 2011, arXiv:1102.1439

Peak-background split bias model

Halo formation much easier with additional long-wavelength fluctuation

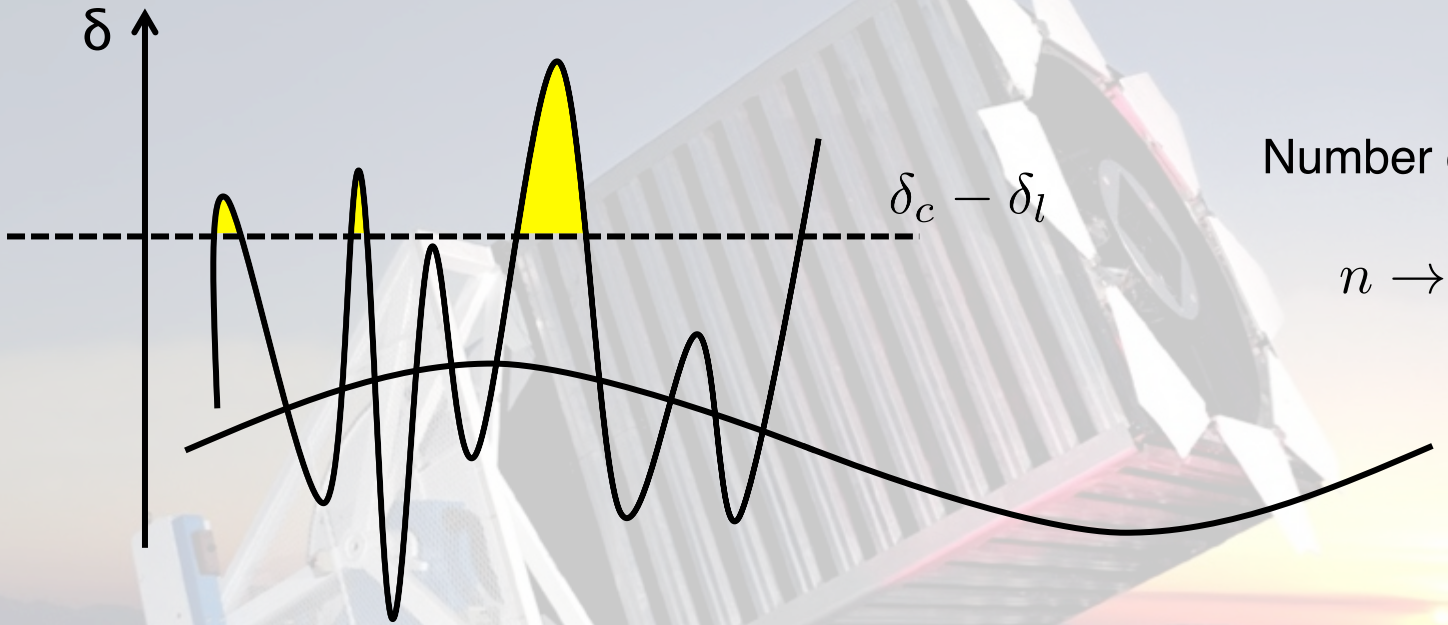

Number density of halos

$$n \to n - \frac{dn}{d\delta_c}\delta_l$$

Leads to a revised density $$(1+\delta_{\rm new}) = \left(1 + \frac{\Delta n}{n}\right)(1+\delta_l)$$

Directly from the large-scale mode

From the change in Number of haloes

To first order, this leads to a bias

$$\delta_{\rm new} = \left(\delta_l + \frac{\Delta n}{n}\right) \qquad b = \frac{\delta_{\rm new}}{\delta_l} = 1 + \frac{\Delta n}{n\delta_l} = 1 - \frac{d\ln n}{d\delta_c}$$

Peak-background split galaxy bias model

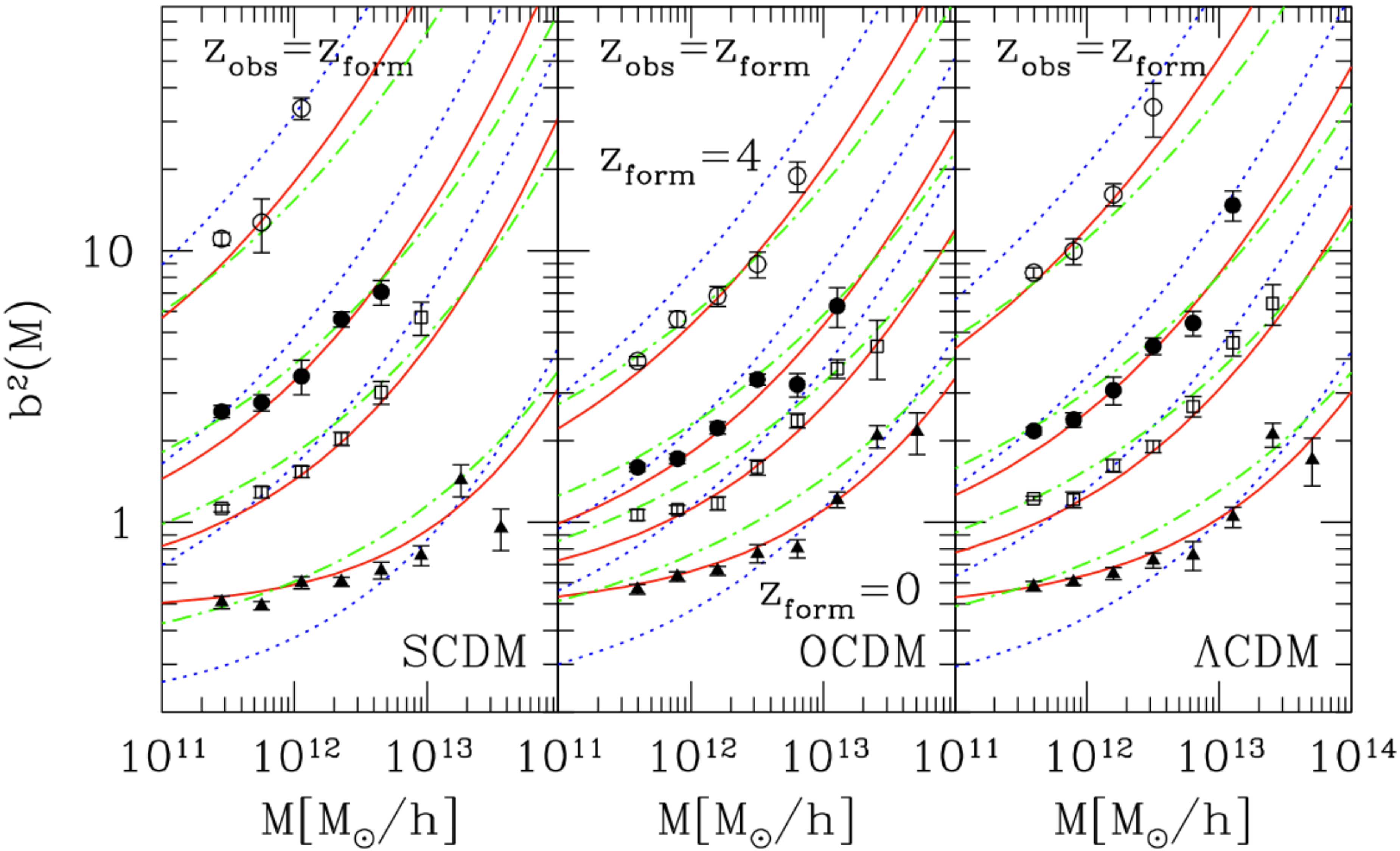

Sheth & Tormen 1999, arXiv:9901122

This is altered by f_{NL} signal

Now split non-Gaussian potential into long and short wavelength components

$$\Phi(\mathbf{x}) = \phi_l + \underbrace{f_{NL}\phi_l^2}_{\text{small}} + (1 + \underbrace{2 f_{NL}\phi_l}_{})\phi_s + f_{NL}\phi_s^2 + \mathrm{cnst}$$

Link between potential and overdensity field shows how changing long wavelength potential component changes “critical density”

$$\delta_l(k) = \alpha(k)\Phi(k) \quad \alpha(k) = \frac{2c^2k^2T(k)D(z)}{3\Omega_m H_0^2}$$

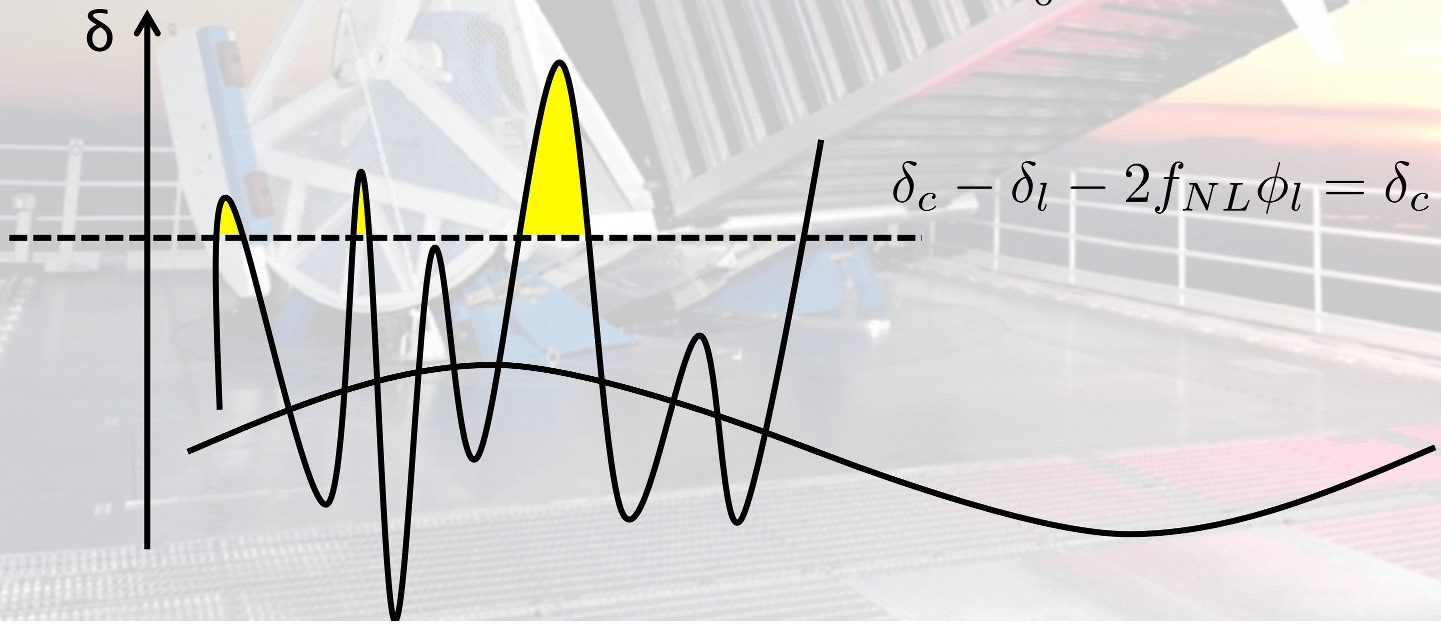

$$\delta_c - \delta_l - 2f_{NL}\phi_l = \delta_c - \delta_l\left(1 + \frac{2f_{NL}}{\alpha(k)}\right)$$

Peak-background split for non-Gaussianity

Halo formation much easier with additional long-wavelength fluctuation

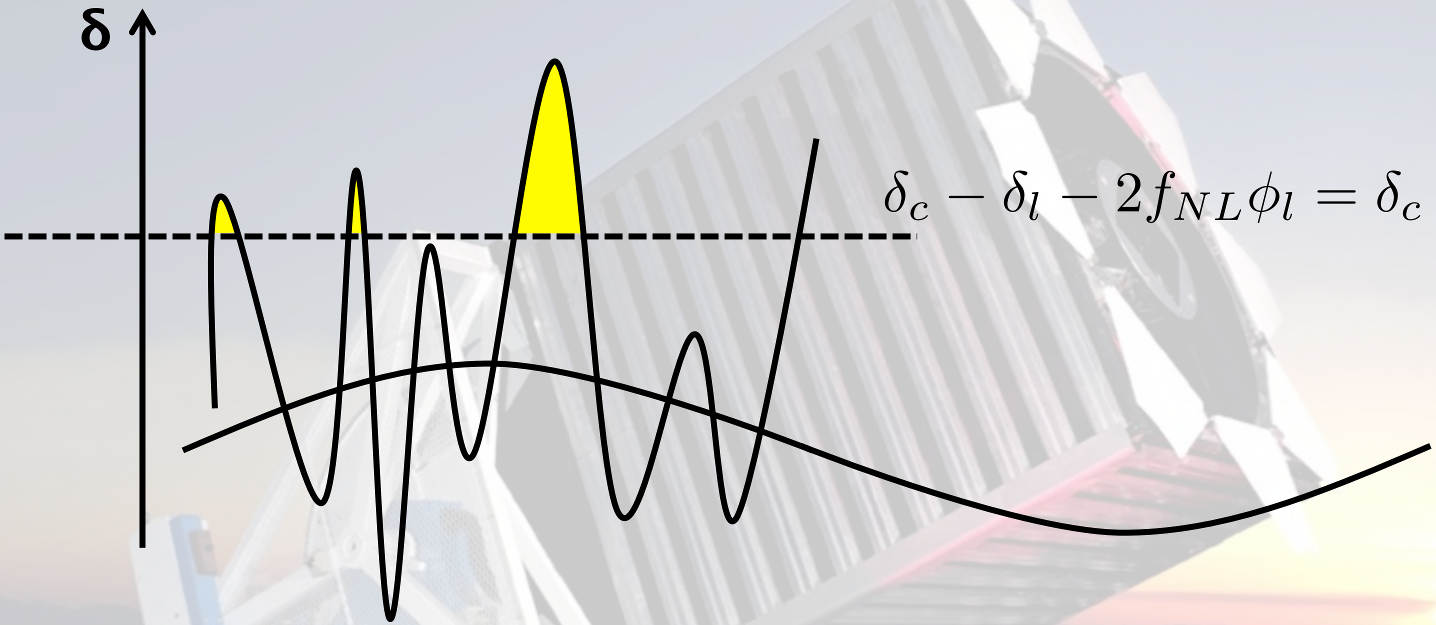

$$\delta_c - \delta_l - 2f_{NL}\phi_l = \delta_c - \delta_l \left(1 + \frac{2f_{NL}}{\alpha(k)}\right)$$

Number density of halos $$n \to n - \left(1 + \frac{2f_{NL}}{\alpha(k)}\right) \frac{dn}{d\delta_c}\delta_l$$

Leads to a revised bias

$$b = 1 - \left(1 + \frac{2f_{NL}}{\alpha(k)}\right) \frac{d\ln n}{d\delta_c}$$

K² dependence in simulations

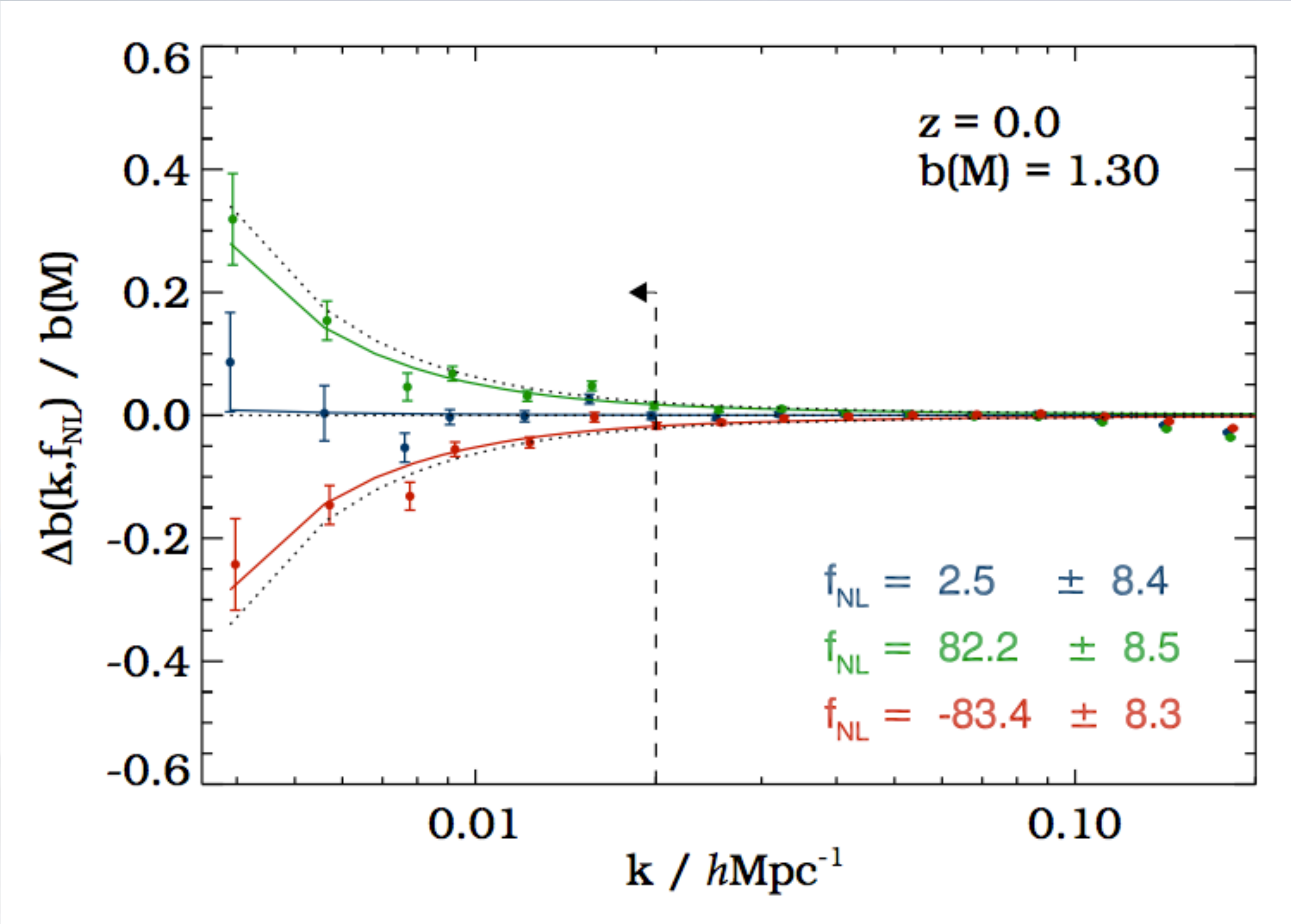

Dalal, Doré, Huterer, Shirokov 2007 ; Smith, LoVerde 2010; Smith, Ferraro, LoVerde 2011; Pillepich, Porciani, Hahn 2008; Desjacques, Seljak, Iliev 2008; Grossi et al 2009; Shandera, Dalal, Huterer 2010; Hamaus et al. 2011

Model testing with data

Bayes theory

Modern observational cosmology relies on Bayes theory

H … Hypothesis to be tested, often a vector of parameters θ
I … Things assumed to be true (e.g. model)
d … Data

sampling distribution of data
often called the Likelihood

$$\mathcal{L}(H) \equiv p(d|H, I)$$

prior

$$p(H|d, I) = \frac{p(d|H, I)p(H|I)}{p(d|I)}$$

posterior probability

normalisation

Assuming θ=(ϕ,ψ), with ϕ interesting and ψ not, **parameter inference** is performed as

$$p(\theta|d, I) \propto \int \mathcal{L}(\phi, \psi)p(\phi, \psi|I)d\psi$$

e.g. review by Trotta 2008; arXiv:0803.4089

Model parameters (describing LSS & CMB)

content of the Universe

total energy density
Ω_{tot} (=1?)
matter density
Ω_m
baryon density
Ω_b
neutrino density
Ω_n (=0?)
Neutrino species
f_n
dark energy eq^n of state
$w(a)$ (=-1?)
or **w_0, w_1**

perturbations after inflation

scalar spectral index
n_s (=1?)
normalisation
σ_8
running
$a = dn_s/dk$ (=0?)
tensor spectral index
n_t (=0?)
tensor/scalar ratio
r (=0?)

evolution to present day
Hubble parameter
h
Optical depth to CMB
τ

parameters usually marginalised and ignored
galaxy bias model
$b(k)$ (=cst?)
or **b,Q**
CMB beam error
B
CMB calibration error
C

Assume Gaussian, adiabatic fluctuations

Multi-parameter fits to multiple data sets

- Given CMB data, other data are used to help break degeneracies (although CMB is now doing a pretty good job by itself) and understand dark energy

- Main problem is keeping a handle on what is being constrained and why
  – difficult to allow for systematics
  – you have to believe all of the data!

- Have two sets of parameters
  – those you fix (part of the prior)
  – those you vary

- Need to define a prior
  – what set of models
  – what prior assumptions to make on them (usual to use uniform priors on physically motivated variables)

- Need a sampling method for exploring multi-dimensional parameter space

degeneracies: CMB

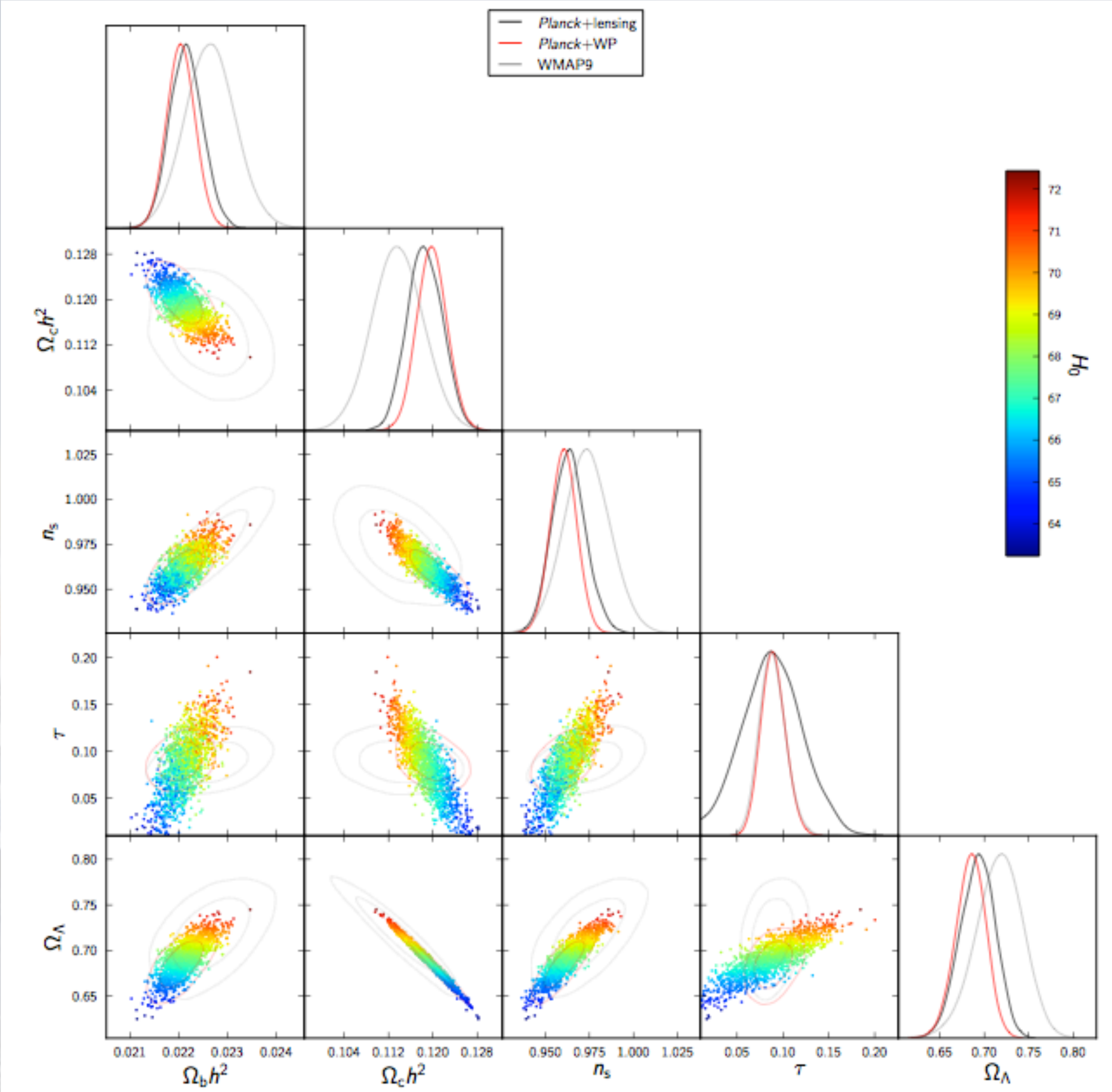

Planck collaboration 2013; arXiv:1303.5076

degeneracies: CMB

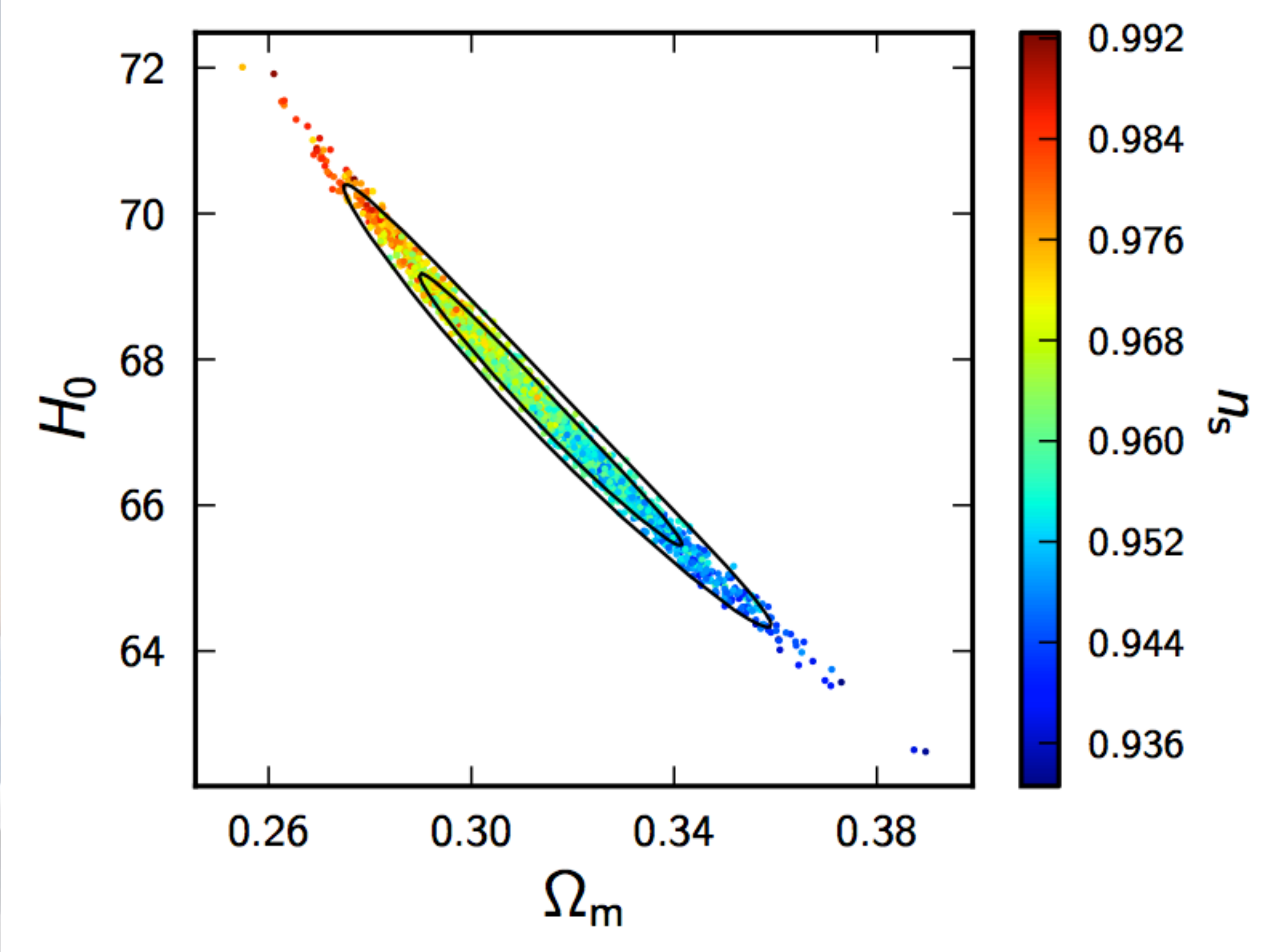

Planck collaboration 2013; arXiv:1303.5076

degeneracies: CMB

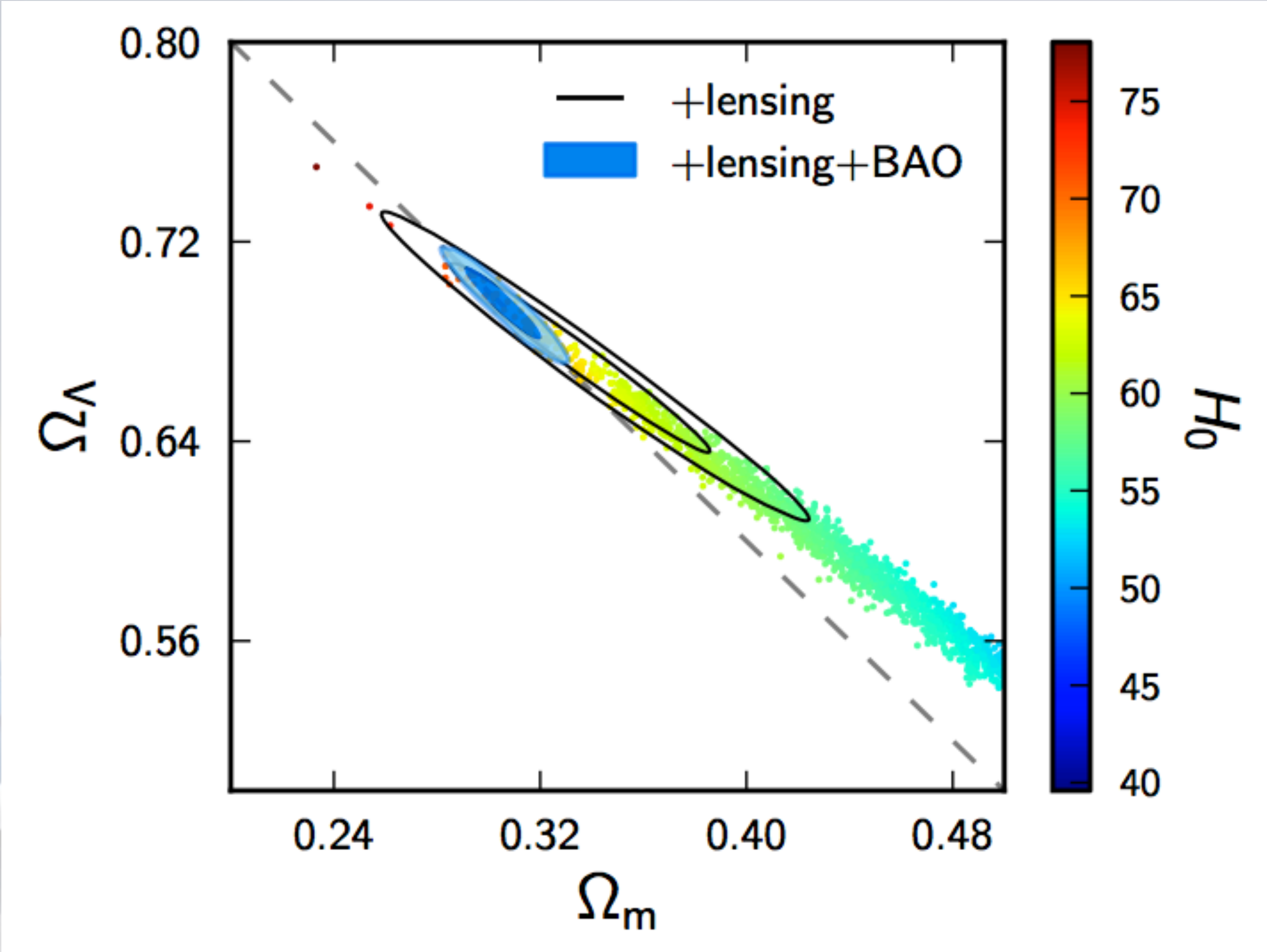

Planck collaboration 2013; arXiv:1303.5076

Bayesian model selection

A lot of the big questions to be faced by future experiments can be reduced to:

Is the most simple model (e.g. Λ) correct?

Bayes theory can test the balance between quality of fit and predictivity

A model with more parameters will always fit the data better than a model with less parameters (provided it replicates the original model).

But does the improvement show the parameter is needed?

$$p(H|d,I) = \frac{p(d|H,I)p(H|I)}{p(d|I)}$$

Bayesian evidence

Bayesian evidence is average of Likelihood under the prior. Splitting into model and parameters

$$p(d|I) = \int_\theta p(d|\theta,M)p(\theta|M)d\theta$$

e.g. review by Trotta 2008; arXiv:0803.4089

Bayesian model selection

Bayes factor is ratio of evidence for 2 models

$$B_{01} = \frac{p(d|I_0)}{p(d|I_1)}$$

Jeffries scale

$\lvert \ln B_{01} \rvert$	Odds	Probability	Strength of evidence
< 1.0	$\lesssim 3:1$	< 0.750	Inconclusive
1.0	$\sim 3:1$	0.750	Weak evidence
2.5	$\sim 12:1$	0.923	Moderate evidence
5.0	$\sim 150:1$	0.993	Strong evidence

Problem: depends on prior on new parameter. More stringent criteria can be set

Other options are available … about a lecture's worth!

e.g. review by Trotta 2008; arXiv:0803.4089

Future surveys: next 4-6 years

Dark Energy Survey (DES)

- New wide-field camera on the 4m Blanco telescope
- Survey started, with first data in hand
- $\Omega = 5{,}000\mathrm{deg}^2$
- multi-colour optical imaging (g,r,i,z) with link to IR data from VISTA hemisphere survey
- 300,000,000 galaxies
- Aim is to constrain dark energy using 4 probes
  LSS/BAO, weak lensing, supernovae
  cluster number density
- Redshifts based on photometry
  weak radial measurements
  weak redshift-space distortions
- See also: Pan-STARRS, VST-VISTA, SkyMapper

DARK ENERGY SURVEY

eBOSS / SDSS-IV

- The new cosmology project with SDSS
- Use the Sloan telescope and MOS to observe to higher redshift
- Basic parameters
  - Ω = 1,500deg^2 – 7,500deg^2
  - ~ 1,000,000 galaxies (direct BAO)
  - ~ 60,000 quasars (BAO from Ly-α forest)
- Distance measurements
  - 0.9% at z=0.8 (LRGs)
  - 1.8% at z=0.9 (ELGs)
  - 2.0% at z=1.5 (QSOs)
  - 1.1% at z=2.5 (Ly-α forest, inc. BOSS)
- Survey will start 2014, lasting 6 years
- Received $10M from Sloan foundation and significant funding from partners

Future surveys: > 4 years

MOS on 4m-telescope

- New fibre-fed spectroscopes proposed
  for 4m telescopes
  - Mayall (BigBOSS)
  - Blanco (DESpec)

    DESI
  - WHT (WEAVE)
  - VISTA (4MOST)
- Various stages of planning & funding
  - DESI has DOE CD-1 in April
  - 4MOST chosen by ESO, 1-year delay
  - WEAVE waiting for UK/Spain/Holland/France
- All capable of observing
  - Ω =5--14,000deg^2
  - 2--20,000,000 galaxies (direct BAO)
  - 1--600,000 quasars (BAO from Ly-α forest)
  - Cosmic variance limited to z ~ 1.4

MOS on 10m-telescope

- New fibre-fed spectroscopes proposed for 10m telescopes
    - Hobby-Eberly (HETDEX)
    - Subaru (PFS)
- Different baseline strategies
- HETDEX
    - 420deg^2 Ly-alpha emitters
    - 800,000 galaxies $1.9<z<3.5$
    - Greig, Komatsu & Wyithe, 2012, arXiv:12120977
- PFS
    - 1400deg^2 ELGs
    - 3,000,000 galaxies $0.6<z<2.4$
    - Ellis et al., 2012, arXiv:1206.0737

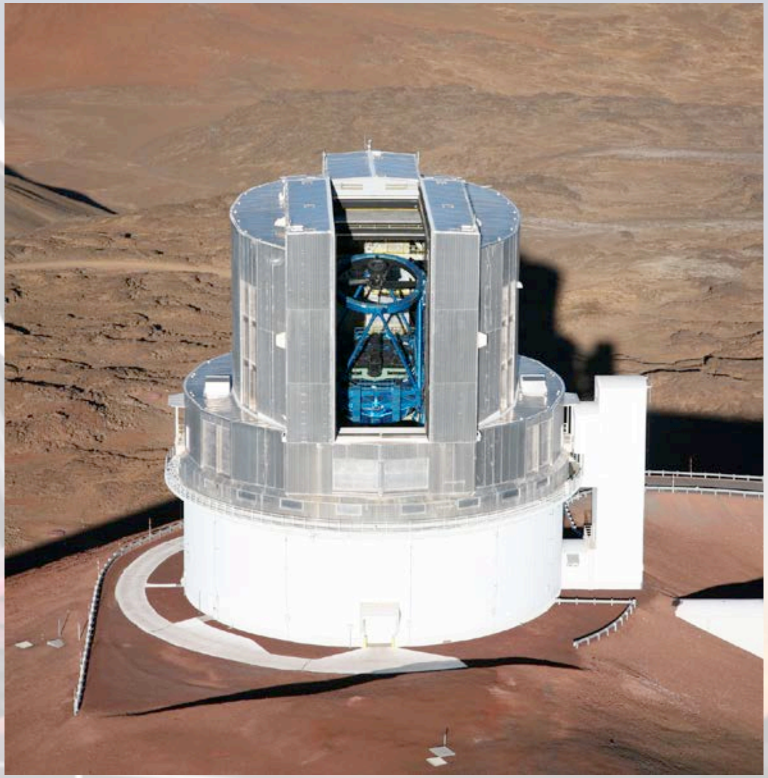

The ESA Euclid Mission

SURVEYS					
	Area (deg2)	Description			
Wide Survey	15,000 (required) 20,000 (goal)	Step and stare with 4 dither pointings per step.			
Deep Survey	40	In at least 2 patches of > 10 deg^2 2 magnitudes deeper than wide survey			
PAYLOAD					
Telescope	1.2 m Korsch, 3 mirror anastigmat, f=24.5 m				
Instrument	VIS	NISP			
Field-of-View	0.787×0.709 deg^2	0.763×0.722 deg^2			
Capability	Visual Imaging	NIR Imaging Photometry			NIR Spectroscopy
Wavelength range	550– 900 nm	Y (920-1146nm),	J (1146-1372 nm)	H (1372-2000nm)	1100-2000 nm
Sensitivity	24.5 mag 10σ extended source	24 mag 5σ point source	24 mag 5σ point source	24 mag 5σ point source	3 10^{-16} erg cm-2 s-1 3.5σ unresolved line flux
Detector Technology	36 arrays 4k×4k CCD	16 arrays 2k×2k NIR sensitive HgCdTe detectors			
Pixel Size Spectral resolution	0.1 arcsec	0.3 arcsec			0.3 arcsec R=250
SPACECRAFT					
Launcher	Soyuz ST-2.1 B from Kourou				
Orbit	Large Sun-Earth Lagrange point 2 (SEL2), free insertion orbit				
Pointing	25 mas relative pointing error over one dither duration 30 arcsec absolute pointing error				
Observation mode	Step and stare, 4 dither frames per field, VIS and NISP common FoV = 0.54 deg^2				
Lifetime	7 years				
Operations	4 hours per day contact, more than one ground station to cope with seasonal visibility variations;				
Communications	maximum science data rate of 850 Gbit/day downlink in K band (26GHz), steerable HGA				

The Euclid spectroscopic survey

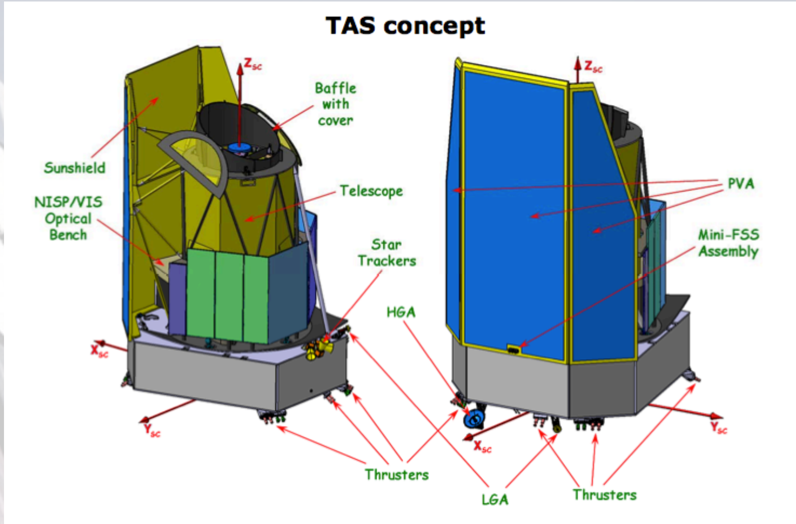

- Wide survey
  - 15,000deg^2
  - 4 dithers
  - NIR Photometry
    - Y, J, H
    - 24mag, 5σ point source
  - NIR slitless spectroscopy
    - 1100-2000nm
    - 3×10^{-16}erg cm^{-2}s^{-1} 3.5σ line flux
    - 3 or 4 dispersion directions, 1 broad wavebands 0.9<z<1.8
    - 45M galaxies

- Deep survey
  - 40deg^2
  - 48 dithers
  - 12 passes, as for wide survey
  - dispersion directions for 12 passes >10deg apart

BAO measurements for future surveys

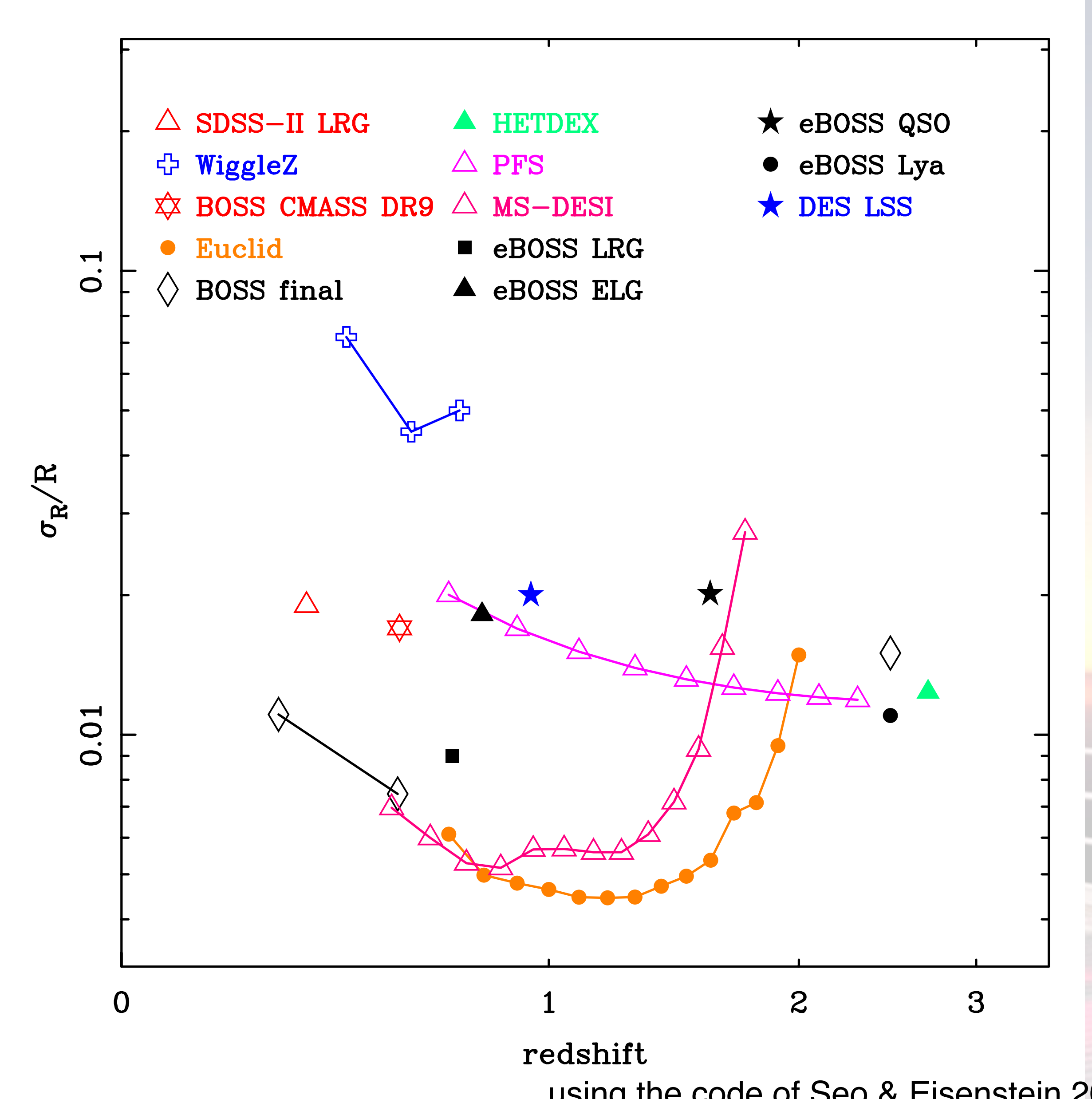

using the code of Seo & Eisenstein 2007, arXiv:0701079

BOSS CMASS DR9 galaxy clustering

BOSS CMASS galaxies at z~0.57

Total effective volume
V_{eff} = 2.2 Gpc^3

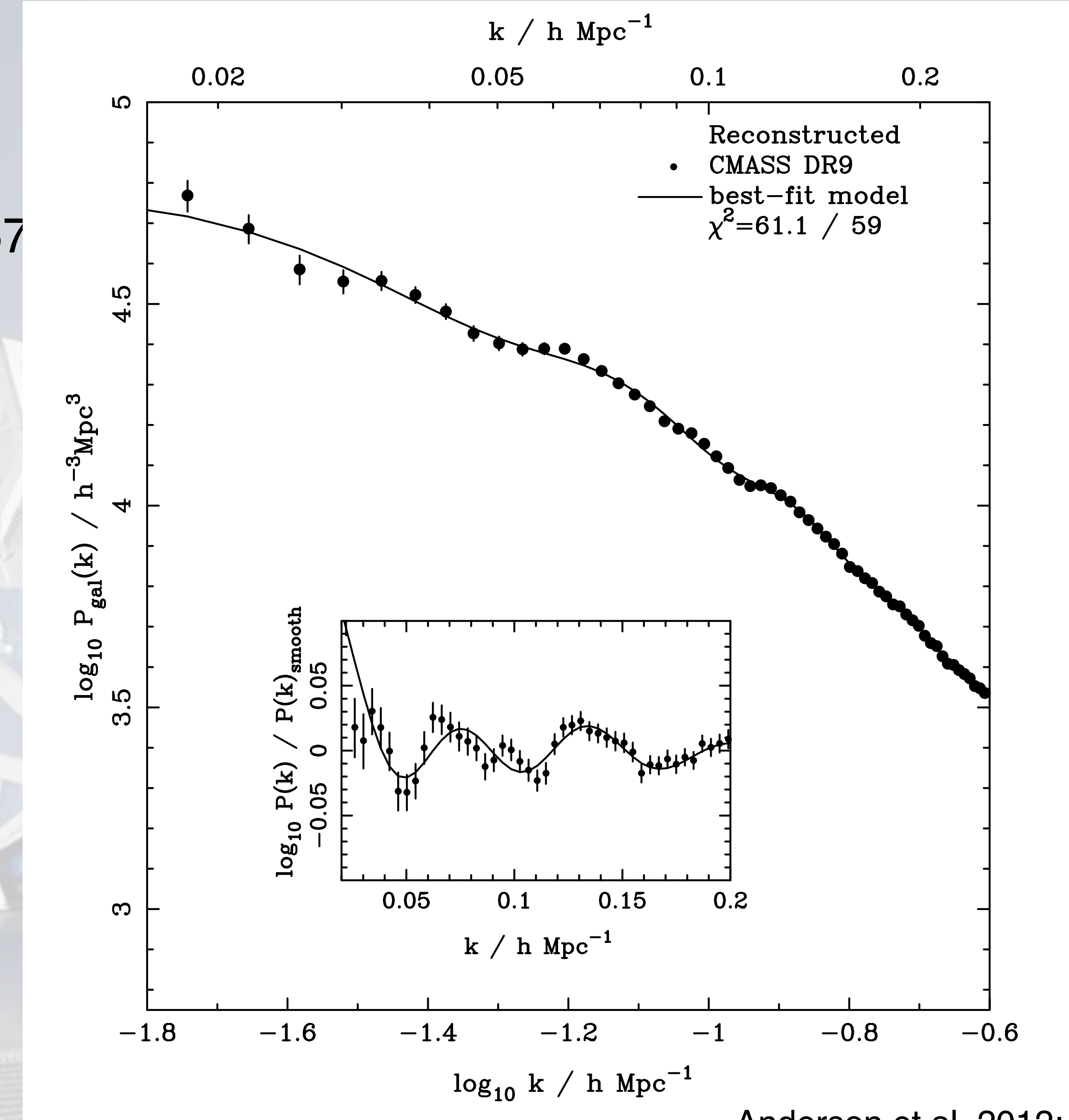

Anderson et al. 2012; arXiv:1203.6565

Predicted Euclid galaxy clustering

Redshift slice
$0.9 < z < 1.1$

Total effective volume (of Euclid)
$V_{eff} = 57.4\ Gpc^3$

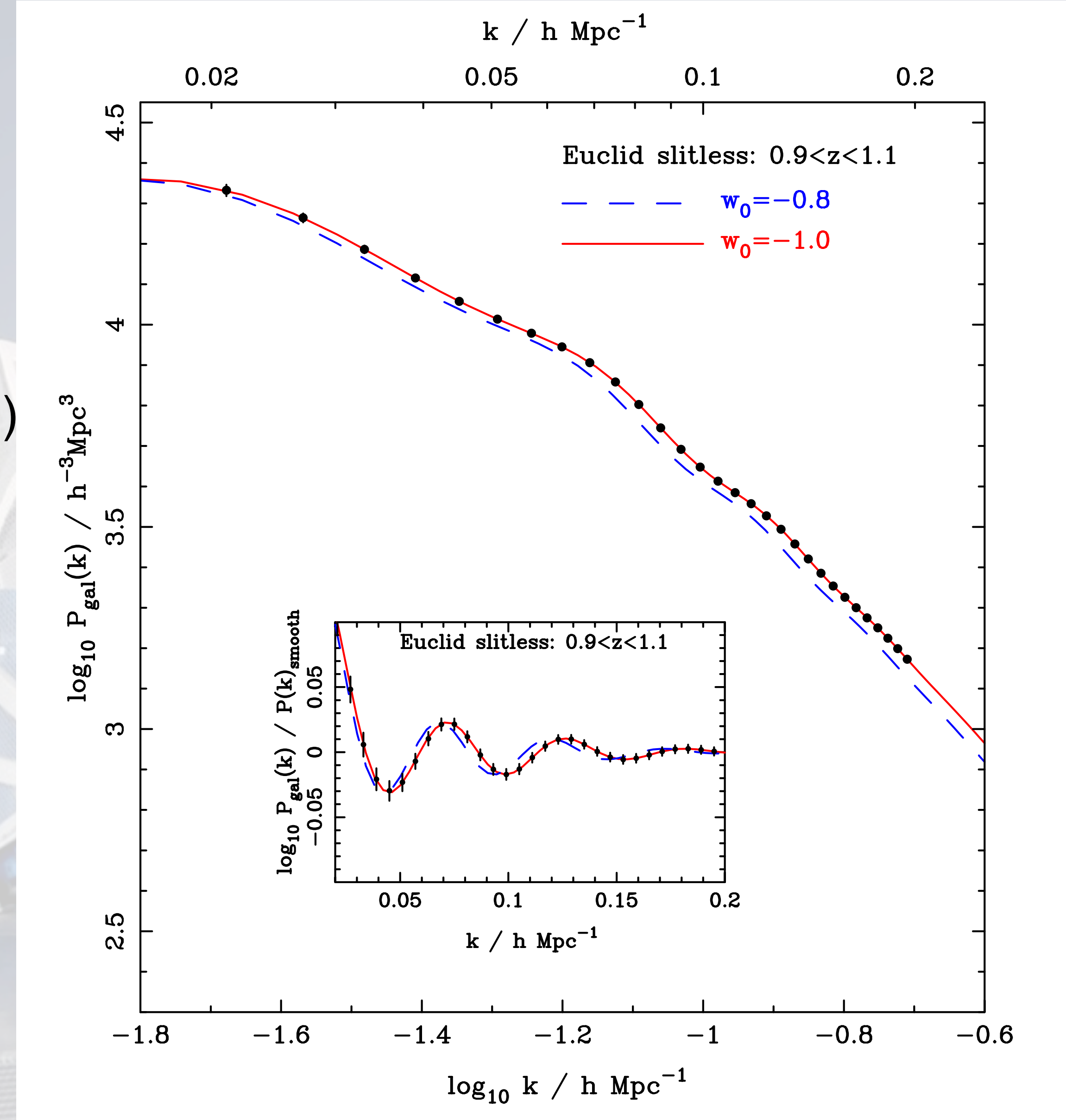

Improvement in precision

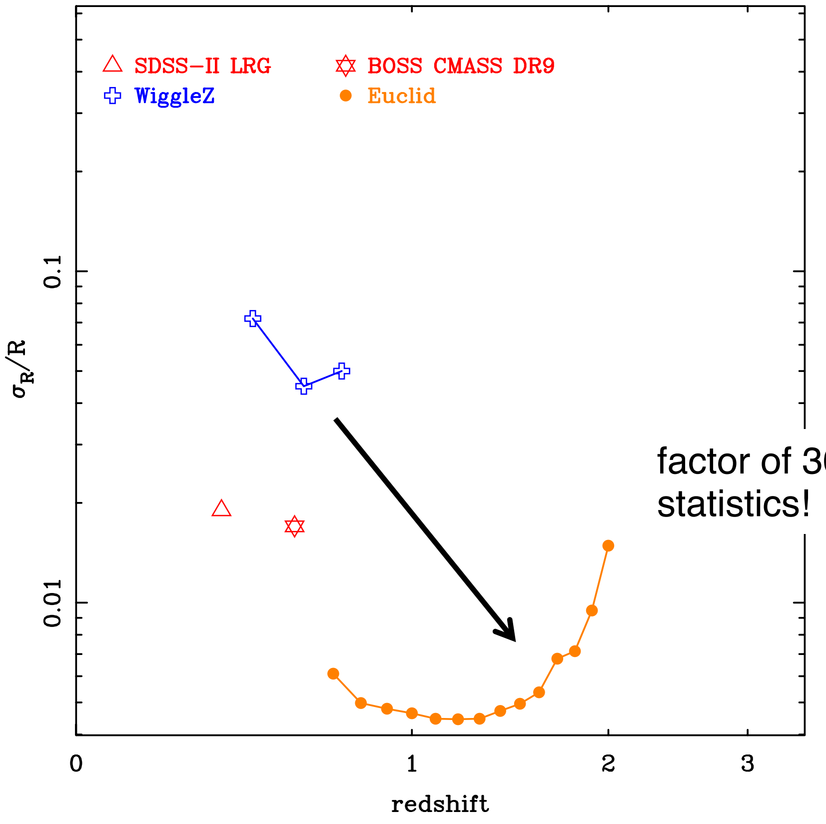

factor of 30 improvement in statistics!

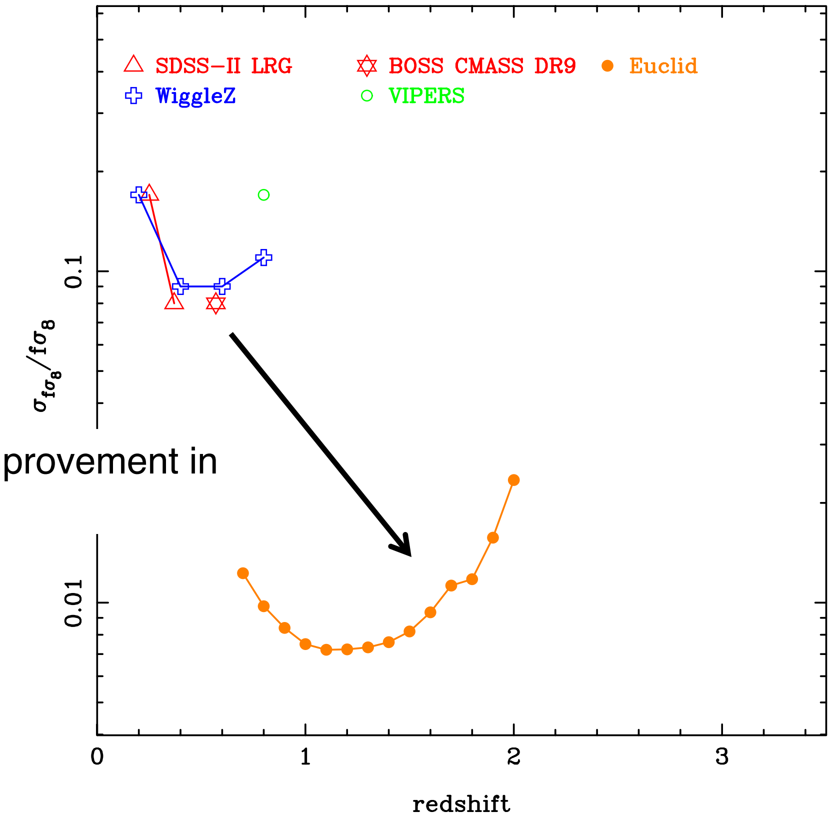

… but what about systematics? …

Testing with subsamples

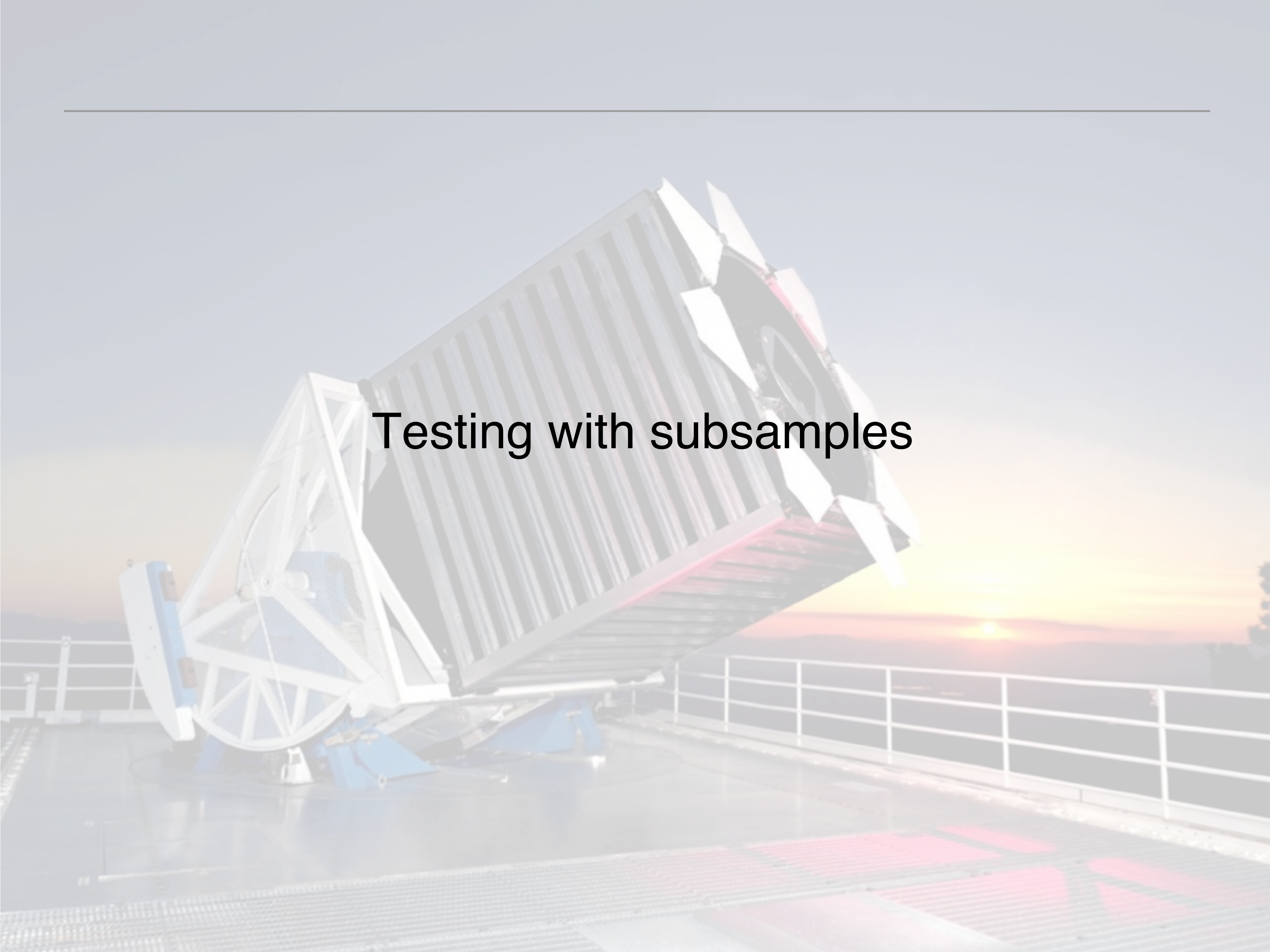

Testing with blue / red subsamples

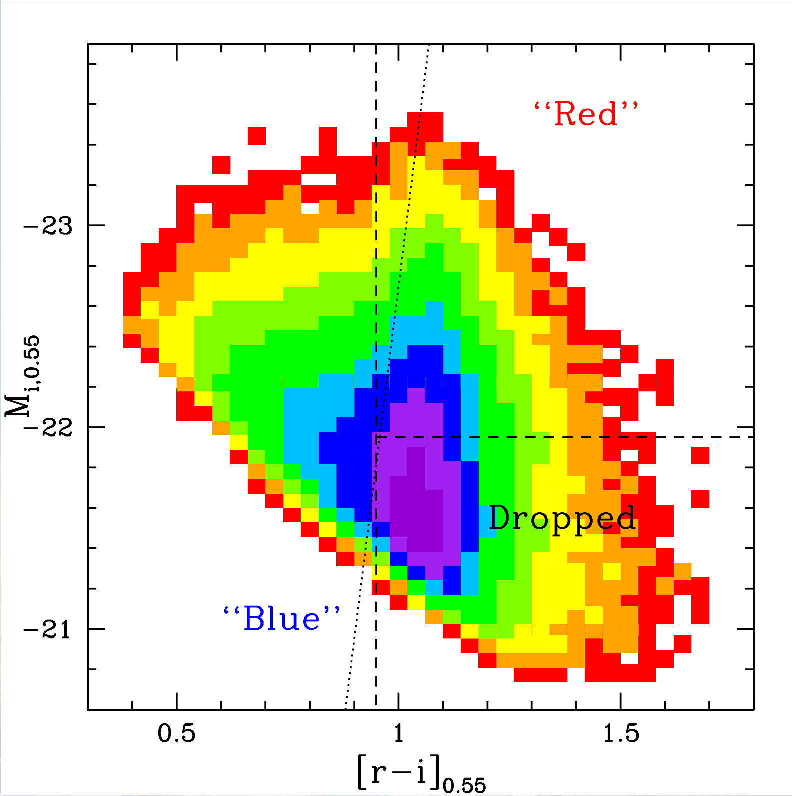

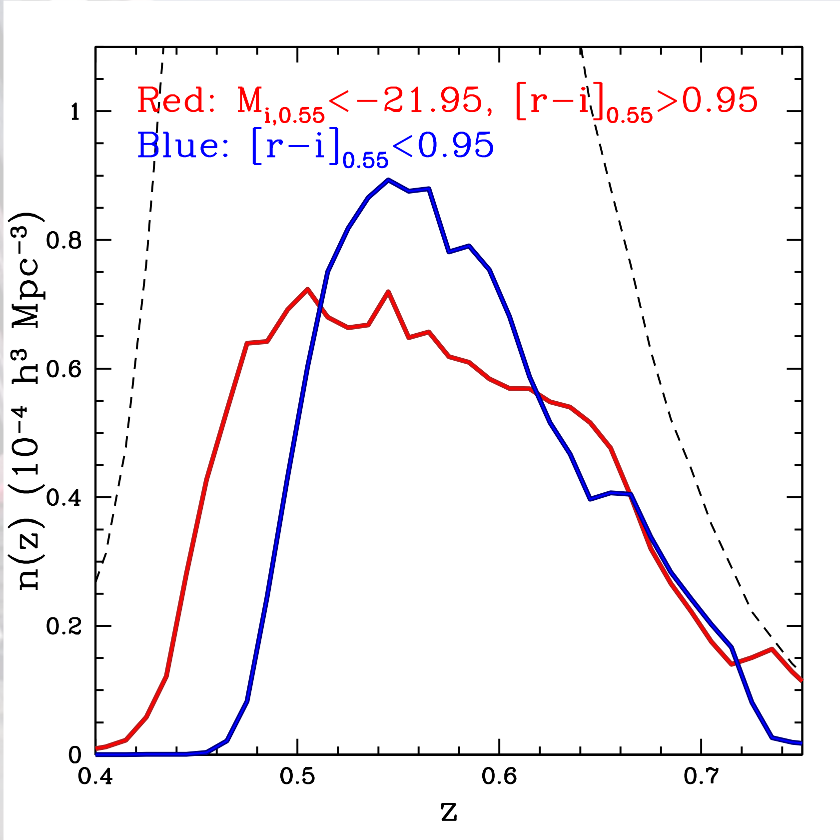

Ross et al. 2013, in prep

Testing with blue / red subsamples

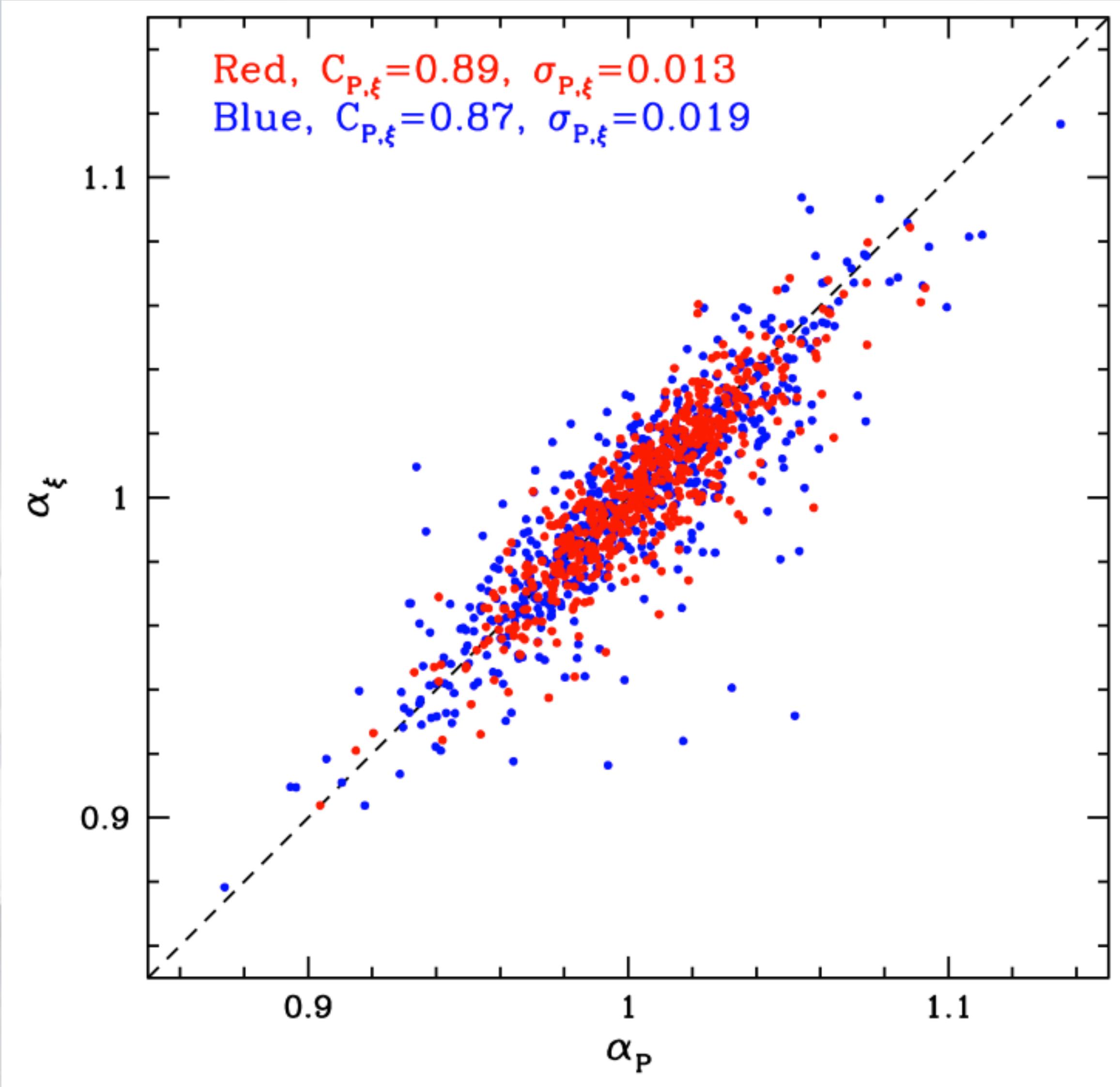

Ross et al. 2014, MNRAS 437, 1109

Getting the likelihood right

Getting the likelihood calculation 100% correct

The Likelihood under the standard assumption of a set of data drawn from a multi-variate Gaussian distribution is given by

$$\mathcal{L}(\mathbf{x}|\mathbf{p},\Psi^t) = \frac{|\Psi^t|}{\sqrt{2\pi}} \exp\left[-\frac{1}{2}\chi^2(\mathbf{x},\mathbf{p},\Psi^t)\right],$$

where $$\chi^2(\mathbf{x},\mathbf{p},\Psi^t) \equiv \sum_{ij}\left[x_i^d - x_i(\mathbf{p})\right]\Psi^t_{ij}\left[x_j^d - x_j(\mathbf{p})\right].$$

now suppose that the covariance matrix (size n_b x n_b) has been calculated from n_s simulations

$$\mu_i = \frac{1}{n_s}\sum_s x_i^s \qquad C_{ij} = \frac{1}{n_s - 1}\sum_s (x_i^s - \mu_i)(x_j^s - \mu_j)$$

then an unbiased estimator of the inverse covariance matrix is

$$\Psi = \frac{n_s - n_b - 2}{n_s - 1} C^{-1}$$

Hartlap J., Simon P., Schneider P., 2007, A&A, 464, 399

Errors in the covariance matrix

Simply providing an unbiased estimator of the inverse covariance matrix is not enough

The inverse covariance matrix also has its own error

$$\langle \Delta\Psi_{ij}\Delta\Psi_{i'j'}\rangle = A\Psi_{ij}\Psi_{i'j'} + B(\Psi_{ii'}\Psi_{jj'} + \Psi_{ij'}\Psi_{ji'}),$$

$$A = \frac{2}{(n_s - n_b - 1)(n_s - n_b - 4)}$$

$$B = \frac{(n_s - n_b - 2)}{(n_s - n_b - 1)(n_s - n_b - 4)}$$

Strictly, we should form a joint likelihood

$$\mathcal{L}(\mathbf{x}, \Psi|\mathbf{p}, \Psi^t) = \mathcal{L}(\mathbf{x}|\mathbf{p}, \Psi)\mathcal{L}(\Psi|\Psi^t),$$

If we don't, this leads to an additional error on the n_p parameters being fitted

$$\langle p_\alpha p_\beta\rangle|_{s.o.} = B(n_b - n_p)F^{-1}_{\alpha\beta},$$

Taylor et al., 2012, arXiv:1212.4359; Dodelson & Schneider 2007, arXiv:1212.4359

Errors in likelihood calculations

Given a set of mocks, we can form two possible estimates of the errors:

1. From the individual likelihood surface from each mock

2. From the distribution of recovered measurements from the set of mocks

These should agree!

The estimates from each are biased in subtly different ways gives errors in the covariance matrix

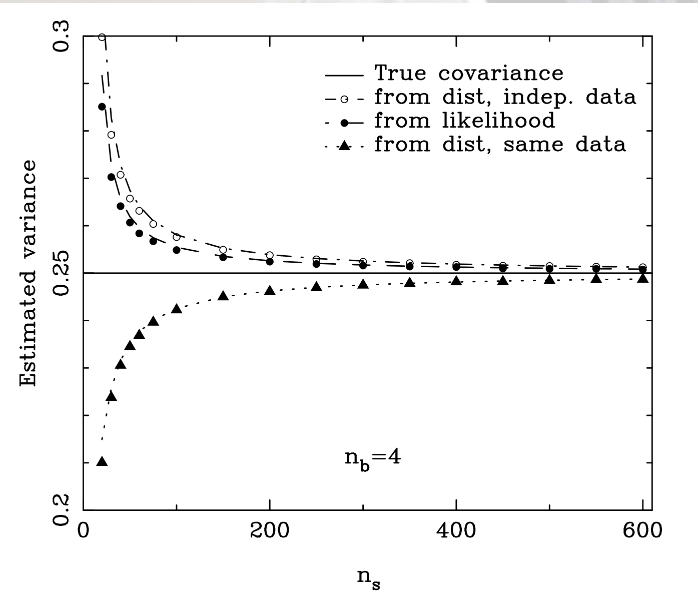

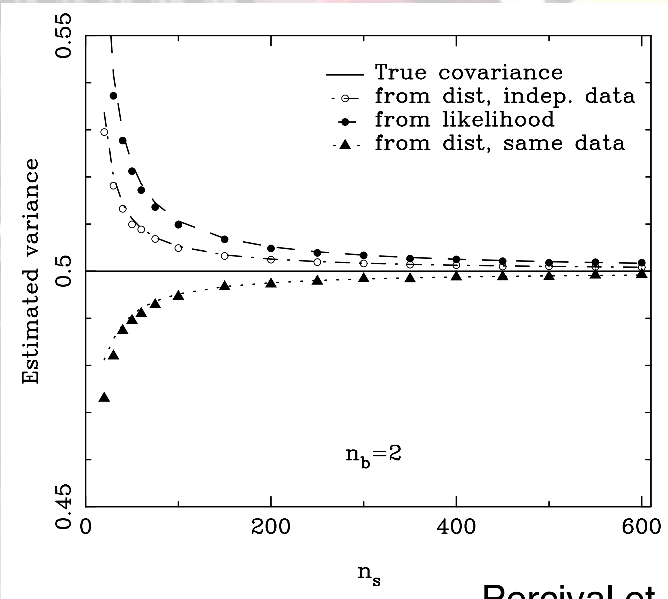

Percival et al., 2013: arXiv:1312.4841

Application to BOSS

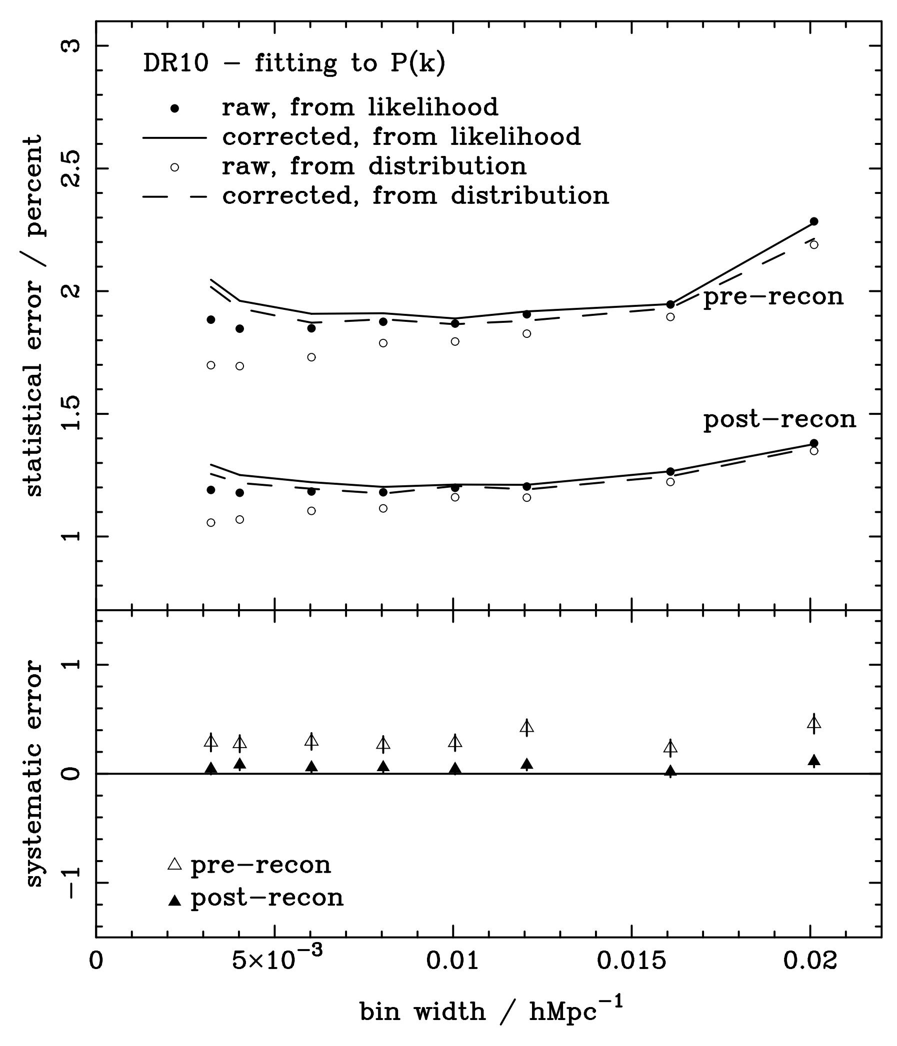

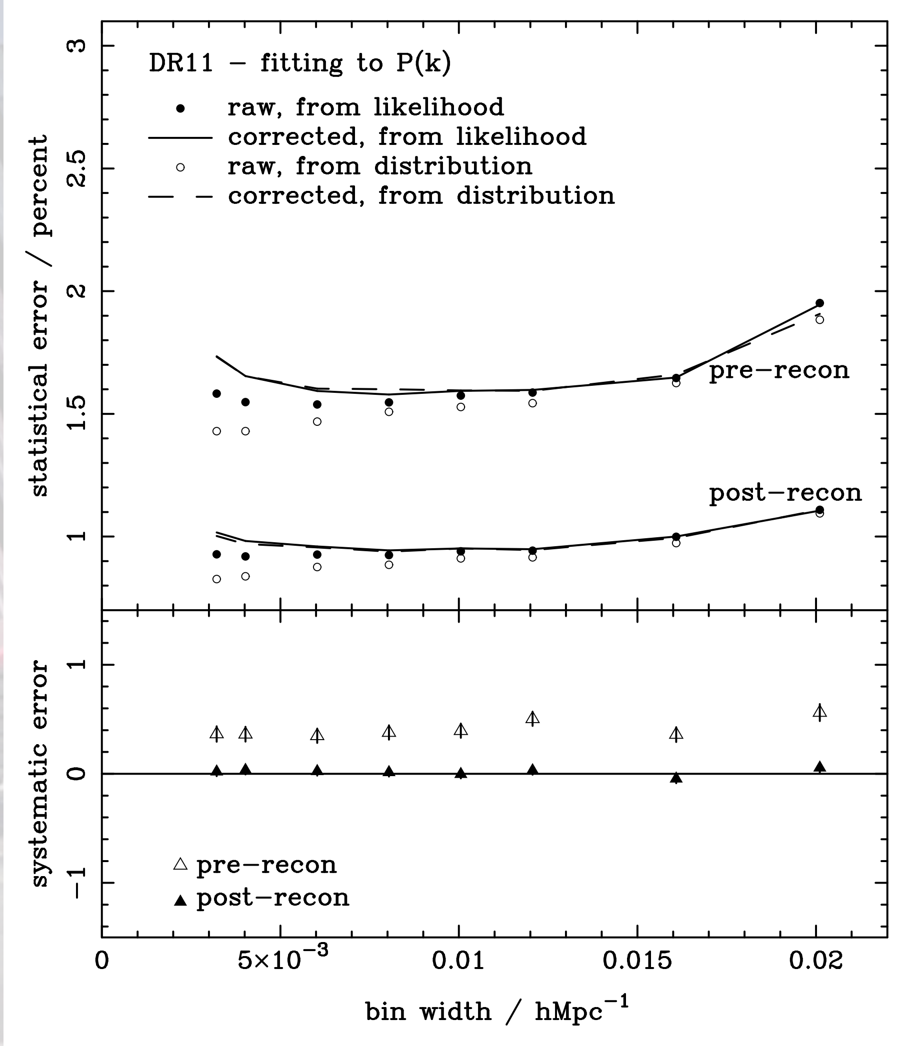

Percival et al., 2013: arXiv:1312.4841

Getting the model right

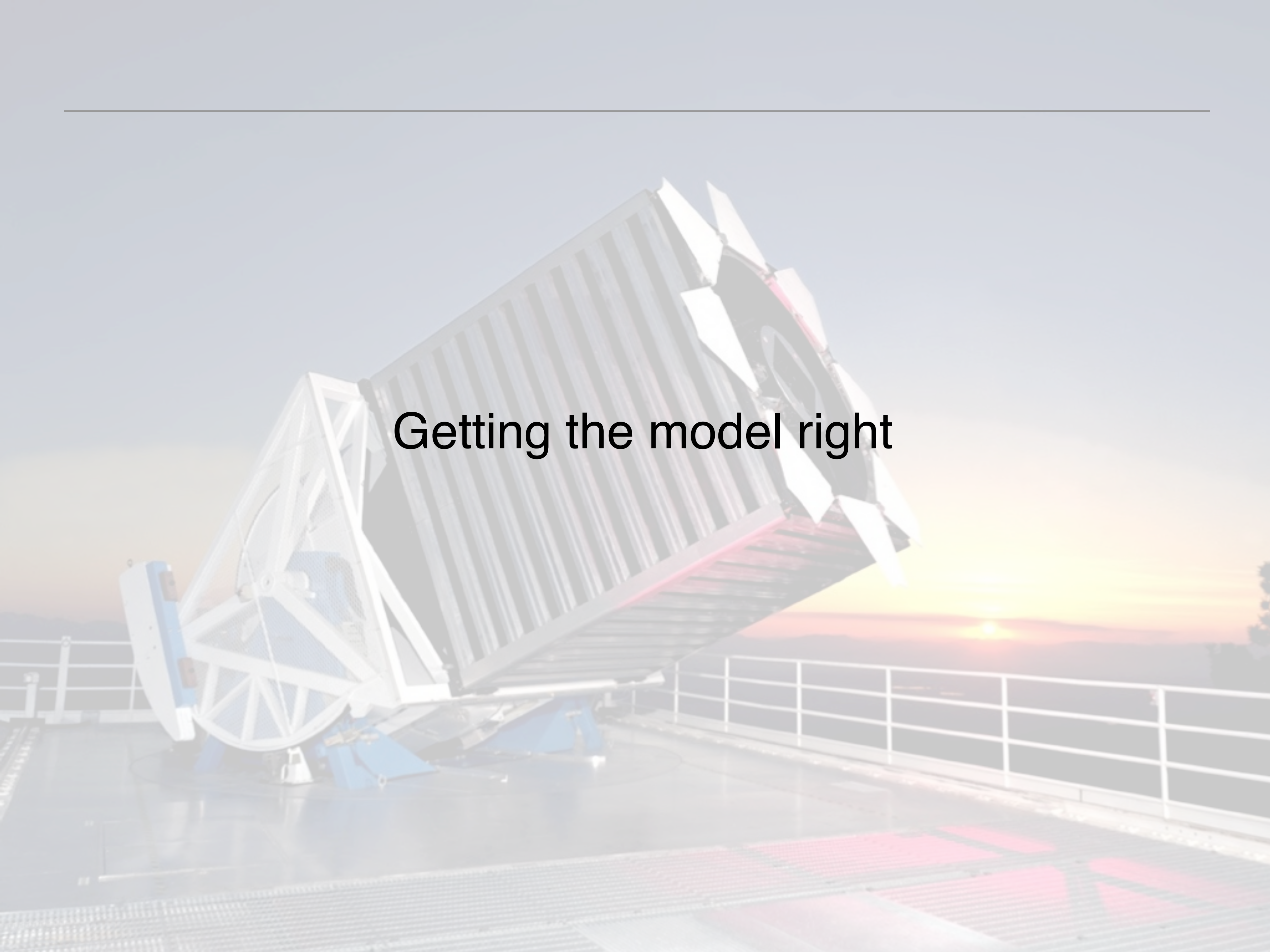

BAO from simulations

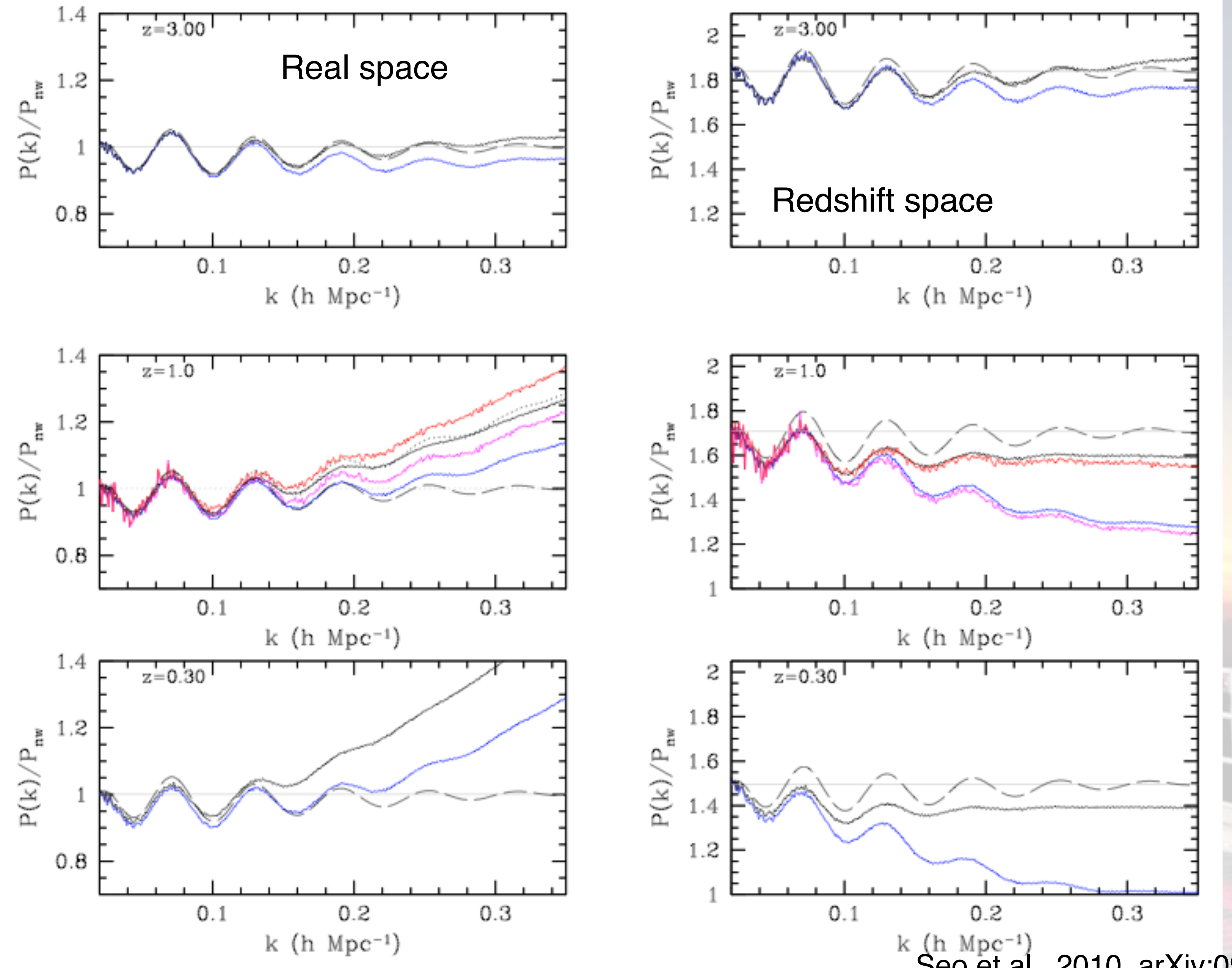

Seo et al., 2010, arXiv:0910.5005

BAO from simulations

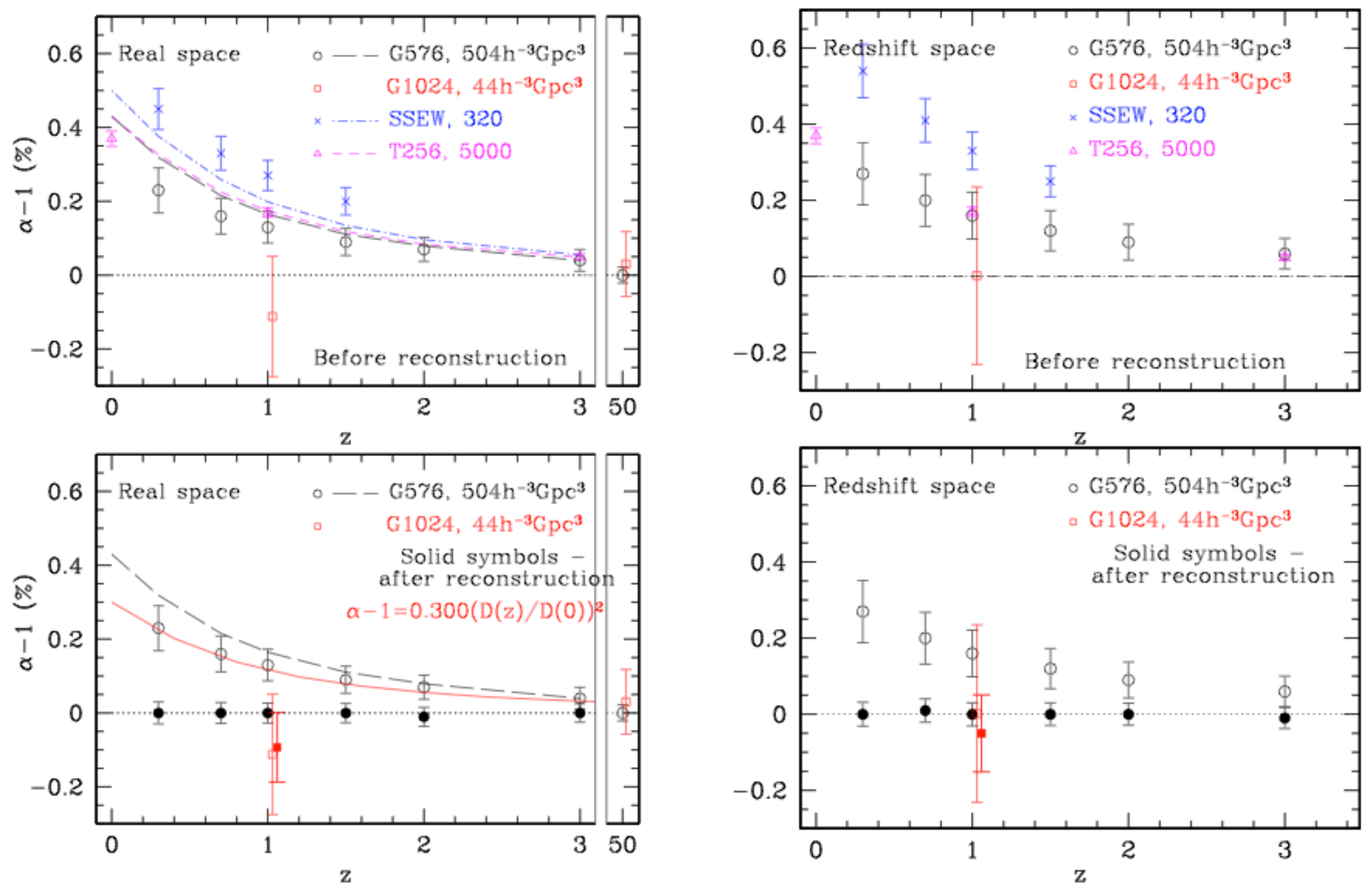

Seo et al., 2010, arXiv:0910.5005

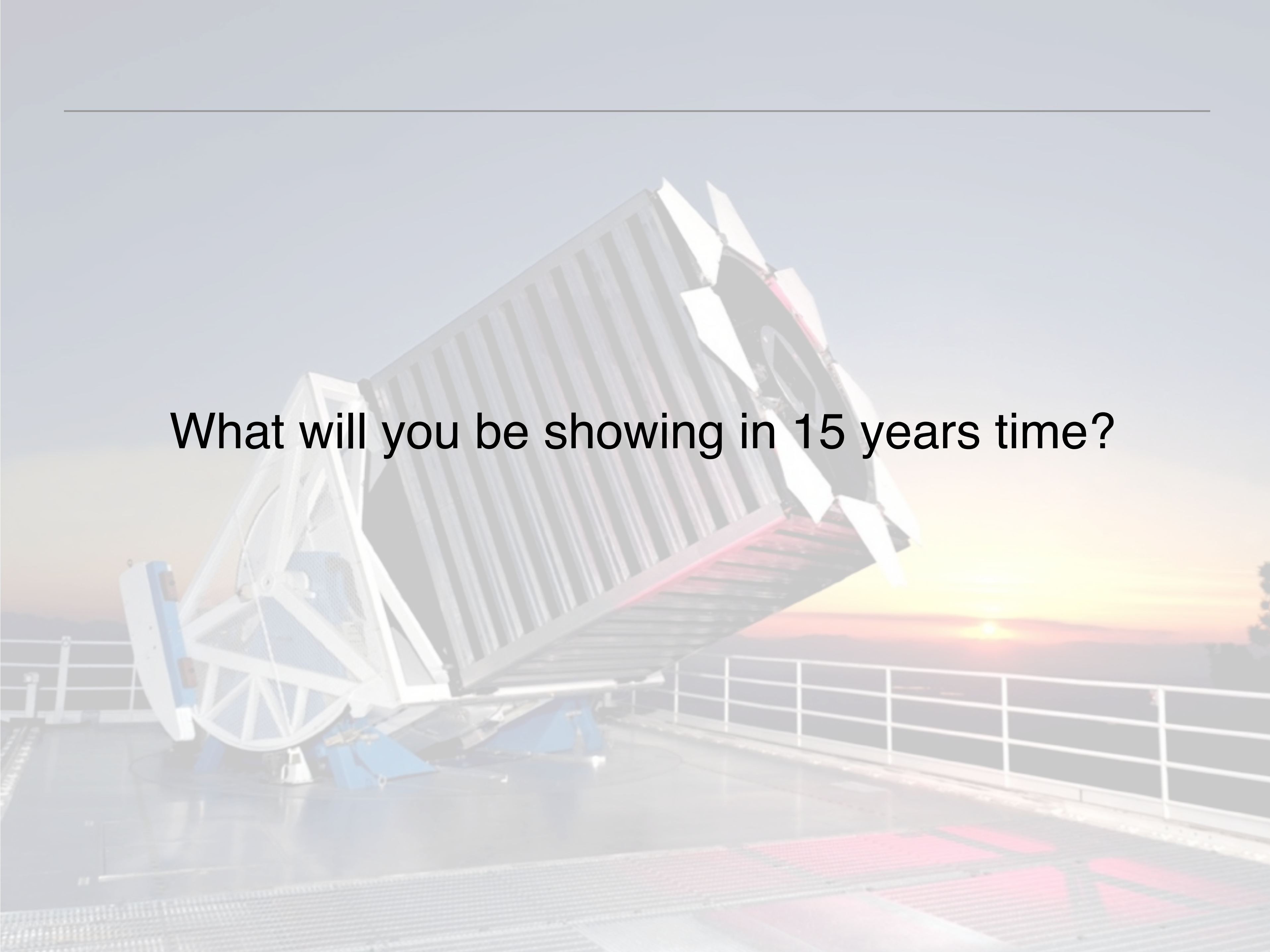

What will you be showing in 15 years time?

At the same time as my PhD …

Photo: U. Montan

Saul Perlmutter

Photo: U. Montan

Brian P. Schmidt

Photo: U. Montan

Adam G. Riess

The Nobel Prize in Physics 2011 was divided, one half awarded to Saul Perlmutter, the other half jointly to Brian P. Schmidt and Adam G. Riess *"for the discovery of the accelerating expansion of the Universe through observations of distant supernovae"*.

SDSS-II LRG BAO vs other data

ΛCDM models with curvature

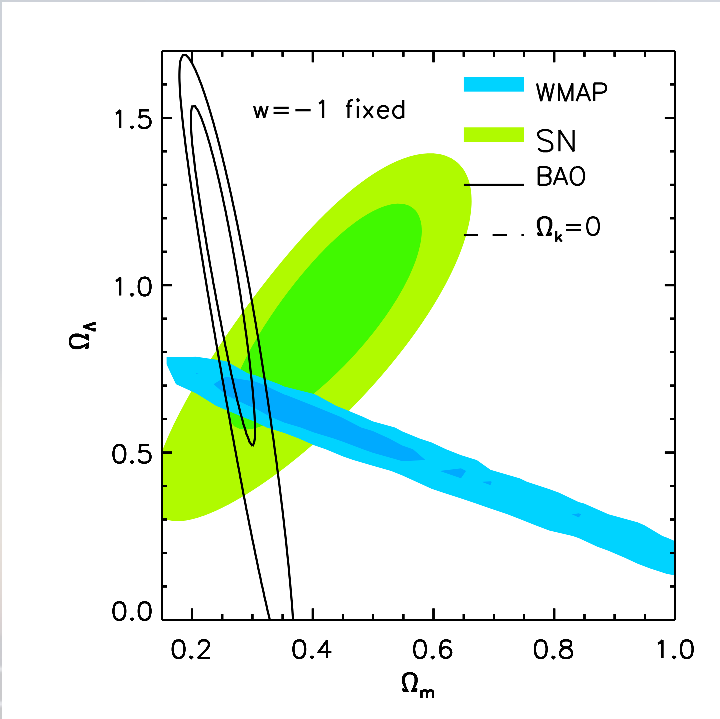

flat wCDM models

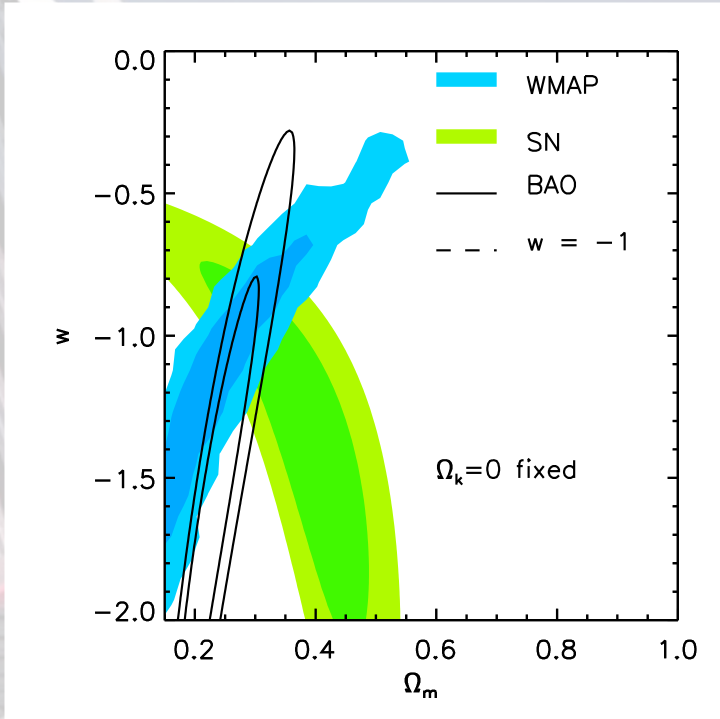

Union supernovae

WMAP 5year

SDSS-II BAO Constraint on $r_s(z_d)/D_V(0.2)$ & $r_s(z_d)/D_V(0.35)$

Percival et al. 2009; arXiv:0907.1660

Euclid BAO predictions

ΛCDM models with curvature

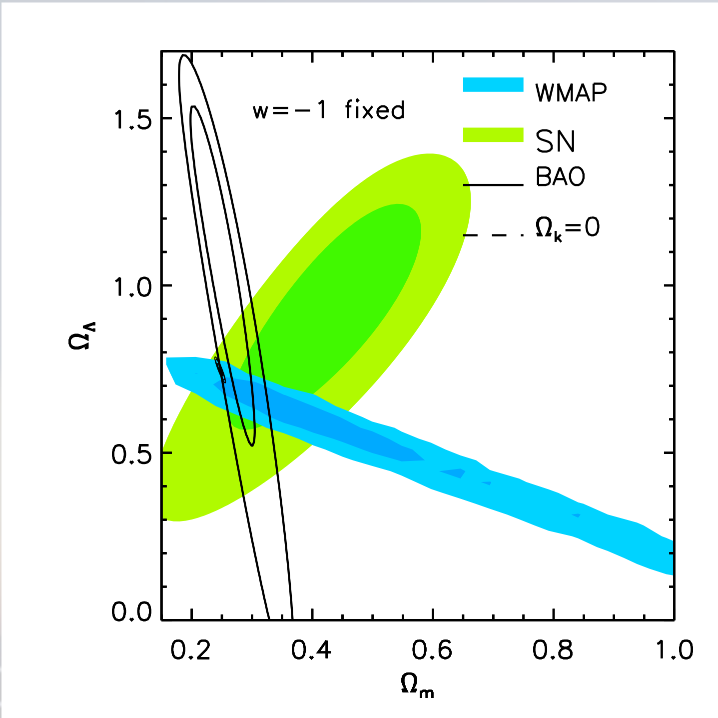

flat wCDM models

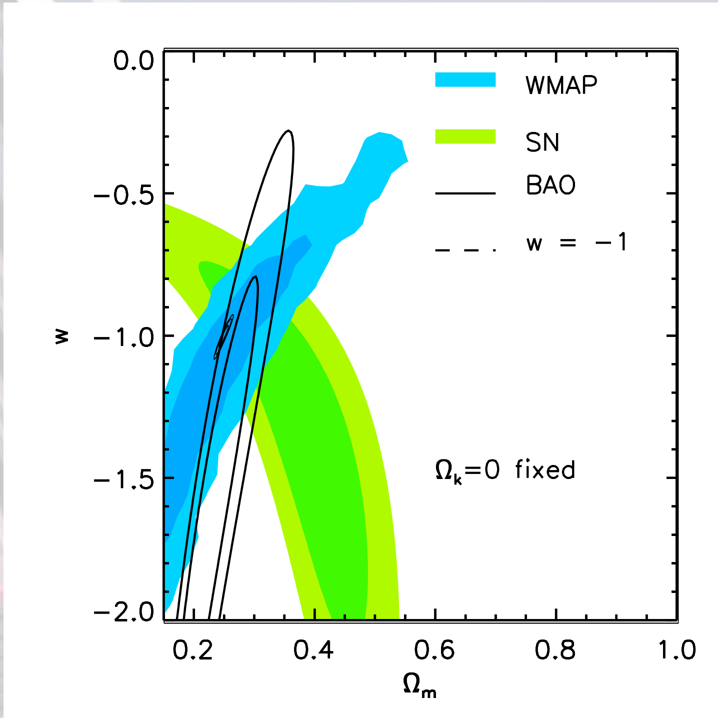

Union supernovae

WMAP 5year

SDSS-II BAO Constraint on $r_s(z_d)/D_V(0.2)$ & $r_s(z_d)/D_V(0.35)$

Cosmology from surveys